

R-09-43

Site investigation SFR

Hydrogeologic modelling of SFR v 0.1

Influence of the ridge on the flow fields for different target volumes

Johan Öhman, Golder Associates AB

January 2010

Svensk Kärnbränslehantering AB

Swedish Nuclear Fuel
and Waste Management Co

Box 250, SE-101 24 Stockholm
Phone +46 8 459 84 00



Site investigation SFR

Hydrogeologic modelling of SFR v 0.1

Influence of the ridge on the flow fields for different target volumes

Johan Öhman, Golder Associates AB

January 2010

Keywords: Hydrogeology, DarcyTools, Trajectories, Flow modelling

This report concerns a study which was conducted for SKB. The conclusions and viewpoints presented in the report are those of the author. SKB may draw modified conclusions, based on additional literature sources and/or expert opinions.

A pdf version of this document can be downloaded from www.skb.se.

Abstract

The primary objective of the ongoing hydrogeological investigations at SFR is to develop a description of the hydrogeological system inside the SFR regional model domain. The descriptive model should provide preliminary parameter values to a mathematical flow model, which will be for safety assessment and design analyses. Preliminary parameter values have recently been reported by /Öhman and Follin 2010/. These are based on the re-interpretation of historic data with respect to the updated bedrock geological model by /Curtis et al. 2009/.

This document demonstrates an application of the current SFR hydrogeological model version 0.1. The flow model is set up in DarcyTools to examine if the pier acts as a local water divide for four suggested layouts of the future expansion of SFR. One of the key findings is that the surface hydrology modelling (soil layers and surface run-off) is critical for providing realistic results. More emphasis should be placed in surface hydrology (and future surface hydrology) in future model versions.

Sammanfattning

Huvudsyftet med de pågående hydrogeologiska undersökningarna vid SFR är att utveckla en beskrivning av de hydrogeologiska förhållandena inom det regionala modellområdet för SFR. Den beskrivande modellen innefattar en preliminär parameterisering av en matematisk flödesmodell, som ska användas för säkerhets- och konstruktionsanalyser. Preliminära parametervärden har nyligen rapporterats av /Öhman och Follin 2010/. Dessa är baserade på en omtolkning av befintliga hydrauliska data med avseende på den uppdaterade berggrundsmodellen som tagits fram av /Curtis et al. 2009/.

Rapporten redogör för en tillämpning av den nuvarande SFR hydrogeologiska modellen, version 0.1. Flödesmodellen implementeras i DarcyTools i syfte att undersöka om piren utgör en lokal vattendelare för fyra föreslagna placeringar av den framtida utbyggnaden av SFR. En av de viktigaste slutsatserna är att beskrivningen av yhydrologin (jordlager och avrinning) har avgörande betydelse för realistiska resultat. Framtida modellversioner bör lägga mer vikt vid beskrivningen av yhydrologi (samt framtida yhydrologi).

Contents

| | | |
|----------|---|----|
| 1 | Introduction | 7 |
| 2 | Objectives and scope of work | 9 |
| 2.1 | Data used | 10 |
| 3 | Preparation of geometrical data | 13 |
| 3.1 | Tunnel geometry | 13 |
| 3.1.1 | The existing SFR | 13 |
| 3.1.2 | Candidate layouts | 13 |
| 3.2 | Surface hydrology | 15 |
| 3.2.1 | Topography | 15 |
| 3.2.2 | River system | 15 |
| 3.2.3 | Modifications to super-regional flow domain | 17 |
| 3.2.4 | Basin-fill and lakes | 18 |
| 3.2.5 | Future river system | 20 |
| 3.3 | Subsurface hydrogeology | 22 |
| 3.3.1 | Hydraulic soil domain (HSD) | 22 |
| 3.3.2 | Hydraulic conductor domain (HCD) | 23 |
| 3.3.3 | Hydraulic rock domain (HRD) | 25 |
| 3.4 | Orientation of computational mesh | 25 |
| 4 | Model set up | 27 |
| 4.1 | Computational grid generation | 27 |
| 4.2 | Conductivity parameterisation | 28 |
| 4.2.1 | Tunnel system and layouts | 28 |
| 4.2.2 | Surface runoff | 29 |
| 4.2.3 | Hydraulic soil domain (HSD) | 29 |
| 4.2.4 | Hydraulic rock domain (HRD) | 30 |
| 4.2.5 | Hydraulic conductor domain (HCD) | 30 |
| 4.3 | Boundary conditions | 32 |
| 4.3.1 | Land lift | 33 |
| 4.3.2 | Future climate | 34 |
| 4.4 | Flow simulations | 35 |
| 4.5 | Particle tracking | 35 |
| 5 | Results | 37 |
| 5.1 | Flow simulations | 37 |
| 5.1.1 | 2000 AD | 37 |
| 5.1.2 | 3000 AD | 37 |
| 5.1.3 | 5000 AD | 39 |
| 5.1.4 | 5000 AD with major future rivers | 41 |
| 5.2 | Particle tracking | 41 |
| 6 | Summary and conclusions | 45 |
| | References | 47 |
| | Appendix A List of geometric objects used in the grid generation | 49 |
| | Appendix B Merging the PFM2.2 and SFR0.1 geologic models | 51 |
| | Appendix C Saltwater density in boundary conditions | 53 |
| | Appendix D Inconsistencies between the PFM2.2 and SFR0.1 geologic models | 57 |
| | Appendix E DarcyTools input file: Grid generation | 63 |
| | Appendix F DarcyTools input file: Flow simulation and particle tracking | 81 |
| | Appendix G Main changes between the preliminary v 0.1 model delivery and the 'final' post review model delivery. | 89 |

| | |
|---|----|
| Appendix H Simulated exit locations from candidate layouts at different stages of land-lift. | 91 |
| Appendix I Simulated flow-field of Candidate layouts. | 97 |

1 Introduction

This document reports the results gained by the interpretation of existing hydraulic data, which is one of the activities performed within the site investigation at SFR. The work was carried out in accordance with activity plan AP SFR-08-022. In table 1-1 controlling documents for performing this activity are listed. Both activity plan and method descriptions are SKB's internal controlling documents.

The first stage of a final repository for low and middle level radioactive operational waste (SFR) was constructed and taken into operation by 1987. An investigation programme for its future expansion was undertaken in 2008 by the Swedish Nuclear Fuel and Waste Management Company (SKB). This expansion of SFR is necessitated by the pending demolition waste from the closed reactors Barsebäck, Studsvik and Ågesta, the additional amounts of operational waste associated with the extended operating time of the remaining nuclear power plants, as well as the future demolition of running nuclear power plants Oskarshamn, Forsmark, and Ringhals /SKB 2008/.

The current investigation program involves new field investigations inside the target area (Figure 1-1), as well as modelling in the disciplines: geology, rock mechanics, hydrogeology and hydrogeochemistry. The modelling is to be developed in three versions that successively incorporate data from the ongoing SFR field investigations and the feedback from the other modelling disciplines. This work follows SKB:s established methodology for modelling /Rhén et al. 2003/ and /Follin et al. 2007/. The first model version, v. 0.0 /Odén 2009/ was primarily a numerical implementation of the previous conceptual hydrogeologic SFR model /Axelsson and Mærsk Hansen 1997, Holmén and Stigsson 2001/ to the computational software DarcyTools v. 3.1.

This successor model version, v. 0.1, incorporates the preliminarily updated geologic model SFR, v. 0.1 /Curtis et al. 2009/ and its hydraulic parameterisation /Öhman and Follin 2010/. This parameterisation is actually based on the same hydraulic data as /Holmén and Stigsson 2001/, but re-evaluated with respect to a preliminary version of the updated structural model of /Curtis et al. 2009/. The development of SFR geologic model v.0.1 was still in progress during this study, and therefore a preliminary version, available per 2008-12-19, was used. The differences between the preliminary and the final model versions are specified in Appendix G. It must be emphasised that this model version 0.1 is uncalibrated with respect to inflow measurements and to inference test data; therefore there are large uncertainties in the model and in many aspects the confidence is low. The data from the ongoing SFR field investigations will be implemented in model versions 0.2, and the final model v. 1.0.

There are four alternative locations considered for the expansion of SFR. The suitability of these candidate target volumes is to be evaluated and compared in a downstream analysis of particle trajectories, which will be performed by the SKB department Safety Assessment. Currently, the detailed geometry of the future layout has not yet been decided. The reason for this is that for optimized performance, the repository layout must be designed with respect to the transient flow field, and thus, the final tunnel design requires input from flow simulations.

The four candidate volumes have been placed with particular respect to their location in the local topography. Just south of the existing SFR, a wave-breaking pier has been constructed on top of a natural ridge, running East-West (Figure 1-1). This ridge forms a local topographical divide between two future sub-catchments: one discharging north to a future Charlie's lake, and the other discharging south into the topographical depression of the Singö zone (Figure 2-1).

Table 1-1. Controlling documents for the performance of the activity.

| Activity plan | Number | Version |
|--|-------------------|---------|
| Hydromodelling of SFR v0.1. Influence of the ridge on the flow fields for different target volumes | SKBdoc ID 1198520 | 0.1 |
| Platsmodellering, Hydrogeologi version 0.1 | AP SFR-08-022 | 0.1 |

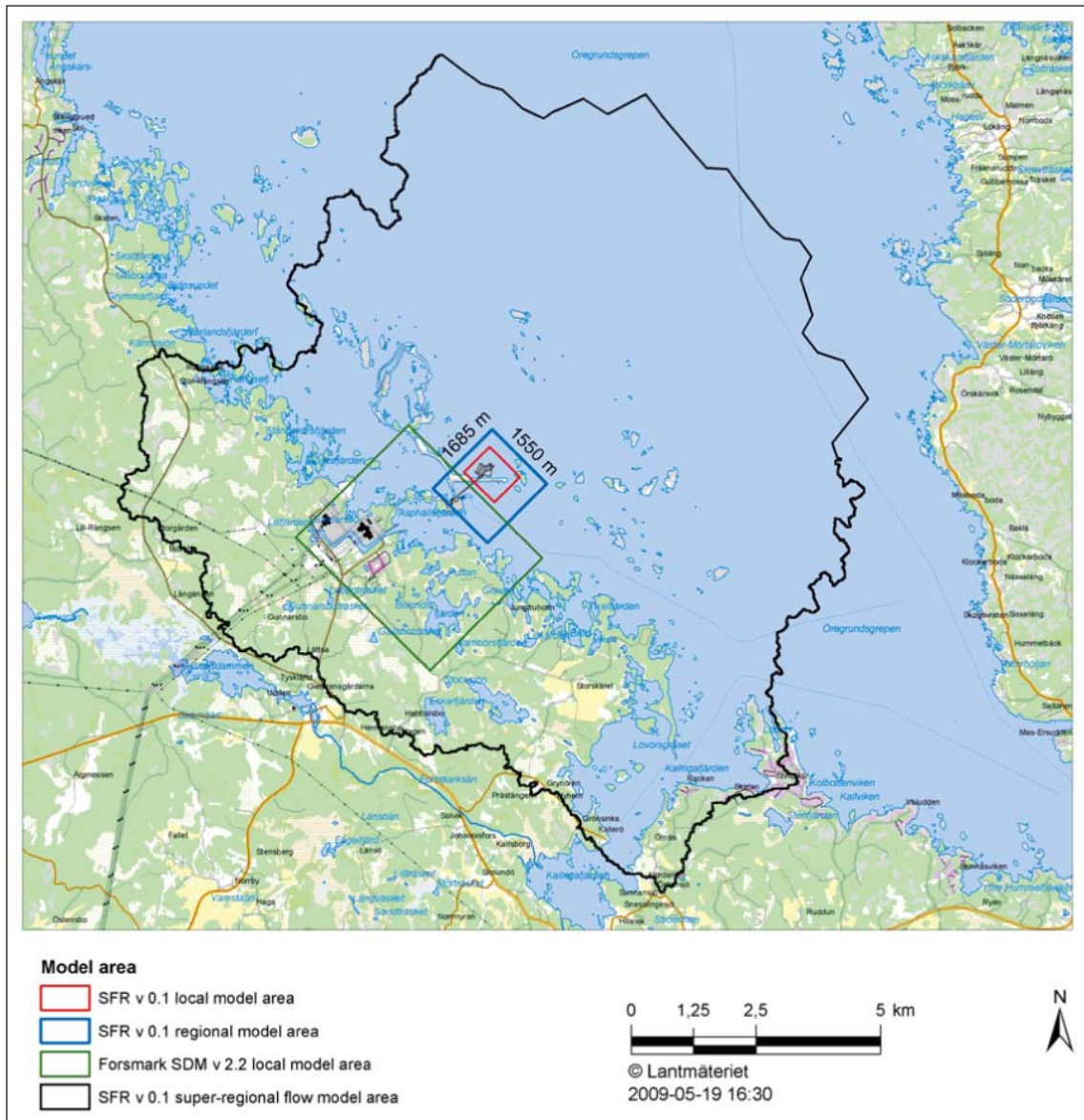


Figure 1-1. Regional (blue) and local (red) model areas for SFR model v. 0.1, as defined in /SKB 2008/, embedded in the super-regional flow model domain (black). The modelling scales in the present SFR investigation are smaller than in the Site Investigations in Forsmark and Laxemar; but the same relative nomenclature is used. For example, the local model area of SFR (red) is considerably smaller than that of the nearby Forsmark Site Investigation, model v. 2.2 (green).

2 Objectives and scope of work

The objectives of this study are to demonstrate the numerical implementation of the updated hydraulic parameterisation /Öhman and Follin 2010/, and to evaluate four alternative extensions of the SFR repository. In particular, it will be investigated if the ridge (Figure 2-1) will act as a water divide between the existing SFR and these four alternative locations. The candidate volumes will be evaluated by means of numerical modelling with the hydrogeological model SFR v 0.1 /Curtis et al. 2009, Öhman and Follin 2010/, as implemented in the computational software DarcyTools v 3.1 /Svensson et al. 2007, Svensson and Ferry 2004, Svensson 2004/. Specifically the following performance measures are of interest:

1. Flow in tunnels (direction etc.)
2. Flow path analyses

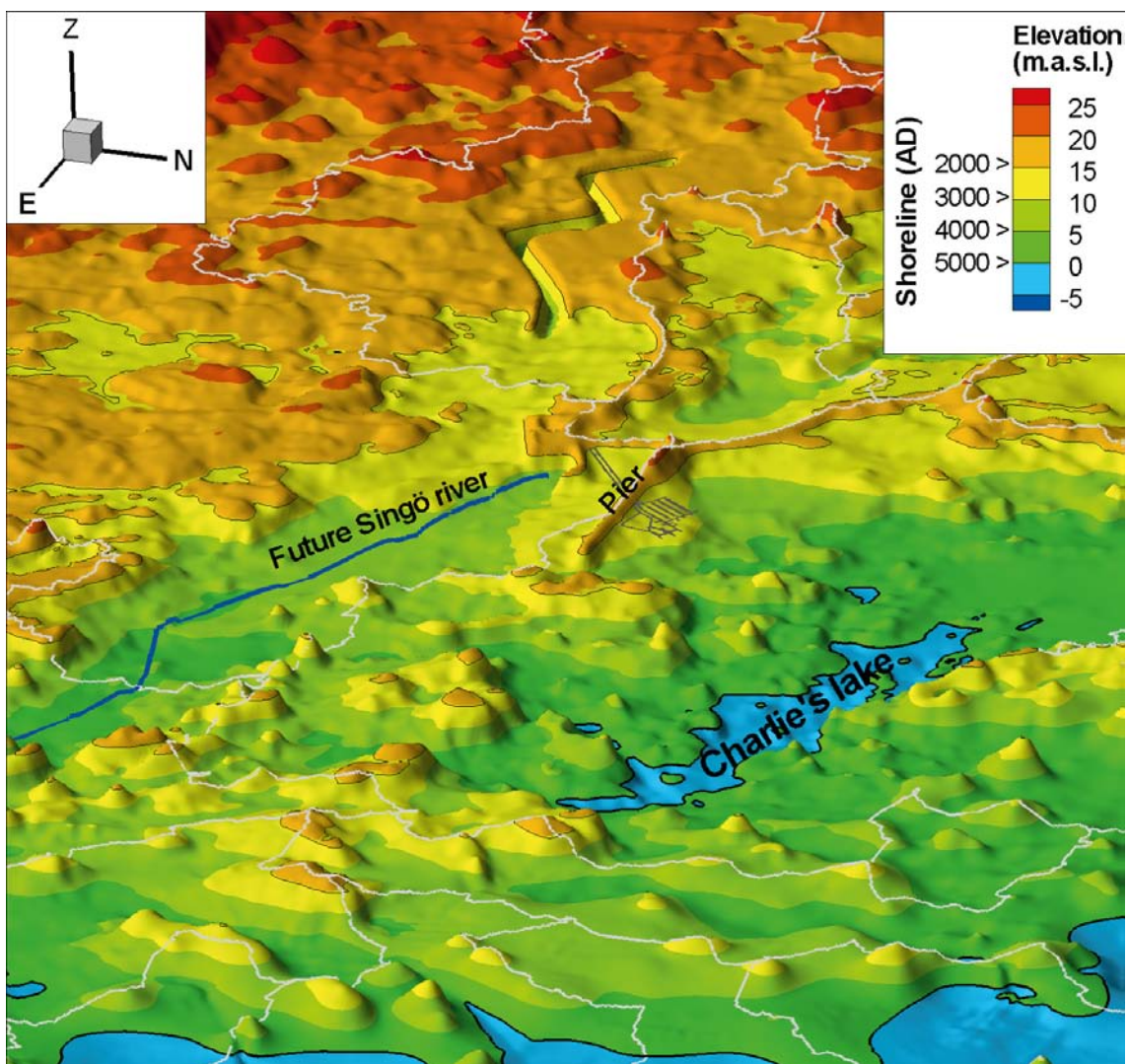


Figure 2-1. Surface hydrology overview of the site with shoreline retreat; the pier forms a topographical water divide between two sub-catchments: Catchment 28, which discharges north to Charlie's lake, and Catchment 32, which discharges south-east along the Singö topographical depression to Kallrigafjärden. The runoff in this depression will be modelled as a "future Singö river". The existing SFR is shown as a horizontal projection and the vertical exaggeration factor is 12.

The modelled process is the groundwater flow, subsequent to the re-saturation of SFR, with consideration to shoreline displacement process. It has been demonstrated that density gradients have a negligible influence on the shallow flow paths from SFR /Stigsson et al. 1998/; therefore groundwater flow is modelled as constant fresh water density in this study. Furthermore, the shoreline withdrawal is not modelled as a transient ongoing process; instead tunnel flow and particle trajectories are analysed as steady-state snapshots at the following times:

- 2000 AD (present)
- 3000 AD
- 5000 AD

The land lift is modelled by successively elevating the topography. As the current seafloor is elevated above sea level, its topography will alter owing to dynamic landscape processes of erosion and sedimentation. The topography is the driving potential for groundwater flow, and therefore the plays an important role for the performance assessment of the candidate layouts.

Technical barriers, such as low permeable tunnel plugs and backfill material at different locations of the tunnel system are excluded in this study.

To some extent, the focus of attention was changed during the course of this study. At the onset of the study, it was expected that focus would be directed towards the analysis of flow patterns between HCDs/HRD. However, the SFR is a very shallow repository relative to the planned deep repository for disposal of spent nuclear fuel. This implies that in comparison to previous DarcyTools applications, the modelling of SFR is sensitive to the HSD parameterisation and surface runoff. For example, in the Task Description it was originally decided that two alternative descriptions of the man-made pier should be modelled as separate model cases and compared:

1. Inclusion of the pier, as defined in the topographical data.
2. Exclusion of any part of the pier extending above an elevation of $z = a1.0$ m.

However, during the course of this study, it was found that the parameterisation of HSD and surface runoff has a larger influence on model results. It was therefore considered necessary to re-direct attention to this matter instead and the primary conclusions of this study concern the recommendations for subsequent model versions.

2.1 Data used

The hydrogeologic model SFR 0.1 is composed of the local and a regional model domain, as defined in /SKB 2008/. These domains are embedded in the surrounding super-regional flow domain (Figure 1-1). The hydrogeology of the local and regional domains is defined geometrically by the preliminary geologic deformation zone model SFR v 0.1¹ /Curtis et al. 2009/, and the hydraulic parameterisation of the hydrogeologic model SFR v 0.1 /Öhman and Follin 2010/. The differences between the preliminary and the final model versions are specified in Appendix G. For traceability, the geometrical data of /Curtis et al. 2009/ have been transferred from the geologic modelling team via SKBdoc (Table 2-1). The surrounding super-regional flow domain has geometric HCD definitions from /Stephens et al. 2007/ and the hydraulic parameterisation of /Follin et al. 2008/.

The geometric definitions of the four candidate volumes were provided by the SKB department Safety Analysis, and downloaded via SKBdoc. The DarcyTools input files that were developed in the hydrogeological model SFR v 0.0, were used as a starting point for this work (Table 2-1), but modified wherever necessary for the current model implementation.

¹ SKBdoc 1224847 – DZ_SFR_REG_v0.1_prelim, Version 0.1, 2010-06-08, (access might be given on request).

Table 2-1. Summary of data used.

| Table/file | Description | Source |
|--|---|---|
| Geometrical data | | |
| SDEADM.POS_FR_GEO_7061 | Super-regional flow domain | |
| SDEADM.UMEU_FM_HOJ_4528, SDEADM.UMEU_FM_HOJ_4529 | Surface topography (DEM) | GIS_08_62 |
| SDEADM.UMEU_FM_VTN_5033 | Subcatchments for future lakes | GIS_09_32 |
| GIS_request09_26.mxd | Regolith depth model (RDM) | GIS_09_26 |
| Alternative candidate volumes for particle release ^{1,2,3,4} | CAD files defining the geometry of candidate volumes | See footnotes |
| Deformation zone geometry ⁵ | Preliminary geometrical deformation zone definitions (RVS) in the Geological model SFR v. 0.1 (available per 090212) | See footnote |
| Extended geometry of ZFM871 ⁶ | Separate RVS definition of ZFM871 | See footnote |
| Deformation zone properties ⁷ | Auxillary geometric definition of zones: orientation, thickness, length | See footnote |
| Existing SFR tunnels and disposal facilities ⁸ | Laser-scanned geometry of the existing SFR (CAD STL format): tunnels and disposal facilities, divided into watertight sections (see Appendix A) | See footnote |
| 861006_DZ_PFM_REG_v22_SJ.dt | Geometric and hydraulic defined HCDs, from PFM2.2 | SKB – TRAC |
| 081006_sheet_joints_v5.ifz | Geometric and hydraulic defined sheet joints, from PFM2.2 | SKB –TRAC |
| FM_SM_shoreequations_2007_AD | Excel sheet with shore-level displacement equations fo the Forsmark area | SKB – TRAC /Pässe 2001, Hedenström and Risberg 2003/ |

¹ SKBdoc 1188004 – Föreslaget läge1, Version 0.1, 2010-09-06, (access might be given on request).

² SKBdoc 1188005 – Föreslaget läge2, Version 0.1, 2010-09-06, (access might be given on request).

³ SKBdoc 1188006 – Föreslaget läge3, Version 0.1, 2010-09-06, (access might be given on request).

⁴ SKBdoc 1188007 – Föreslaget läge4, Version 0.1, 2010-09-06, (access might be given on request).

⁵ SKBdoc 1224847 – DZ_SFR_REG_v0.1_prelim, Version 0.1, 2010-06-08, (access might be given on request).

⁶ SKBdoc 1228773 – DZ_PFM_REG_v22.01-SFR_hydro_H2, Version 0.1, 2010-06-08, (access might be given on request).

⁷ 1224861 – DZ_SFR_REG_v0.1-zone-report, Version 1.0, 2010-06-08, (access might be given on request).

⁸ SKBdoc 1223130 – Befintligt skannat SFR i STL-format, Version 0.1, 2010-06-08, (access might be given on request).

3 Preparation of geometrical data

There are several types of geometrical data which are used to define the computational mesh of grid cells in DarcyTools. These must be pre-processed and converted into an “object” file format that is required for the DarcyTools grid generation. The geometric objects must be defined by water-tight surfaces, in order to ensure a unique geometrical definition. Underground constructions, such as tunnel geometry and candidate layouts (Section 3.1), are available in CAD-format. These data are converted into a standard triangle mesh, by means of the inbuilt DarcyTools module OGN. The surface topography data is available as a 20 x 20 m² DEM. The topography data has many applications in the model set up (Section 3.2). After pre-processing, the topography data is converted into the triangle mesh format using a Fortran code for input into the DarcyTools model. Surface river systems are derived with GIS analysis and transformed into linear meshes (Section 3.2).

The subsurface hydrogeologic model is divided into the three units: the Hydraulic Soil Domain (HSD), the Hydraulic Conductor Domain (HCD), and the Hydraulic Rock Domain, after /Rhén et al. 2003/. The geometrical definition of HCDs inside the regional and local model domains are taken from the geologic model SFR v 0.1 /Curtis et al. 2009/, and the surrounding geometrical definition of HCDs in the super-regional flow domain are taken from the SDM-site v 2.2 of the Forsmark Site Investigation /Stephens et al. 2007/ (Section 4.2). The HCDs are converted from their original definition in RVS into the DarcyTools format for “deterministic fractures”. Deterministic fractures are defined by a triangulated central plane, with locally variable properties, such as HCD thickness, transmissivity, porosity, and storativity.

3.1 Tunnel geometry

3.1.1 The existing SFR

The tunnel geometry of the existing SFR repository has been laser-scanned and is available in CAD format. The geometric definition has been subdivided into a set of sequentially linked CAD objects, each being defined as a stand-alone closed volumetric shape. This is important for the grid generation in DarcyTools, as all geometric objects must be watertight to avoid ambiguity in geometric definitions. The CAD objects are then fused into larger tunnel sections which are of particular interest for the calibration and evaluation of inflow to tunnels (Figure 3-1). These tunnel sections are: 1) the individual storage facilities collection, 2) the intersection with ZFMWNW0001 (Singö deformation zone), and 3) areas for which separate inflow measurements exist /Axelsson et al. 2002, Axelsson 1997/. These objects, coloured and named by group (Figure 3-1), are specified in Table A-1. It should be noted that no inflow calibration is undertaken in the current study; the dividing of tunnel sections has been a preparation step for coming model versions.

3.1.2 Candidate layouts

There are four alternative locations considered for the expansion of SFR. The suitability of these candidate target volumes is to be evaluated and compared in a downstream analysis of particle trajectories, which will be performed by the SKB department Safety Assessment. These trajectories are calculated at different times (i.e. stages of land lift; Section 4.3.1), by releasing a large number of particles (i.e. inert water parcels) uniformly within the candidate volumes and tracking the flow field downstream until reaching the sea, which is the final outflow boundary of the model (see Section 4.5). The locations of these candidate volumes have been provided by Safety Assessment. The four candidate volumes have been placed with particular respect to their location in the local topography, with the consideration that the man-made pier may form a water divide between two sub-catchments: one discharging north to Charlie’s lake, and the other discharging south into the topographical depression of the Singö zone (Figure 2-1).

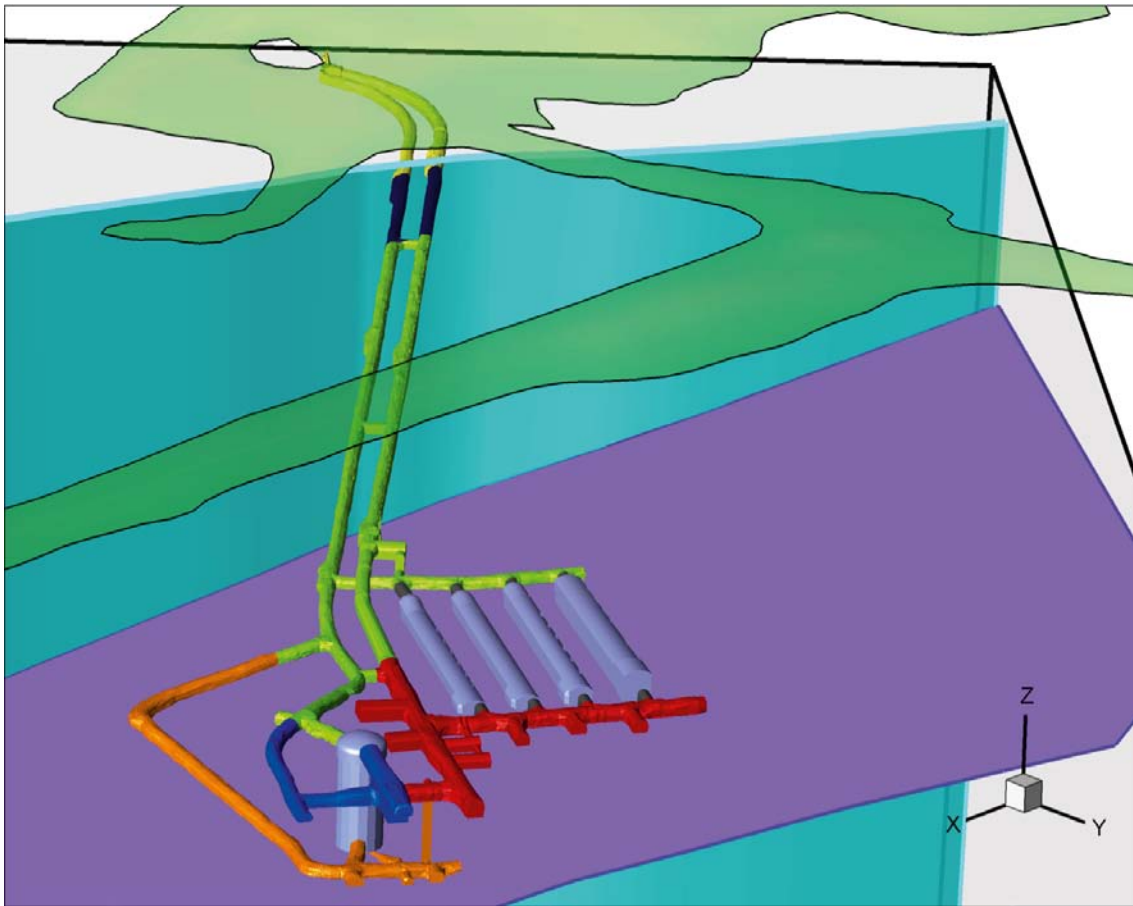


Figure 3-1. Tunnel objects discretised by areas of tunnel inflow; storage facilities (grey), access tunnels above and below the intersection with Singö deformation (yellow, respectively, green), NBT (orange) and tunnels downstream storage caverns (red) and silo (blue).

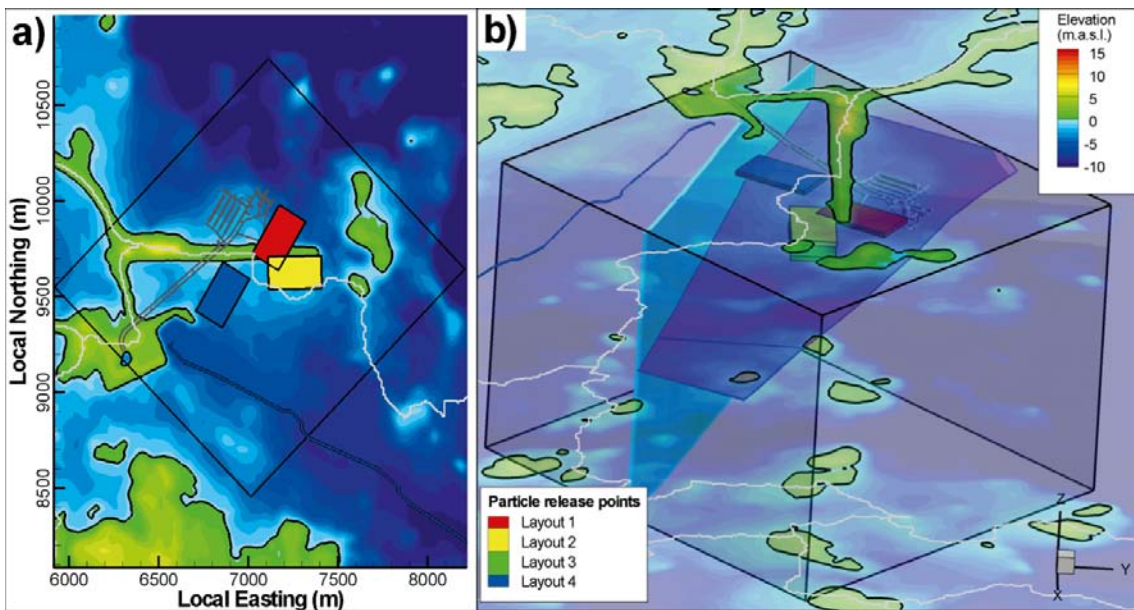


Figure 3-2. Location of particle release points in relation to the pier, the existing SFR, and topographical water divides (grey lines); a) top view and b) 3D-view with ZFMWNW0001 (Singö) and ZFM871 (zonH2), perspective from the East. Note that Layout 3 (green) is located right below Layout 2.

The detailed geometry of the candidate layouts has not yet been decided. The reason for this is that the repository layout should be designed with respect to the transient flow field in order to optimize its performance, and thus, the final tunnel design requires input from flow simulations. For the purpose of the current study, the candidate volumes will be represented by simple rectangular cuboids (Figure 3-2). One layout (Layout 1; Figure 3-2) is oriented parallel to the existing SFR and located partly underneath the pier partly and extending North. Its downstream trajectories can be expected to discharge close to those from the existing SFR, as the layout is located in the same catchment as SFR (Figure 3-2). Two layouts (Layouts 2 and 3; Figure 3-2) are located just South side of the pier with an orientation parallel to the pier. Layout 2 has an elevation approximately similar to Layout 1 (–65 to –85 m.a.s.l. RHB70), while Layout 3 is located twice as deep (–130 to –145 m.a.s.l. RHB70). Layout 4 is also parallel to the existing SFR, but located South of the pier in its entirety and at shallower depth (–55 to –70 m.a.s.l. RHB70). The postulation is that the downstream trajectories of Layout 4, will follow completely different routes compared to the existing SFR, as they are separated by a local topographical divide (Figure 3-2).

3.2 Surface hydrology

3.2.1 Topography

The ground surface topography, or more specifically its slope, is intimately related to the hydraulic gradients that constitute the driving potential of the flow model. Thus, the topography controls both surface runoff as well as the deeper groundwater flow, and consequently, the topography data has a central role in setting up the flow model; it is involved in defining appropriate model domain boundaries, assigning boundary conditions, the discretisation of the computational mesh, describing surface runoff patterns, etc.

The topography of the SFR super-regional flow domain is available by means of a Digital Elevation Map (DEM) defined at 20 x 20 m² resolution (Figure 3-3). This DEM was combined from high resolution DEM (10 x 10 m²) of the present day's land area, detailed lake level measurements, and several overlapping types of data on seafloor topography /Strömngren and Brydsten 2008/. The topographical gradients within the model domain are low, and particularly so for the current seafloor that will be elevated above present sea level within 5000 AD owing to land lift (Section 4.3.1). Note that during this time frame the topography is exposed to landscape dynamic processes and will alter due to sedimentation and erosion /Brydsten 2006/. Such processes are not modelled in the present study; instead a simplified case with "major future rivers" is tested in order to examine the sensitivity to the description of surface runoff (Section 3.2.5).

3.2.2 River system

The top boundary of the super-regional flow domain (i.e. ground surface) is assigned prescribed flux. The net precipitation (precipitation – evotranspiration) in the area has been estimated to 150 mm/year /Johansson and Öhman 2008/. The topographical gradients are low in the SFR area, and this condition is even more accentuated for the later simulation time periods, 5000 AD, as the seafloor is elevated above present sea level owing to land lift (Section 4.3.1). The landscape dynamics, such as sedimentation and erosion /Brydsten 2006/, are not considered here. Consequently, part of the net precipitation will become surface runoff that follows topographical depressions until either discharging into the sea, or possibly infiltrating downstream. The surface runoff at present days date can be calibrated to match lake levels and stream discharge measurements. In comparison, it is more difficult to ensure a realistic representation of the future river systems from analysis of seafloor topography as complex landscape dynamic processes will transiently transform the topography as it is elevated out of the sea /Brydsten 2006/. An alternative description of the future major river system is discussed in Section 3.2.5.

At present DarcyTools has no separate algorithm for modelling surface runoff. Instead, surface runoff is mimicked by solving the Darcy groundwater flow equation for grid cells with artificially high horizontal hydraulic conductivity, which are identified as river cells. This mimicked river flow takes place in surface grid cells along topographical depressions. The surface runoff from an arbitrary point at ground surface to the nearest river is facilitated by an artificial depth trend in horizontal hydraulic conductivity. This depth trend is globally assigned to the top 20 m of the computational grid (see section 4.2.3). The

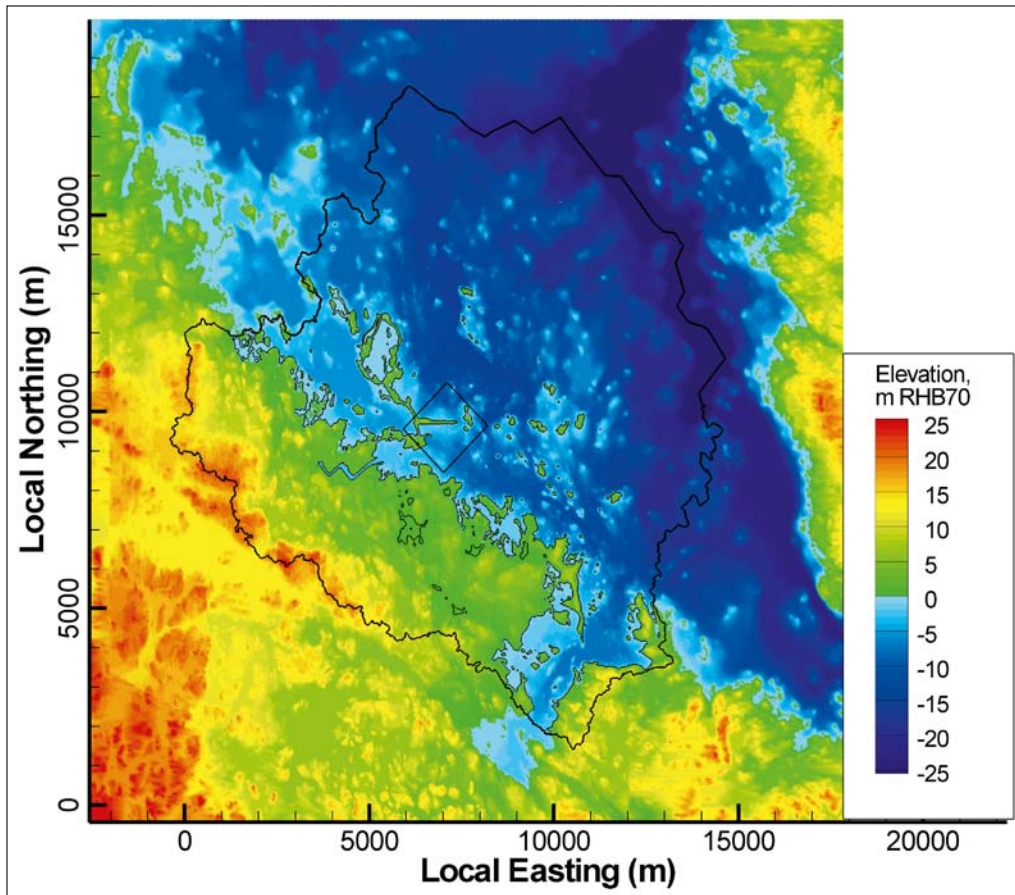


Figure 3-3. Ground surface topography data, available as a Digital Elevation Map (DEM) resolved at a 20 x 20 m resolution. Regional model area and super-regional flow model area shown with black lines. Local origo set to Northing = 6692000, Easting = 1626000.

surface runoff occurs in river systems that are interconnected by lakes, which can be identified from topographical depressions. This mimicked surface flow can potentially conceal convergence errors in the flow solution of the deep rock, as the surface flows are considerably larger in magnitude (see discussions in Chapters 5 and 6).

These anticipated river systems are identified and defined by means of Geographic Information System (GIS) analysis of the topographical data (Section 3.2.1). The software ArcGIS was used with the extensions SpatialAnalyst and ArcScan. The methodology can briefly be described as follows:

1. The topographical DEM was basin-filled using the hydrology tool "Fill" (without specifying z limit) to define the spatial extent of lakes
2. The hydrology tool "Flow Direction" and was applied for the filled DEM with calculation of "Flow Accumulation"
3. Riverlines with "Flow Accumulation" from less than 100 upstream DEM pixels (20 x 20 m) were neglected
4. Riverlines were fused into connected river systems. The elevation of these river systems are defined by the local ground surface level, but assigned a vertical extent of ± 1.0 m to eliminate the risk of discretisation errors.

The analysis above produces two geometric objects that are later used to represent surface runoff in the DarcyTools computational mesh. These are: 1) a linear river system connected to the sea (Figure 3-4), and 2) closed volumes defining potential lakes (Section 3.2.4). The lakes are defined

by the volumes between the bottom of the lake (i.e. the original topography DEM) and the maximum lake level possible (i.e. the basin-filled topography DEM). Note that this “maximum lake level” is only a tool used in the grid generation in order to avoid erroneous identification of the sea discharge boundary (Section 3.2.4); it does not constrain the actual simulated lake level (as shown for example in Figure 5-4).

3.2.3 Modifications to super-regional flow domain

Boundary conditions define how the model interacts with domains outside of the domain studied. These boundary conditions are generally based on the conceptual understanding of the hydro-geologic system, and therefore entail a certain degree of approximations and simplifications. The effects that these simplifications impose on the flow solution can be minimised by: 1) using a large embedding domain to exile errors far away from the domain of interest (i.e. the SFR v 0.1 regional domain), and 2) define natural boundaries that form a closed flow system. If the flow domain forms an independent large-scale catchment area, all of its vertical sides can be assigned a no-flow condition. Strictly speaking, this condition requires boundaries to be aligned parallel to flow. To define a flow domain with proper vertical no-flow boundaries it is therefore convenient to assume that the groundwater table follows the topography. Thus, the boundaries of the super-regional flow domain are geometrically defined by, either topographical divides (assuming divergent recharge), or the deep seafloor trench (the so-called Gräsörännan; assuming convergent discharge; Figure 3-4). This makes the geometric definition of the super-regional flow domain intimately related to the analysis of surface runoff. It should be noted however, that the flat topography of the SFR area causes uncertainty in this type of analyses.

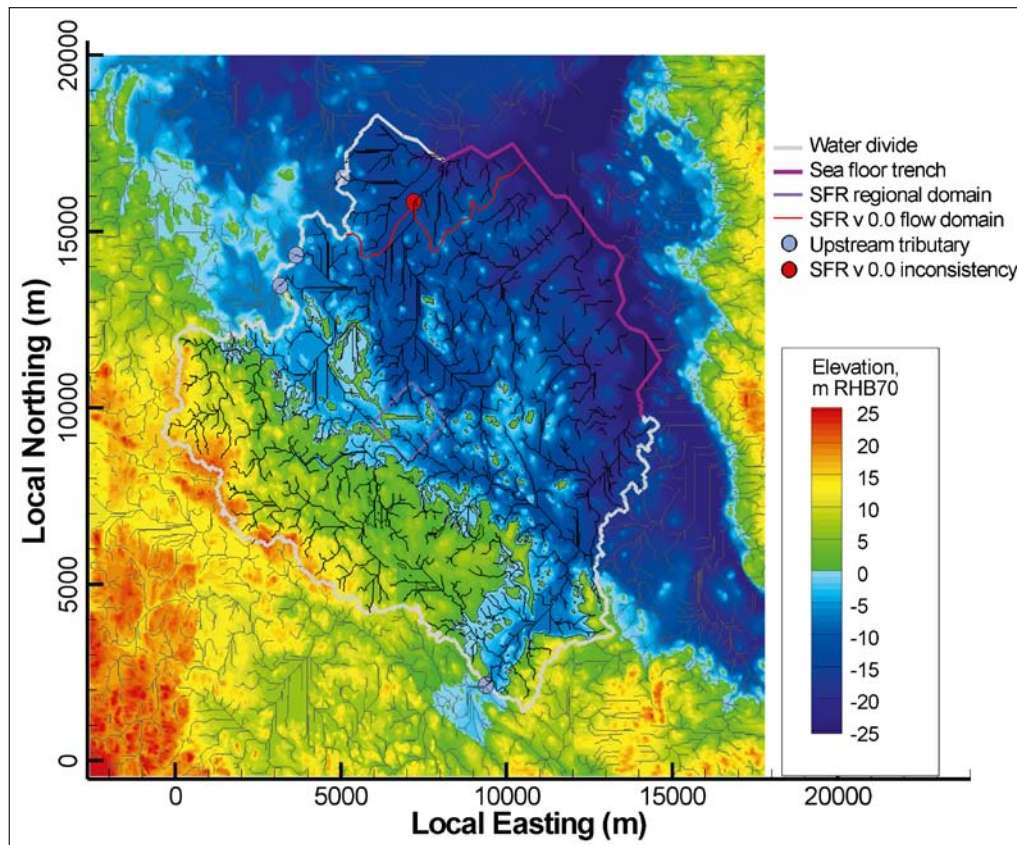


Figure 3-4. Surface river system derived by means of Geographic information system (GIS) analysis. Super-regional flow boundaries defined by water-divides (grey), or, a trench in the sea floor (purple). The flow boundary of SFR v 0.0 (red line) was extended north due to avoid assigning a no-flow boundary across a river system (red marker). Local origo set to Northing = 6692000, Easting = 1626000.

The super-regional flow domain used in this study is actually a sub-catchment area, with four points of inflow from upstream catchments (grey markers; Figure 3-4). In particular, the inflow to Kallrigaffjärden, at the Southern corner of the domain (Figure 3-4) comes from the enormous upstream catchment 42. For a similar situation at Laxemar, it was found that neglecting a large upstream area resulted in an overestimation of flow path lengths from a deep repository, by about 20%, and breakthrough times by about 30% /Holmén 2008/. In the present study, the inflow from upstream catchments is assumed to have a negligible influence on simulated flow paths. The reason for this is the comparatively shallow depths of the SFR candidate layouts are (Section 3.1.2), relatively to the Laxemar deep repository, as it is generally accepted that the shallow flow field is dominated by local topography, while the regional/superregional flow occurs at greater depths.

During review of the SFR v 0.0 model, an inconsistency was identified in the geometrical definition of the super-regional flow domain. This inconsistency is likely to cause errors for simulation times exceeding 5000 AD. As stated above, the lateral no-flow boundaries of the super-regional flow domain must follow either water divides or the seafloor trench. However, the northern domain boundary of the v 0.0 version was accidentally defined along a local water divide between two local sub-catchments (red line in Figure 3-4), which cannot be assumed to be a no-flow boundary. In other words, the sub-catchment north of the red line in Figure 3-4 (catchment #12) is in fact a downstream catchment area, and must therefore be included in the SFR v 0.1 flow domain. This can for example be confirmed by inspection of the river system that discharges from Charlie's lake. In the SFR v 0.0 model, this river system inconsistently terminates against a no-flow boundary (red marker in Figure 3-4), while in the expanded SFR v 0.1 flow domain it discharges into the seafloor trench. The termination of the river in the v 0.0 model occurs at -15 m (RHB 70), which implies that the SFR v. 0.0 flow domain is inconsistent for simulation times after 5000 AD. In order to ensure connection to the sea for simulation times after 5000 AD, the SFR v. 0.1 super-regional flow domain was therefore expanded north by including half of catchment #12 (Figure 3-4).

3.2.4 Basin-fill and lakes

Preliminary simulations demonstrated that deep lakes can inflict numerical errors in the flow solution of DarcyTools. The reason is that the seafloor is a hard-coded discharge boundary of the numeric model (Section 4.3), and with the retreating shoreline, owing to land lift (Section 4.3.1), the definition of this boundary changes transiently. Therefore, DarcyTools uses an in-built algorithm that to identify which computational cells are in contact with the sea for any given time, or more precisely, for any given sea level displacement relative to the present day's sea level. The relation of sea level displacement with time is shown in Figure 4-4b. Based on this relative sea level displacement to topography (both levels defined in RHB70), the inbuilt DarcyTools-algorithm identifies all computational cells in contact with the seafloor and assigns prescribed head equal to sea level. The criteria for identifying the discharge boundary are that computational cells: 1) belong to the top layer of the grid, and 2) has a cell centre located below the relative sea-level. Unfortunately, this implies that local topographical depressions that are isolated from the sea (i.e. the bottom of a deep lake) can be mistaken for seafloor (Figure 3-5a). The implication of this is that lakes are erroneously prescribed sea-level head, instead of its actual lake level. In other words, it produces an erroneous flow solution, as the head values of such lakes are erroneous and conservation of mass is lost.

This was circumvented by constructing the computational mesh in DarcyTools based on a basin-filled DEM (Figure 3-5b). The basin-fill algorithm levels out all inland depressions, and thus, ensures that no inland computational cells are below sea level and can be mistaken for the seafloor. On the order of thousand years, shallow lakes are expected to choke-up by sedimentation and vegetation and transform into bogs /Holmén and Stigsson 2001, Brydsten 2006/. However, lakes function as essential connectors between different segments of the river system, and simply eliminating lakes from the flow model would be detrimental for the representation of surface runoff. Therefore, geometrical lake objects were defined as the closed volumes between its bathymetry in the original DEM and its maximum water level (Figure 3-5c). Lakes are then mimicked in the flow model by assigning an artificially high hydraulic conductivity to computational cells inside such lake volumes (analogous to the river system, Section 3.2.2). The full set of lake objects are shown in Figure 3-6.

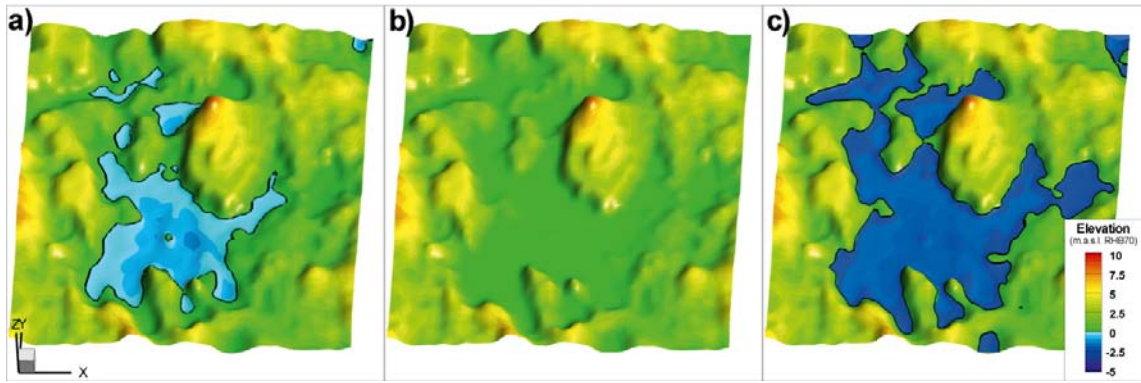


Figure 3-5. Lake Bolundsfjärden is taken as an example to demonstrate topographic basin-filling: a) in the topographical DEM part of its bathymetry is below the current sea level (-1.3 m, RHB70), b) to avoid erroneous association to the sea, the DEM is filled to its basin threshold, $+0.75$ m.a.s.l. RHB70, c) the lake geometry is defined as the volume between the lake bottom and its maximum water level.

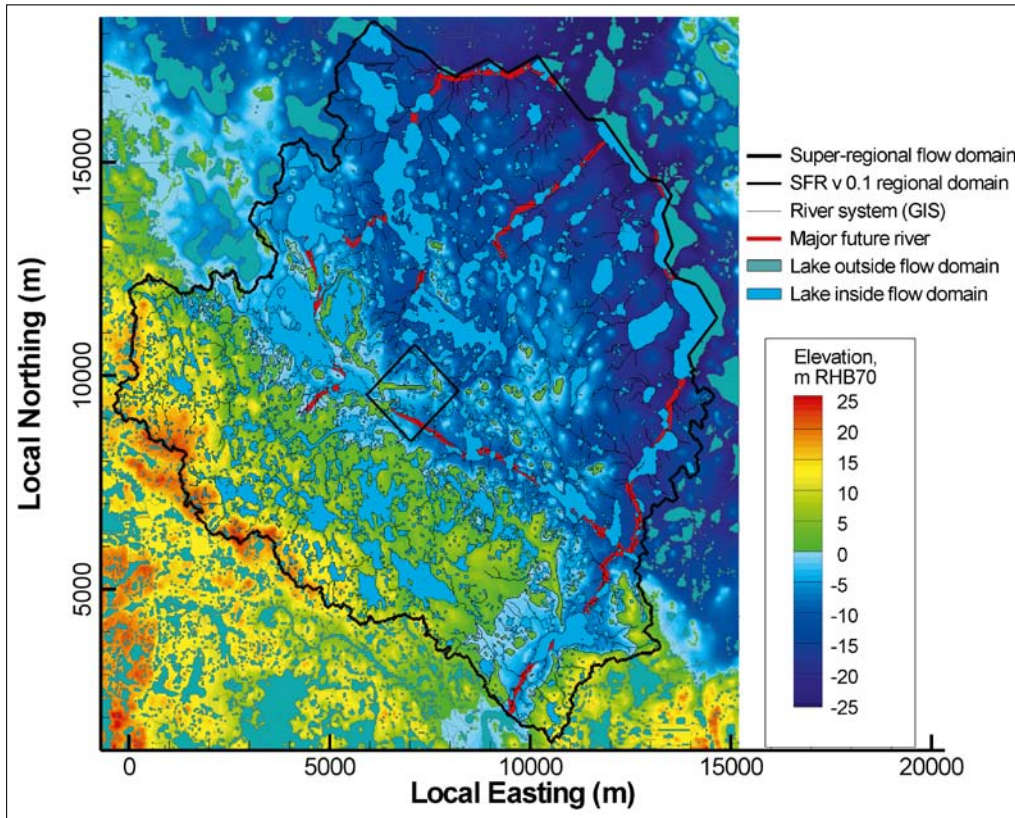


Figure 3-6. Lake objects defined by means of Geographic information system (GIS) analysis and major future rivers, based on /Brydsten 2006/. Note that the lake objects appear overestimated compared to the actual number of lakes in the domain /Strömgren and Brydsten 2008/; however, many lake objects are very shallow (< 1.0 m) and will therefore be eliminated in the grid generation (cf Figure 4-2). Local origo set to Northing = 6692000, Easting = 1626000.

3.2.5 Future river system

The current surface runoff can be calibrated to match lake levels and stream discharge data, whereas the characterization of future river systems based on analysis of seafloor topography is highly uncertain. The reason for this is that over the time it takes for the seabed to rise out of the sea (on the order of thousands years), it is subject to dynamic landscape processes that successively transforms its topography /Brydsten 2006/. This landscape alteration is not a uniform process; wave erosion re-suspends postglacial silt and clay which is re-deposited in sheltered topographical depressions (future lakes) and surface runoff erodes hill slopes and the future rivers may carve deeply into riverbed sediments. The erosion depth in riverbeds depends on material, postglacial clay and silt, as well as glacial clay are easily eroded, while the coarser materials, particularly the bedrock, form bounds for further erosion (Brydsten 2008, personal communication). For example: in sediment profile observations of the seafloor in the Forsmark/SFR area, all postglacial clay has been eroded at depths shallower than 5 m /Brydsten 2006/. This implies that, for example, all postglacial clay found at 15 meters water depth (an average thickness of 1.5 m) can be expected to erode within the next 2,000 years.

The river system has an important role in the flow model, namely draining the ground surface from excess net precipitation to prevent the simulated water table from rising above the ground surface. The altering landscape causes uncertainties in:

1. the route of future rivers (GIS analysis is based on present topography),
2. the riverbed depth (considering runoff erosion and sedimentation), and
3. a reasonable parameterization in fictive conductivity to mimic river flow.

Note that, the fictive conductivity values assigned to the present day's rivers and lakes have been calibrated to match surface water data /Odén 2009/. This calibration provides fictive conductivity values that produce realistic river flows, given the topographical gradient along rivers. However, it is highly uncertain if this parameterization applies also to the future river system, as its relief is highly uncertain. Furthermore, river flow accumulates along its route to the sea, as its upstream catchment area increases. Therefore, the future river system will be more extensive and carry more water compared to the present day's river system. It seems likely that the future river system requires a higher fictive conductivity value, in order to carry this higher flow. A plausible approach could be setting the fictive river conductivity proportional to the flow accumulation of the river (see Section 3.2.2).

In this study, a simple approach was tested in order to explore the significance of the surface runoff parameterisation. A second set of "major future rivers" were defined to explore the impact of riverbed depth and their parameterization (Figure 3-6). These major future rivers are superimposed on top of the existing "minor" river system (e.g. Figure 3-4). These major river systems are intended to represent accumulated flow from large upstream catchments. The geometric routes of these major future rivers are defined with reference to /Brydsten 1999/. In reality, the riverbed depth depends on type and thickness of quaternary deposit material. In this analysis it is set to a constant value of 4.0 m for major rivers, and 1.0 m for "minor" rivers. A river bed depth of 4.0 m seemed reasonable as a first crude estimate, as the average soil depth is 5.6 m within the Site Investigation Forsmark area /Hedenström et al. 2008/, and rivers form along topographical depressions with sediment layers that are deeper than average.

In the present study, the major future river running south-east of the pier is of particular importance. It follows the topographical depression of the Singö zone to a downstream junction at Kallrigafjärden, where it meets another future river from the large catchment 42 south of the super-regional flow domain, and turns north. The characterisation of the Singö river is expected to have large influence on modelled surface runoff south of the pier. In particular, this riverbank depth controls the local effluent groundwater level and in turn, the upstream hydraulic gradients. In other words, the characterisation of this Singö river can be expected to have a large influence on the overall predicted performance of the candidate layouts.

The man-made pier is constructed from blasted rock, the soil type of the natural ridge underlying the pier is till, and the islands east of the pier is bedrock (Figure 3-7); none of these materials are easily eroded. The riverbed of the future Singö river, running South-East from the pier, has a top regolith layer (Z1) of clay and sand (Figure 3-7). Note that the river trajectory is not defined inside the lakes; instead a straight line is drawn between its entry and exit points. The soil type is postglacial clay between 0–3 km river length, postglacial sand between 3–5.9 km, and again postglacial clay

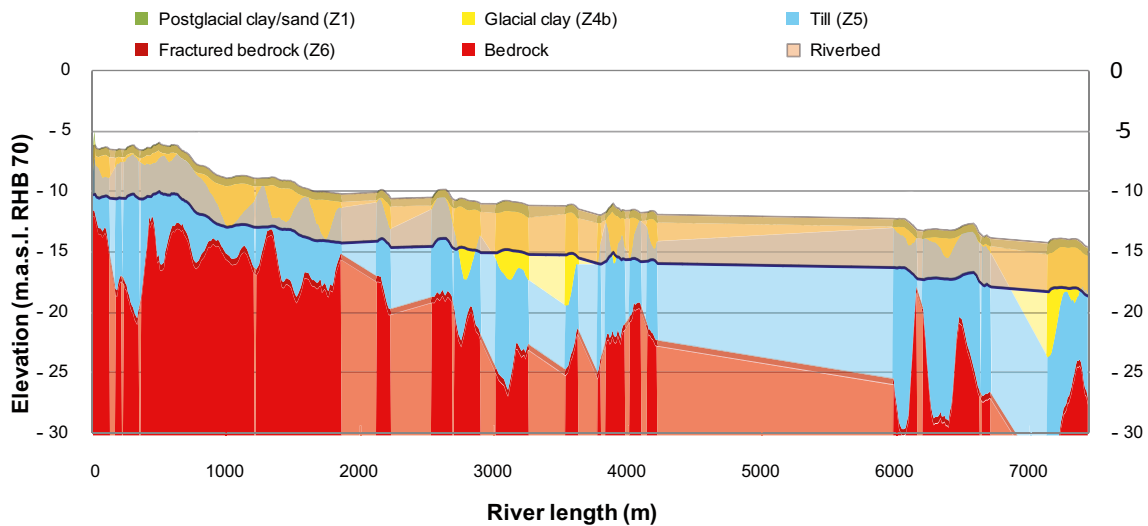


Figure 3-8. Vertical cross-section of the quaternary deposits along the future river running south-east of the pier, which has been assumed to be 4 m deep. The quaternary deposit layers have been approximated from the regolith depth model /Hedenström et al. 2008/ by krieging. Note that the river trajectory is undefined inside lakes (see Figure 3-7), and therefore regolith layers have been linearly interpolated between its entry and exit points of lakes (translucent colours).

3.3 Subsurface hydrogeology

The flow model is composed of the three conceptual hydraulic domains, HSD, HRD and HCD (Figure 3-9). The conductivity parameterisation of these sub domains is described in Section 4.2.

3.3.1 Hydraulic soil domain (HSD)

The HSD is geometrically defined by the regolith depth model /Hedenström et al. 2008/, which provides the geometrical definition of six layers of quaternary deposits (Z1–Z6) and three sediment lenses inside lake basins (L1–L3). The top layer, Z1, should be linked to the geological soil type map. These layers and lenses have been parameterised hydraulically and calibrated against point-water head measurements by means of Mike-SHE flow modelling /Bosson et al. 2008/, as summarized by /Follin et al. 2008/.

In the current model the HSD is geometrically defined as a constant thickness of 20 m, which is common practise in DarcyTools modelling.

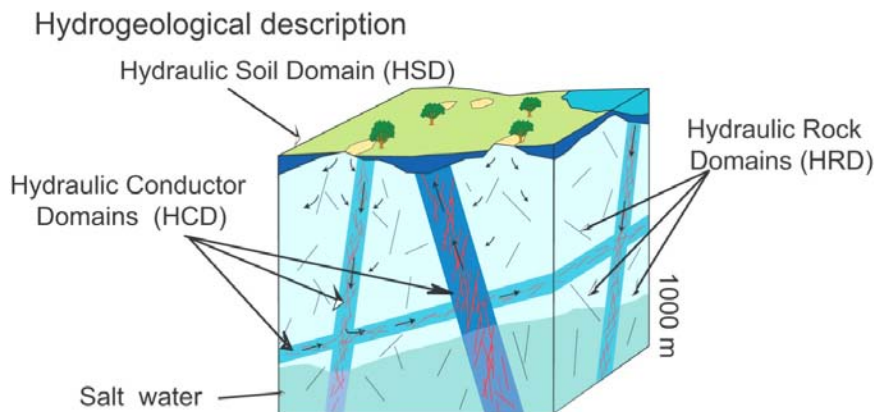


Figure 3-9. The hydraulic sub domains of a hydrogeological model; taken from /Rhen et al. 2003/.

3.3.2 Hydraulic conductor domain (HCD)

The HCDs are geometrically modelled as a central plane with a perpendicular width. The central plane is defined by a triangulated mesh with its local properties, such as thickness, transmissivity, porosity, and storativity, specified constants that may vary from one triangle to another. This is the DarcyTools format for “deterministic fractures”, after conversion from their original definition in RVS. Inside the super-regional flow domain the geometrical HCD definition is taken from the deformation zone model SDM-site v 2.2 of the Forsmark Site Investigation /Stephens et al. 2007/, and the hydraulic parameterisation is taken from /Follin et al. 2008/. Inside the regional and local model domains the geometrical HCD definition is taken from the geologic SFR v 0.1 model /Curtis et al. 2009/, with hydraulic parameterisation according to /Öhman and Follin 2010/. The merging of the two geologic models is demonstrated in Appendix B.

The sheet joints are not included in neither of the geological models. Instead, both their geometric and hydraulic parameterisation is taken from /Follin et al. 2008/. It should also be noted that the sheet joints extends across the interface between the SFR regional and super-regional domains (Figure 3-10). Therefore, the sheet joints must not be considered in the merging process of HCD models, described below, but instead they are superimposed afterwards.

The two geologic models are merged into a single HCD model. This is done in the following steps (see details in Appendix B):

1. Any part of the HCDs in the SDM-site v 2.2 of the Forsmark Site Investigation that enter the SFR regional domain v 0.1 are cut away (see Figure 3-10). This procedure requires re-meshing along the intersection line between the HCD and the regional model volume (as shown in detail in Appendix B).
2. The removed parts HCDs are replaced with definitions according to the SFR geologic model v 0.1 /Curtis et al. 2009/.
3. The agreement in HCD geometry at the domain boundary is evaluated. Inconsistencies are listed in Table 3-1, and demonstrated in Appendix D.

Table 3-1. Geometric HCD inconsistencies between geologic models PFM2.2¹ and SFR 0.1²

| HCD | Comments | Action |
|------------|--|---|
| ZFM871 | Large discrepancy between models | Replaced by separate RVS definition of ZFM871 |
| ZFMNNE0725 | Does not enter the SFR regional domain in PFM2.2, but included in the SFR model. | None |
| ZFMNNE0869 | Extends across domain boundaries in PFM2.2, but strictly inside SFR regional domain, in the SFR model. | PFM2.2 definition replaced by SFR0.1 |
| ZFMWNW0809 | The PFM2.2 definition crosses corner of SFR regional domain, but excluded in SFR 0.1. | PFM2.2 definition retained inside SFR regional domain 0.1 |
| ZFMNNE0808 | The PFM2.2 definition crosses corner of SFR regional domain, but excluded in SFR 0.1. | PFM2.2 definition retained inside SFR regional domain 0.1 |
| ZFMENE0060 | The PFM2.2 definition crosses corner of SFR regional domain 0.1, but excluded in SFR 0.1. | PFM2.2 definition retained inside SFR regional domain 0.1 |
| ZFMWNW1127 | The PFM2.2 definition crosses the SFR regional domain; replaced by ZFMWNW0001 and ZFMWNW0804 in SFR 0.1. | None |
| ZFMENE1057 | The PFM2.2 definition strictly inside SFR regional domain 0.1; removed in SFR 0.1. | PFM2.2 definition removed |
| ZFMWNW0001 | Unconnected across the domain boundaries. | None |
| ZFMWNW0813 | Unconnected across the domain boundaries. | None |
| ZFMWNW0835 | Unconnected across the domain boundaries. | None |
| ZFMWNW0836 | Unconnected across the domain boundaries. | None |
| ZFMWNW1056 | Unconnected across the domain boundaries. | None |
| ZFMNW0805 | Unconnected across the domain boundaries. | None |

¹ PFM2.2 refers to the geologic model SDM-Site Forsmark /Stephens et al. 2007/

² SFR 0.1 refers to the preliminary SFR geologic model v 0.1 /Curtis et al. 2009/

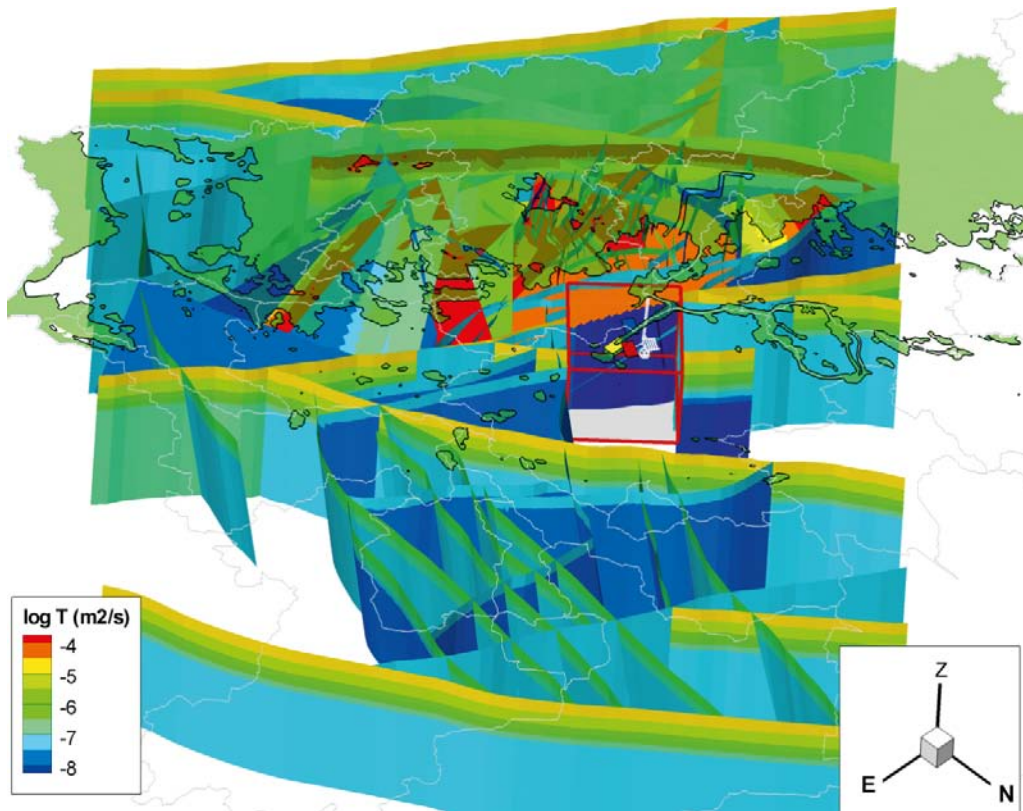


Figure 3-10. HCDs of the SFR super-regional flow domain v 0.1. The HCD geometry is taken from /Stephens et al. 2007/ and the hydraulic parameterization is taken from /Follin et al. 2008/. Any part extending into the SFR regional domain (red box) is removed, with exceptions listed in Table 3-1. Also, note that the sheet joints (orange sheets crossing the regional domain) are not truncated from the regional domain.

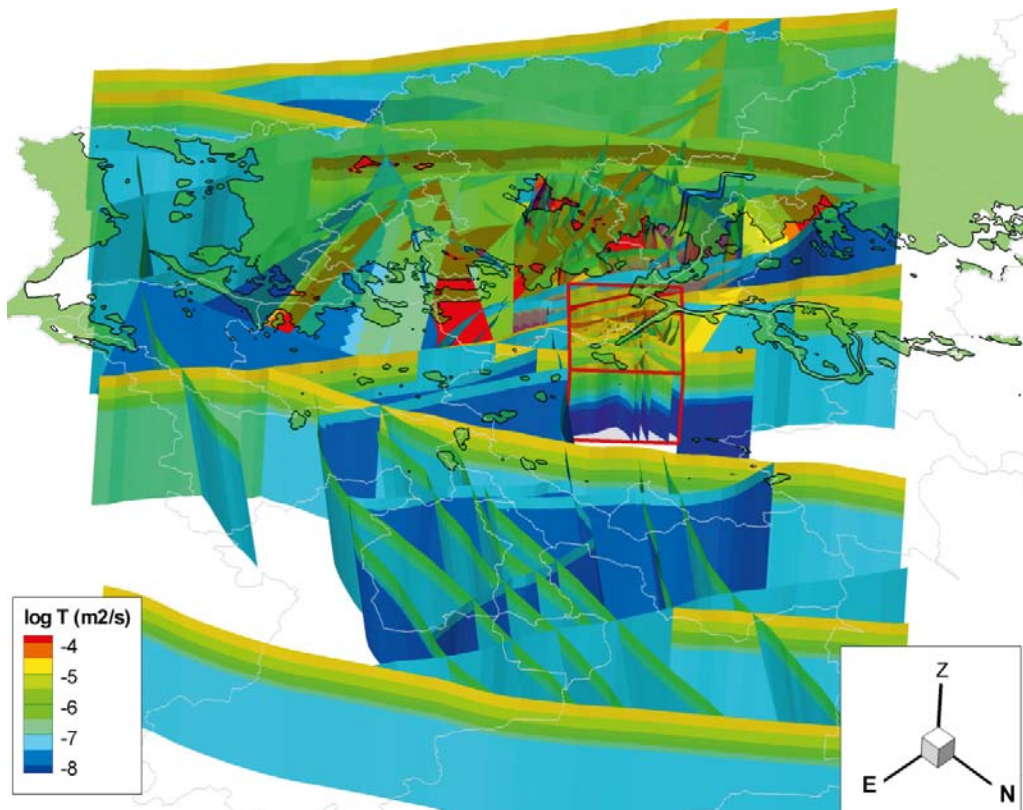


Figure 3-11. HCDs of the SFR regional domain v 0.1 merged with its surrounding super-regional flow domain. The regional SFR HCD geometry is taken from /Curtis et al. 2009/ and the hydraulic parameterization is taken from /Öhman and Follin 2010/.

The SFR v 0.1 geologic model is based on recent lineament data, that were unavailable during the interpretations of /Stephens et al. 2007/. Therefore, geometrical inconsistencies exist between the two models, which results in HCD discontinuities across the interface between domains. All such inconsistencies are listed in Table 3-1, and illustrated in Appendix D. For example, a HCD which has been defined by /Stephens et al. 2007/ in the super-regional flow domain may barely intersect a corner of the regional model. If this HCD is excluded from the SFR v 0.1 geologic model (see Table 3-1), the merging process described above will result in a discontinuity of the HCD. In such cases it was decided to allow exceptions from the method described above, and retain the PFM2.2 definition inside the SFR v 0.1 Regional domain. In order to ensure continuity in ZFM871 (zonH2) across the domain interface, it was decided necessary to remove the zone from both geologic models and use a separate geometric definition, which extends across both domains (see Table 2-1).

3.3.3 Hydraulic rock domain (HRD)

The HRD is geometrically defined as the complement to the HSD and HCD units. In other words, the HRD is the rock volume remaining after the definitions of HSD and HCD. In the current model, the HRD is a single, uniform domain, but in the next model version, SFR v 0.2, the possibility in subdividing the HRD into separate fracture domains, analogous to the SDM-Site Forsmark Site Investigation will be studied.

3.4 Orientation of computational mesh

DarcyTools uses a Cartesian computational grid, which is constrained to alignment with the axes: North, East and Elevation. In many cases this is practical, as it allows grid cell references to, for example: “east of a specified plane”, or “below a certain level”, etc. However, in other situations the inflexible coordinate system may be unfeasible, for example in the calculation of tunnel inflows. Tunnel inflows provide important calibration data for the flow model, but an unfavourably oriented computational mesh versus tunnel orientation and the hydraulic gradient may complicate the calculations of total tunnel inflow /see discussion in Odén 2009/. A mesh that is non-parallel to flow forces the modelled flow into a zigzag pattern between grid cells (i.e. a flow representation decomposed into its vector components), which risks double-counting flow in the calculation of total flow over a tunnel wall. Furthermore, the cell-jump particle tracking method (Section 4.5) requires the mesh to have a parallel orientation to flow in order to avoid excessive numeric dispersion.

This may be particularly important for the flow modelling of SFR, as the tunnels were purposely constructed parallel to the future flow field, with the intent to maximise the performance of the repository. Calibration to unsaturated tunnel inflow is beyond the scope of the current study (Section 2). Nevertheless, it was decided to explore a method to implement grid rotation in DarcyTools. The method used here can be summarized as:

1. All input geometries (all data in Sections 3.1 to 3.3, see complete list in Appendix A) are transformed into a local coordinate system, using Equation (3-1).
2. The computational grid is generated from rotated input geometries (Section 4.1), and flow is solved in the local coordinate system.
3. The flow solution is transformed back into the original coordinate system (RT90 2.5 gon W).

The coordinate transformation was done by the following horizontal rotation,

$$\begin{bmatrix} x' \\ y' \end{bmatrix} = \begin{bmatrix} \cos \alpha & \sin \alpha \\ -\sin \alpha & \cos \alpha \end{bmatrix} \begin{bmatrix} x_p \\ y_p \end{bmatrix} + \begin{bmatrix} x_0 \\ y_0 \end{bmatrix} \quad 3-1$$

where $[x', y']$ is the rotated point in local coordinates, $x_p = \text{Easting} - 1632400.0$, $y_p = \text{Northing} - 6701200.0$, $x_0 = 6400.0$, $y_0 = 9200.0$, and the counter-clockwise rotation angle $\alpha = 32.58817^\circ$. The rotation angle α was calculated based on the SFR tunnel orientation in CAD, and is fairly close to the rotation angle for transformation between the RT90, 2.5 gon W and the T-U coordinate system (39.4118°).

4 Model set up

4.1 Computational grid generation

The computational mesh is set up in a Cartesian system aligned parallel to the disposal tunnels of SFR. The reason for this is to facilitate the flow calculations and subsequent particle tracking (see discussion in Section 3.4). Once a flow solution and particle trajectories have been obtained, the results can then be back-rotated into the original coordinate system (cf Figure 4-1 and Figure 4-2). The grid is unstructured, which means that it is flexible for local refinement, within nested sub domains. For example, the Super-regional domain is coarsely meshed at a 128 m scale, the mesh inside the Regional domain is refined to 16 m scale, and finally the tunnels and disposal facilities are refined to 2 m scale (see Table 4-1). The DarcyTools command “Blur” is used to smoothen the transition in meshing scales across domains. The vertical resolution is set to a maximum of 1.0 m at ground surface, and a blur level of 1. This means that the top 10 m is meshed at a minimum 1.0 m scale, while below 10 m depth the vertical meshing scale grows exponentially, $\Delta z = 1\text{ m}, 2\text{ m}, 4\text{ m}, 8\text{ m}, 16\text{ m}$ (see Figure 4-1). The meshing has a higher resolution in practise. For example the top 20 m are meshed by approximately 45 cells inside the SFR Regional domain (see Figure 5-2). Also the horizontal discretisation is refined at ground surface to 64 m, or, in the presence of lakes or rivers, to 32 m.

In this grid generation, the computational cells are also assigned marker values (e.g. Figure 4-1a). These markers are useful for identifying cells or sub volumes within the computational mesh that have special properties or serve a particular purpose in the flow simulations. The cell markers can for example represent: domains, lakes, rivers, different tunnel sections (e.g. Figure 3-1). The reason for marking these cells is to facilitate later commands that require reference to a subgroup of computational cells, e.g. assigning specific conductivity values (in the DarcyTools file *propgen.f*), or tunnel areas over which inflow should be calculated (in the DarcyTools file *fif.f*), or volumes for particles release (in the DarcyTools file *cif.xml*). The complete file for grid generation is shown in Appendix E.

The candidate layouts are to be assigned a high hydraulic conductivity (10^{-5} m/s ; Section 4.2.1) and their presence entails a locally refined computational mesh (see Table 4-1). Consequently, the introduction of a layout volume implies a disturbance in the modelled flow field. The four candidate layouts are not intended to co-exist; only the layout with best location will be put into effect and will co-exist with the existing SFR. Therefore, in order to evaluate the four alternative layouts independently (i.e. “undisturbed” by other candidate layouts) four separate grids were required; these grids contain the existing SFR tunnel system, co-existing with a candidate layout volume, one at the time. For later comparisons of travel times and particle exit locations, a separate grid with only the existing SFR was also generated.

Table 4-1. Discretisation of the computational grid.

| Domain/feature | | Horizontal isotropic resolution, Δx (m) | Vertical resolution, Δz (m) |
|--|----------|---|-------------------------------------|
| Super-regional flow domain | | 128 | 128 |
| SFR Regional domain | | 16 | 16 |
| Ground surface | Blur = 1 | 64 | 1 |
| Lakes and rivers | | 32 | 1 |
| Tunnels, existing SFR, and candidate layouts | Blur = 2 | 2 | 2 |

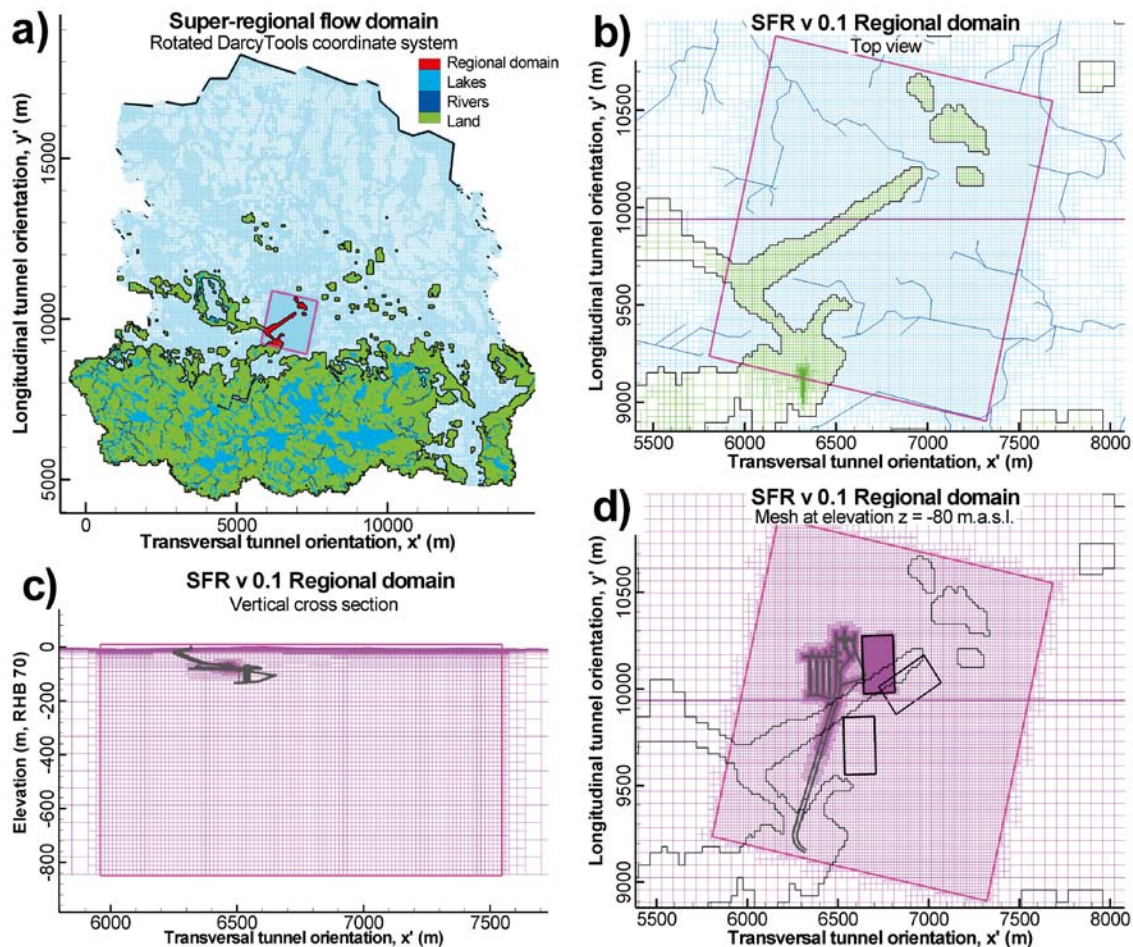


Figure 4-1. Computational grid in DarcyTools set up in a Cartesian coordinate system aligned with repositories of the existing SFR; a) surface hydrology of the super-regional domain, b) close-up of the Regional domain, c) a vertical cross-section of the Regional domain, and d) the Regional domain mesh at an elevation of -80 m.a.s.l.

4.2 Conductivity parameterisation

The computational mesh is composed of the three conceptual hydraulic domains, HSD, HRD and HCD (Section 3.3).

4.2.1 Tunnel system and layouts

The influence of technical barriers on flow at SFR has been modelled by /Holmén and Stigsson 2001/. In the current analysis it was decided to exclude the modelling of technical barriers, such as backfill material, tunnel plugs, etc. The reason for this is that the methodology and material performance criteria for the future sealing of the storage facility have not yet been decided. Until such details have finally been decided it is preferred that the Safety Case is based on highly pessimistic assumptions. Furthermore, the analysis of flow interaction between HCDs and the storage facilities is facilitated, if the tunnel inflow is not hampered by low-permeable flow in tunnels. Therefore, the conductivity of all constructions the tunnel system of the existing SFR, including its storage facilities, and the four candidate layout volumes was set to 10^{-5} m/s, following the specifications of the activity plan. This is the same value as was used in the predictions of the SFR 0.0 model /Odén 2009/.

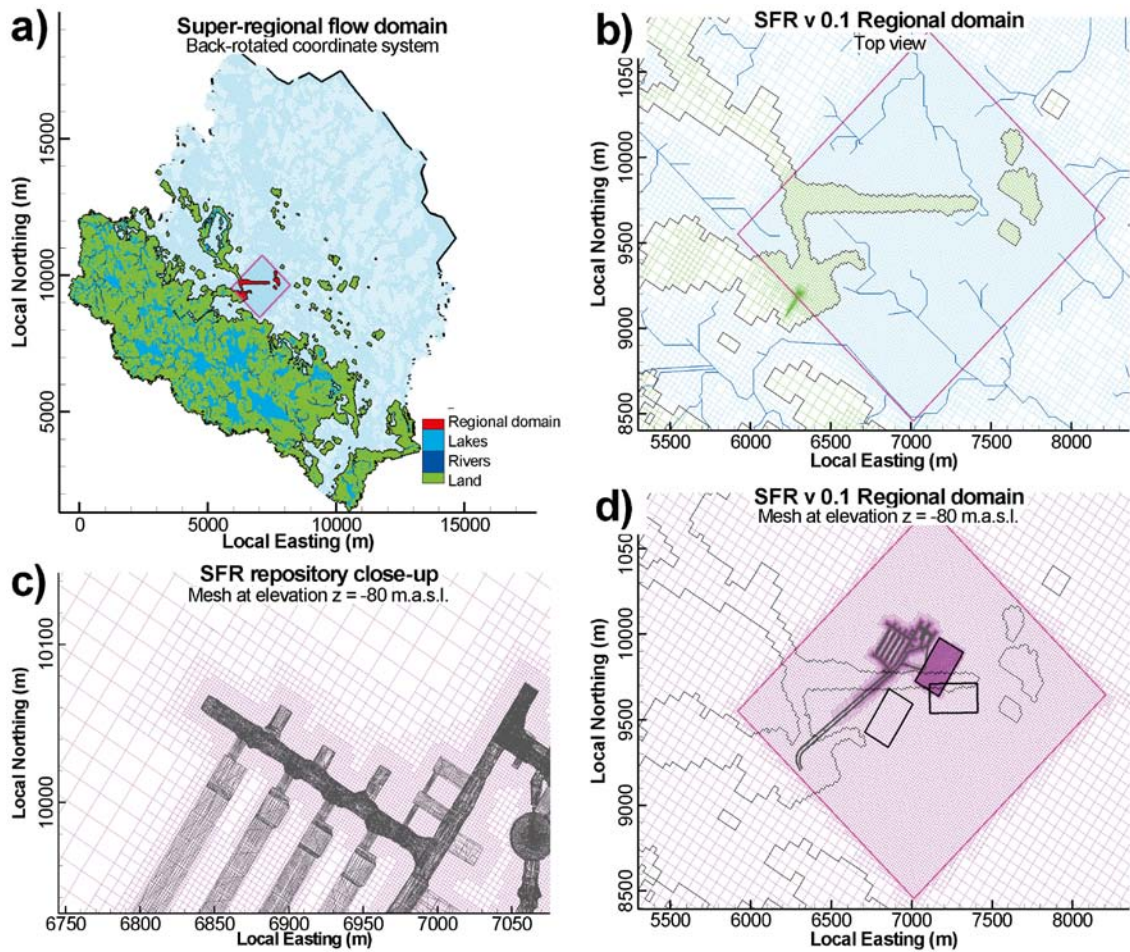


Figure 4-2. The computational mesh rotated back into the RT90 coordinate system; a) super-regional domain, b) close-up of the Regional domain, c) a close-up of the SFR repository, and d) the Regional domain mesh at an elevation of -80 m.a.s.l. including candidate layout 1. Local origo set to Northing = 6692000, Easting = 1626000.

4.2.2 Surface runoff

All surface grid cells that are partly in contact with the minor river system, completely enclosed by lake object volumes, or partly in contact with the future major rivers are assigned fictive horizontal conductivity values to mimic surface runoff. Note that in this contact, minor rivers have a vertical tolerance of ± 1.0 m from the ground surface, while the vertical tolerance for major rivers extends from $+1$ m above ground surface and down to a depth of 4.0 m below ground surface. Minor rivers are assigned a horizontal conductivity of 0.2 m/s /Svensson 2008/ (personal communication). Currently existing lakes are also assigned the same value, since they are part of the calibrated surface system. Future lake objects and all future major river systems are assigned a 100 times larger value: 20 m/s. It should be noted that the low conductivity of lake sediments are not incorporated in the parameterization of lakes. The reason for this is the artificial parameterization of HSD, as explained below.

4.2.3 Hydraulic soil domain (HSD)

In the DarcyTools modelling it is common practice to assign a fictive high horizontal conductivity to the top-layer of the computational grid /Svensson 2004/ (personal communication) (i.e. to arbitrary top-layer cells, excluding river and lake cells). The purpose is to facilitate horizontal flow from an arbitrary top-layer grid cell to its nearest downstream river or lake cell. This high horizontal conductivity value is only active as long as the grid cell is saturated. If the groundwater level should drop below the computational cell, an in-built DarcyTools function decreases the fictive high horizontal

conductivity in order to prevent surface runoff occurring in de-saturated cells. An exponential depth trend model for the top 20 m of the computational grid is used for a gradual transition in conductivity to the underlying HRD. This type of smooth transition is recommended in order to avoid difficulties with numerical convergence /Svensson 2008, personal communication/. The following exponential equation for soil conductivity is assigned to the top 20 m layer of computational cells:

$$K_h(d) = \max (K_{h0} 10^{-d/C}, 10^{-7}); d \leq 20 \text{ m} \quad 4-1$$

where d is the depth below ground surface, C is the depth interval over which conductivity drops one order of magnitude and set to 3 m, K_{h0} is the saturated horizontal conductivity at ground surface, and set to 0.005 m/s. The vertical conductivity is set to a constant 10^{-6} m/s within the top 20 m. All values are taken from /Odén 2009/.

4.2.4 Hydraulic rock domain (HRD)

In the current model version, it was decided to model the HRD with homogeneous hydraulic conductivity (spatially constant). The complete calibration of effective conductivity versus measured tunnel inflows under the present unsaturated condition, see /Follin et al. 2007/, was beyond the scope of the SFR v 0.1 model. Therefore it was decided to rely on previous findings on effective HRD conductivity of SFR. By means of simulating unsaturated tunnel inflow, /Holmén and Stigsson 2001/ calibrated an effective conductivity, K_{eff} , equal to 6.5×10^{-9} m/s, which was associated to a model domain roughly corresponding to the SFR v 0.1 regional domain. Similarly, /Holmén and Stigsson 2001/ calibrated an effective conductivity of 1.5×10^{-8} m/s to a large surrounding flow domain (i.e. roughly corresponding to the SFR v 0.1 super-regional flow domain). These values were also used in the SFR v 0.0 model /Odén 2009/. A probabilistic approach to calibrate the HRD and the HCDs effective conductivity by conditioning tunnel leakage to data was presented by /Holmén 2005/. The upper 25 m of the HRD was assigned a random effective conductivity, ranging from 5×10^{-9} to 5×10^{-7} m/s, while the lower HRD conductivity was defined as one order of magnitude less conductive.

The geometrical difference in flow domains does not pose an obstacle for applying the effective values calibrated by /Holmén and Stigsson 2001/ in the present model. On the other hand, the different levels of detail in the HCD representation between the two models, does form a discrepancy in the distinction between HCD and HRD between the two models, particularly inside the SFR v 0.1 local domain. A larger number of discrete HCD features are resolved in the current model, which, in a strict sense, makes its HRD definition incongruent to that of /Holmén and Stigsson 2001/. Therefore, it is not straightforward that it is appropriate to use the same HRD parameterization.

It was nevertheless decided to use the effective conductivity values of /Holmén and Stigsson 2001/ as effective HRD values for the regional, respectively, super-regional domains. The reason for this is that, without actually undertaking the time consuming calibration process for unsaturated tunnel inflow of the current model, the /Holmén and Stigsson 2001/ values are considered to be reasonable estimates of effective conductivity on tunnel-inflow scale for the current modelling stage. No potential depth dependency was considered in the HRD conductivity, see discussion in /Öhman and Follin 2010/.

4.2.5 Hydraulic conductor domain (HCD)

HCD conductivity is calculated from width and transmissivity which is imposed onto the computational mesh proportionally to the fraction of grid cell volume inside the HCD, /Svensson et al. 2007/. The HCD widths are taken from /Curtis et al. 2009/, while the transmissivity is taken from /Öhman and Follin 2010/.

However, in retrospect an error was found in the implementation of depth trend. The intention was to use the same logarithmic slope, $k_T = 232$ m, as used by /Follin et al. 2008/ (i.e. depth over which transmissivity changes an order of magnitude). Instead, k_T was accidentally set to 534 m, which corresponds to lower estimations of effective T_0 at ground surface and a weaker transmissivity decline with depth. Note however, that at an approximate depth of 100 m, which is the depth of the existing SFR facility, the error in HCD parameterisation is negligible. This is not a coincidence; the reason for this is that most underlying data (HCD intercepts) are available close to the present SFR facility, and T_0 was calculated by depth-trend extrapolation to ground surface, see /Öhman and Follin 2010/.

Table 4-2. HCD parameterisation.

| HCD ¹⁾ | Alias | Count of T ₀ | Used in v 0.0, log T ₀ ²⁾ | Parameterised, log T ₀ ³⁾ | Implemented in v 0.1, log T ₀ ⁴⁾ |
|-------------------------------------|-------|-------------------------|---|---|--|
| zfm871 | H2 | 15 | -5.8 | -4.5 | -5.0 |
| zfmnw0805 | Zon8 | 8 | -5.4 | -4.9 | -5.4 |
| zfmne0870 | Zon9 | 5 | -7.7 | -5.6 | -4.5 |
| zfmne0869 | Zon3 | 5 | -4.7 | -4.0 | -4.5 |
| zfmwnw0001 | Singö | 2 | -3.3 | -3.6 | -4.3 |
| zfmnw1035 | - | 3 | | -3.3 | -4.4 |
| zfmwnw0804 | - | 2 | | -3.8 | -4.9 |
| zfmnnw0999 | - | 2 | | -6.0 | -6.1 |
| zfmnnw1209 | Zon6 | 2 | -5.7 | -5.1 | -5.0 |
| zfmwnw0813 | - | 1 | | -2.9 | -3.5 |
| zfmwnw3262 | - | 1 | | -4.6 | -5.9 |
| zfmwnw2496 | - | 1 | | -4.2 | -4.6 |
| zfmwnw3259 | - | 1 | | -4.2 | -4.6 |
| zfmne2308 | - | 1 | | -5.4 | -4.6 |
| Generic HCDs (random population) | | 50 | | -5.1 | -4.6 |

¹⁾ Geological and geometrical definition, including HCD thickness /Curtis et al. 2009/

²⁾ Derived from parameterisation by /Axelsson and Mærsk Hansen 1997/, calibrated by /Holmén and Stigsson 2001/, and also used by /Odén 2009/.

³⁾ HCD parameterisation based on re-evaluation of existing SFR data in the context of the updated structural model /Öhman and Follin 2010/. These recommended values were intended to be implemented in the current study (i.e. based on Continuum approach, and max fraction outside HCD = 0.5).

⁴⁾ Actual values implemented in this numerical implementation, owing to an error in the logarithmic slope of the depth trend.

In other words, HCD transmissivity is conditioned at the depths of HCD intercepts, and therefore the error takes on its minimum at approximately 100 m depth. Although, this error is annoying and regrettable, its consequences are expected to be small in relation to the overall uncertainty: the present predictions 1) are made with an uncalibrated flow model, 2) uses a strongly simplified representation of future topography, and 3) there exists large uncertainties in the parameterisation of HCDs, see discussion in /Öhman and Follin 2010/.

In the translation from HCD transmissivity to cell conductivity, the HCD conductivity does not necessarily exceed the HRD. In fact some of the HCDs inside the Super-regional domain translate into cell conductivities below the HRD value (Figure 4-3a). This occurs for low HCD transmissivity (Figure 3-10) which are discretised with coarser cell size than its actual HCD width. In these cases, the cell conductivity is increased to its HRD value.

There are seven HCDs defined inside the SFR Regional domain that terminate against the interface between the Regional and Super-regional domains (black ovals; Figure 4-3b). The reason for this is that these lineament data are based on surface lineaments /Curtis et al. 2009/ that were unavailable at the time when the HCDs of the Super-regional domain were defined /Stephens et al. 2007/. This is expected to restrain for particle transport outside of the Regional domain. The south-western part of the SFR Regional domain contains three highly transmissive sheet joints (orange/yellow area; Figure 4-3b) that terminate against the Singö deformation zone. Inside the SFR Regional domain these sheet joints are resolved as three discrete features, but the coarse discretisation of the Super-regional domain blends them into a single conductive volume (Figure 4-3c).

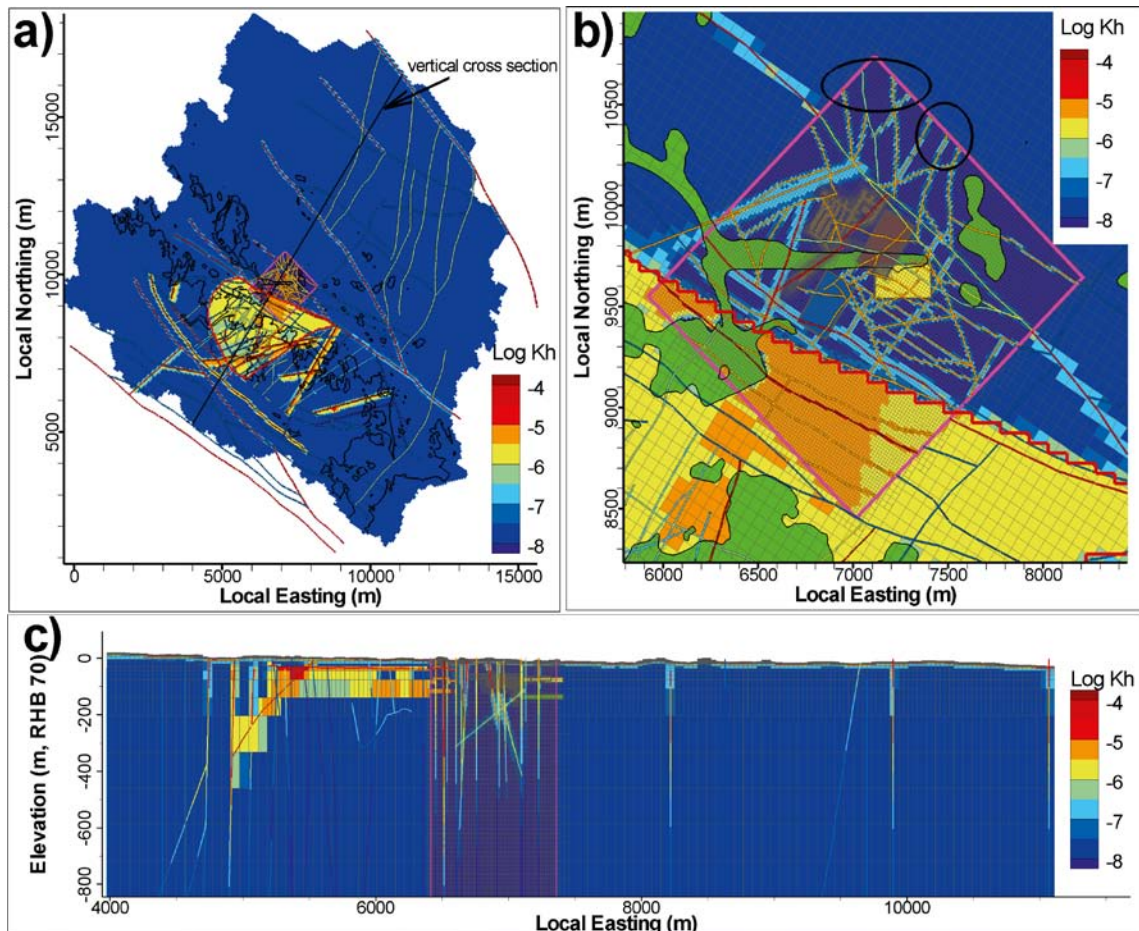


Figure 4-3. The conductivity field in a horizontal plane at elevation $z = -80$ m.a.s.l. (RHB 70); a) super-regional domain, b) close-up of the Regional domain, and c) a vertical cross section. The conductivity field of the computational mesh is overlain the intersection of the HCD transmissivity model (Figure 3-11) at $z = -80$ m.a.s.l. (RHB 70). Note that the logarithmic colour scale refers both to horizontal conductivity and transmissivity. Local origo set to Northing = 6692000, Easting = 1626000.

4.3 Boundary conditions

There are three types of boundary conditions assigned to the super-regional flow domain (Table 4-3). All computational cells located within the top layer of the grid and above sea level are assigned prescribed flux, which is set equal to the net precipitation. The net precipitation of the area is approximately 150 mm/year /Johansson and Öhman 2008/, and translates to the DarcyTools input parameter <pme> equal to 4.7×10^{-9} /Svensson et al. 2007/ (see Appendix F).

All vertical sides, and also to the bottom of the super-regional domain, correspond to the no-flow condition. In effect this simply means that no cells exist outside the Super-regional domain, and therefore no exchange of mass can take place across these boundaries. The no-flow condition constrains the orientation of simulated flow to be parallel to the boundaries (as the flow vector component normal to the no-flow boundary is set to zero by definition). Therefore it is imperative to: 1) use a large flow domain with no-flow boundaries located far from the region of interest (cf. Super-regional flow domain and Regional domain, Figure 3-3), and 2) to define no-flow boundaries with respect to catchment areas (see Section 3.2).

The seafloor grid cells are assigned a prescribed head condition in terms of dynamic pressure, P_{dyn} , which is calculated as the excessive pressure of the overlying Baltic, relative to the modelled freshwater

$$P_{dyn} = \rho_{sea} gh - \rho_{fresh} gz \quad 4-2$$

Table 4-3. Summary of boundary conditions.

| Flow boundary | Assigned to | Condition | Value |
|---------------------------------------|---|-----------------------|--|
| Net precipitation ¹⁾ | Top layer of gridcells, located above sealevel | prescribed flux | 150 mm/yr, or $\langle pme \rangle = 4.7E-9$ |
| Water divide ²⁾ | Vertical sides of super-regional domain | No-flow ³⁾ | – |
| Low-permeable deep rock ⁴⁾ | Bottom of super-regional domain (z = –850 m.a.s.l.) | No-flow | – |
| Sea discharge | Top layer of gridcells, located below sealevel, depending on land lift (Figure 4-4) | prescribed head | Depending on depth, eq (4-2) |

¹⁾ Net precipitation defined as precipitation – evotranspiration.

²⁾ Definitions of water divides taken from established future catchments /SKB 2008/. In order to maintain a reasonable size of the flow domain, a few upstream catchments were excluded, see Figure 3-4.

³⁾ Inflow from upstream catchments neglected, see Figure 3-4.

⁴⁾ Lower model boundary taken from /SKB 2008/.

where ρ_{sea} is the density of the overlying Baltic, g is the constant of gravitational acceleration, and h is the depth below sea level (i.e. height of overburden saltwater column), and z is elevation (RHB 70). Two different values for Baltic seawater density were tested for the seafloor boundary condition:

1. Brackish water density ($\rho_{sea} = 1,004 \text{ kg/m}^3$)
2. Fresh water density ($\rho_{sea} = 1,000 \text{ kg/m}^3$, for model consistency, as groundwater flow is assumed to be freshwater)

The first option corresponds to the actual density of the Baltic, and is the default value for modelling the seafloor boundary in DarcyTools /Svensson, personal communication/. In the current study, it has been assumed that impact of variable density on flow is negligible, such that the groundwater flow can be modelled as freshwater (Section 2). Unfortunately, the use of a saltwater boundary condition in a freshwater model causes a numerical inconsistency (see Appendix C). This inconsistency can be described as an everlasting density-driven saltwater intrusion, which cannot reach steady state without incorporating variable fluid density in the flow solution.

Therefore, the second option was used instead; the density of the Baltic was set equal to the density of the simulated groundwater. This reduces eq. (4-2) to $P = \rho_{fresh} g z_{sea}$, where z_{sea} is the elevation of the sea (RHB 70), and as a result, it eliminates all density driven gradients along the seafloor (see Appendix C). It may seem odd to use fresh water density in the calculation of excessive saltwater head at the seafloor boundary, but in reality this approach translates to the assumption of low density differences below the sea. This is a realistic assumption, since salt-water intrusion (which is a neglected process in the current model setup) tends to level out the density differences below sea. Which of the values, 1,000 or 1,004 kg/m^3 , is used for ρ_{sea} is of less importance. It is more important that to acknowledge the fact that both fluid densities, the groundwater and the overlying Baltic, will have approximately the same density at the discharge boundary to the sea. Furthermore, the shallow bay of Öregrundsgrepen can be expected to have lower density than in the proper Baltic (1,004 kg/m^3), and to continue decreasing over time with the retreating shoreline.

4.3.1 Land lift

The future flow field in the SFR domain will change significantly owing to the land lift, which has been demonstrated in previous analysis e.g. /Holmén and Stigsson 2001/. The slow, uniform, upward-directed flow regime of the currently undersea repository will within a few thousand years develop into to an inland repository with a horizontal flow field that is controlled by local deviation in topography. The land lift is not uniform across the Forsmark domain, which causes a slow large-scale tilt; on the time scale of 10,000 years the tilt of the super-regional model is about 1 m (Brydsten 2008, personal communication). With respect to other uncertainties in the current model version, the effects of tilting were considered negligible. The land lift within the model domain is modelled as vertical displacement, according to equations by /Pässe 2001/ and /Hedenström and Risberg 2003/ (Figure 4-4).

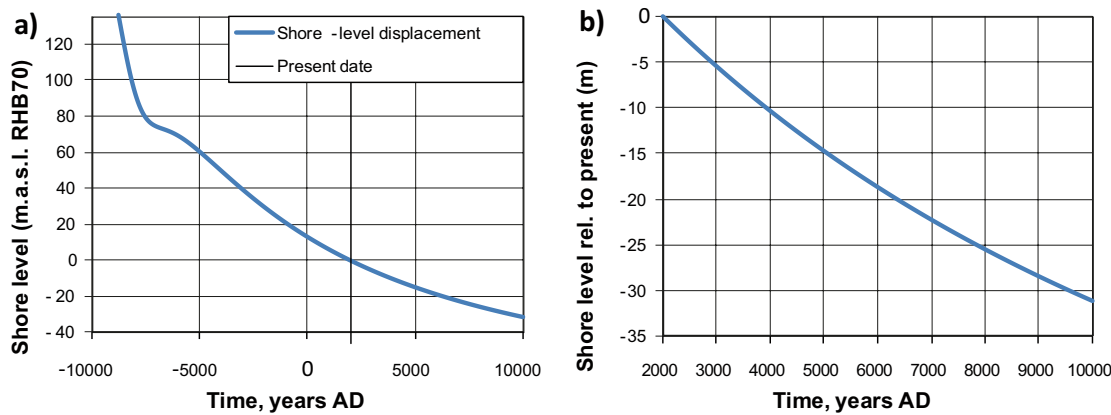


Figure 4-4. Predicted land lift for the Forsmark area (based on equations by /Påsse 2001/ and /Hedenström and Risberg 2003/).

Table 4-4. Parameters used for the Forsmark area.

| Parameter | As m | Bs Year ⁻¹ | Af | Bf | Tf | E m | U m |
|-----------|---------|--------------------------|----|-------|--------|---------|----------|
| Value | 270.4 | 7,230 | 93 | 1,000 | 11,600 | -2.2923 | -33.7133 |

This is numerically implemented in DarcyTools by vertically lowering of the sea level relative to the present days date (Figure 4-4b), which is specified in the DarcyTools input file fif.f. In order to reduce computational time, the land lift is not modelled transient (i.e. continuously), but by solving steady state flow fields for three specific time steps: 2000 AD, 3000 AD, and 5000 AD. One additional simulation is done for 6000 AD, in order to examine if the change flow field is small enough to assume a stationary flow field thereafter – independent of subsequent land lift.

4.3.2 Future climate

Over the time scales considered in the land lift scenarios, the climate will change from its present condition. A warm period owing to solar forcing and greenhouse gas emissions has been modelled for the nearest thousands of years /Kjellström et al. 2009/, resulting in a net precipitation twice as high as currently. During this warm period the sea levels are expected to rise owing to the thermal expansion of sea water and melting of the Greenland ice sheet and the West Antarctic ice shelves. The magnitude of this sea-level rise is highly uncertain, but 7–14 m was used as an upper bound. Even with the current net precipitation, the SFR area is considered to be a saturated recharge area, and therefore additional precipitation is expected to result in surface runoff. An increase in surface runoff would therefore have no direct influence on groundwater flow, but rather in terms of landscape dynamic processes, such as erosion and sedimentation rates. The rising sea levels are not expected to be detrimental for SFR performance, as it is currently subject to an undersea flow regime. Instead, rising sea-levels could be interpreted as a delay in the transition of SFR from its current undersea flow regime to its future inland flow regime, driven by land lift (4.3.1).

The warm period will be superseded by a period of permafrost and, eventually, the next glaciation cycle. These cold periods are expected to impose radically different hydraulic conditions for the SFR repositories. However, they are not expected to occur within the time span considered in this study (i.e. not before 10,000 AD).

Future climate scenarios are not considered in this study. The current net precipitation is used (Table 4-3) and the relation between land lift relative sea-level is calculated according to Section 4.3.1.

4.4 Flow simulations

Steady state flow fields were solved for the stage of land-lift at 2000 AD, 3000 AD, and 5000 AD. A separate model case was solved for 5000 AD, where future major rivers have been implemented (see Section 3.2.5). For each land-lift scenario, five different configurations of repositories are compared: the existing SFR alone, versus the existing SFR and either of the four candidate volumes. All in all, the array of four land-lift scenarios, each with five different layout configurations, results in 20 different model setups, for which steady state flow is solved. The actual simulation time ranges from a couple of days for the 2000 AD cases, up to 3–4 weeks for the 5000 AD scenario with major future rivers.

One objective in this study is to examine if the pier is acting as an important water divide between sub catchments 28 and 32 (see Section 2). It was originally planned that the influence of the man-made pier on the water divide should be evaluated by comparing the flow solutions of two cases of topography input:

1. The pier is included in the flow model, as defined in the DEM, and
2. Any part of the pier exceeding an elevation of $z = -1.0$ m (RHB 70) is removed from the flow model (numerically implemented by constraining the DEM locally so as not to exceed $z = -1.0$ m).

However, during the course of this study, it was found that the flow solution is more sensitive to the parameterisation of the HSD and surface runoff than it is to the topographical representation of the pier. It was therefore decided to address this question by argumentation, and to focus more attention to the representation of surface runoff instead.

4.5 Particle tracking

Particle tracking is performed in steady state flow solutions. A released particle represents an inert water parcel, and its downstream particle trajectories represent alternative flow paths. Thus, important processes to transport modelling of chemical compounds, such as longitudinal dispersion, sorption, matrix diffusion, chemical reactions, etc. are not considered here.

DarcyTools provides two alternative particle algorithms: 1) the vector method for porous media, and 2) the complete-mixing cell-jump method which /Svensson et al. 2007/. The former is the classical method to trace deterministic trajectories, which strictly follow the locally variable flow vector field. The method is deterministic in the sense that if two particles released at the same point, they will also exit at the same predestined location. The continuous adaptation to the local flow field in this method relies on the assumption that the flow field is differentiable in space. Thus, strictly speaking, this method applies only to porous media and not to the ECPM-type of conductivity field that is used in DarcyTools. A technical difficulty with this method is how to control the vector updating in a highly heterogeneous flow field with regards to resolution in space and time.

In the latter method, particle motion is constrained to the actual flow solution, namely the flow vector components. It is therefore fully compatible with the DarcyTools ECPM concept, and consistent in its continuum approximation of the medium. In this method, particle motion is modelled in terms discrete jumps from its current location in a given cell centre to any of its adjacent downstream cell centres; which of these downstream cells is randomly chosen proportionally to the flux in that direction. Conceptually, the cell centres can be interpreted as junctions between fracture network paths, at which complete mixing occurs; the fracture network flow between cell centres are available from the DarcyTools flow solution under its assumption of a valid continuum approximation. In contrary to the former method, this method includes a random component; particles released at a single point randomly take different routes at each cell centre, with a probability proportional to relative downstream inter-cellular flux.

The drawback of this method is that, since its particle trajectories are constrained to the flow vector components, an inappropriate discretisation of the computational mesh forces particles into a zigzag pattern between grid cells, which results in an excessive numeric dispersion transversally. For example, consider a Cartesian grid where the hydraulic gradient is oriented 45° versus the mesh. In this grid the particles are prevented from following the gradient, but instead they are re-directed at each cell centre, which results in an artificial spreading of the plume. This artefact can be reduced by rotations of the computational mesh with consideration to the flow field (see Section 3.4). It should also be noted that this artefact is evident for porous media, but less obvious in fractured media. The reason is that fracture flow does not always follow the global hydraulic gradient, but is constrained to geometry of the connected fracture network.

In reality, the fracture flow at fracture junctions is best described as channelized, with a certain degree of mixing. Thus, the truth lies somewhere between the two particle-tracking algorithms. The vector method is conservative in terms of simulated concentrations and transit time, as it represents high channelling, while the cell-jump method is conservative in terms of simulated exit locations, as it tends to exaggerate the transversal dispersion. In this study, the latter was selected, as one of the objectives is to study possible exit locations.

Approximately 35,000 particles are released with a uniform distribution inside each disposal volume of the existing SFR and one of the candidate volumes, and traced downstream to the discharge boundary.

5 Results

5.1 Flow simulations

One objective in this study is to examine if the pier is acting as an important water divide between sub catchments 28 and 32 (see Chapter 2). It was originally planned that the influence of the man-made pier on the water divide should be evaluated by comparing the flow solutions of two cases of topography input:

1. The pier is included in the flow model, as defined in the DEM, and
2. Any part of the pier exceeding an elevation of $z = -1.0$ m (RHB 70) is removed from the flow model (numerically implemented by constraining the DEM locally so as not to exceed $z = -1.0$ m).

However, during the course of this study, it was found that the flow solution is more sensitive to the parameterisation of surface runoff than it is to the topographical representation of the pier. It was therefore decided to address this question by argumentation, and to focus more attention to the representation of surface runoff instead.

5.1.1 2000 AD

At the present stage of land lift (2000 AD), it is only the man-made part of the pier that extends above sea level and constitutes the possibly basis for a water divide. Thus, the question to if the pier acts as a water divide currently depends solely on its ability to hold a groundwater potential above sea level. In other words it is a question which depends on material property, and cannot be evaluated by simple comparing the two topographical representations suggested above.

The preliminary flow simulations in this section demonstrate how sensitive the SFR flow model is to the HSD parameterisation and surface run-off (see discussions below). During the course of this study it was realised that the HSD parameterisation must be significantly improved in order to analyse the effect of the pier in a realistic way, i.e. testing different material properties and topographies, as opposed to the currently used fictional HSD model (Section 4.2.3). At this early modelling stage, it was decided to focus more on the identification of technical modelling difficulties than on the actual model results. These difficulties must be solved for later flow model versions.

5.1.2 3000 AD

In 3000 AD the shoreline will have retreated to -5.65 m (RHB 70) and the man-made pier will be located on top of a ridge with an elevation of 5 m till (Figure 5-1). The soil type in this underlying ridge is till (Figure 3-7). In this scenario the topographical removal of the man-made part of the pier could potentially address its significance for acting as a water divide. However, the groundwater level inside the underlying ridge is low and does not follow the topography (Figure 5-1). It is therefore very unlikely that a simulation case with topographic removal of the man-made pier would provide any response on the solved groundwater table, at least not with the current HSD parameterisation.

The HSD is modelled as an artificially high horizontal conductivity assigned to the top 20 m of the computational grid in order to imitate surface runoff (see Section 4.2.3). During the iterative calculations for a converging flow solution, an inbuilt DarcyTools algorithm then decreases conductivity for drained cells in order to find the equilibrium between net precipitation, runoff, and infiltration (Svensson, personal communication).

In the current analysis of the pier at 3000 AD, the simulated groundwater table is located at 7 m depth inside the pier, which is barely above sea level (Figure 5-1; Figure 5-2). The horizontal conductivity of all cells above groundwater level is reduced by a factor 1000 (Figure 5-2), but nevertheless the non-adjusted horizontal conductivity just below the groundwater table is high still enough ($K_h = 10^{-5}$ m/s) to drain all net precipitation of the pier. As a comparison, in the surface numerical modelling of Site

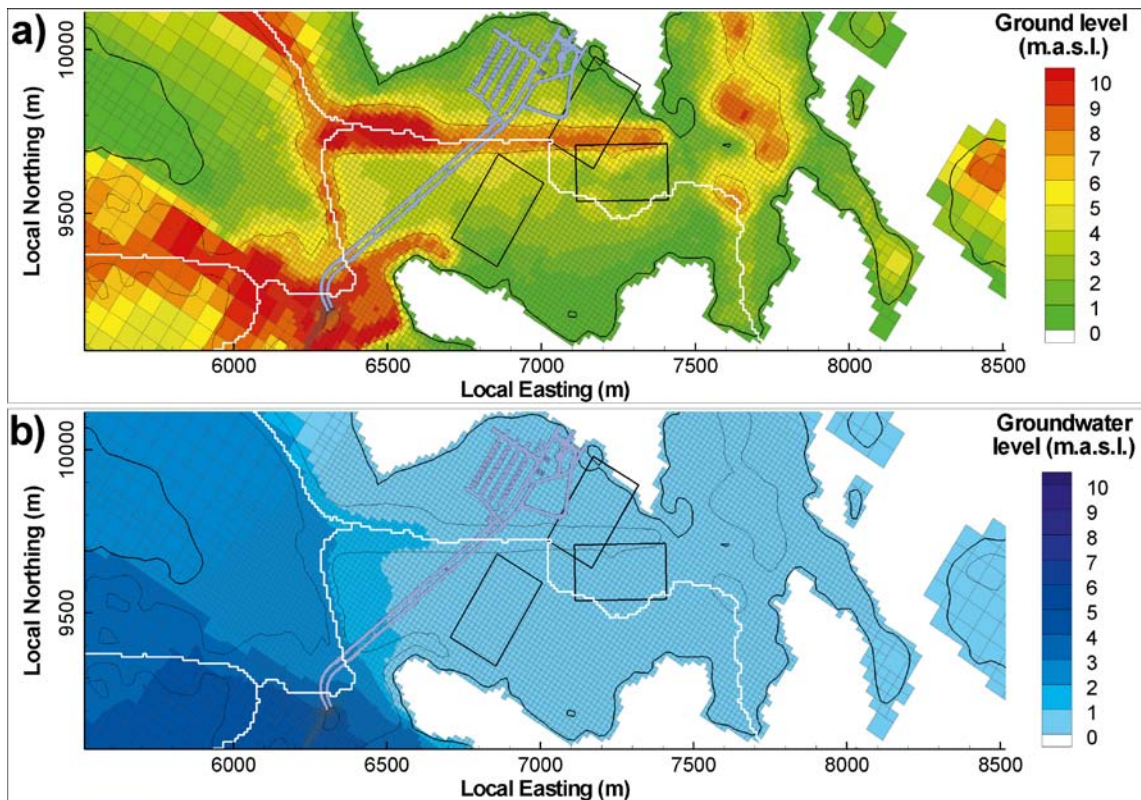


Figure 5-1. Simulated groundwater level in the vicinity of the pier at 3000 AD (shoreline at $z = -5.65$ m RHB 70); a) despite its topographical relief, the groundwater level inside the pier, b) is close to sea level.

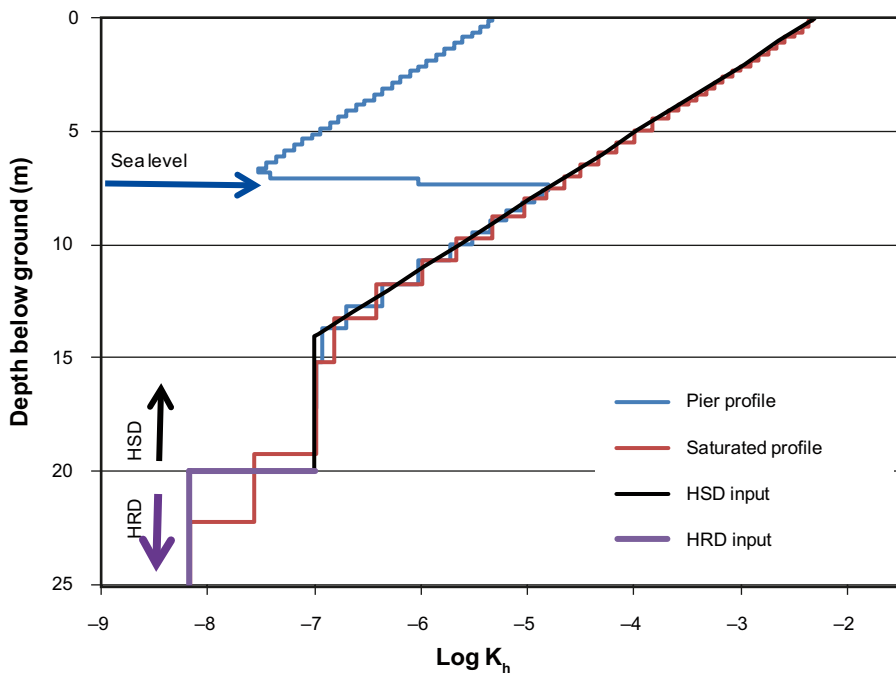


Figure 5-2. Vertical profiles of horizontal HSD conductivity with depth at 3000 AD. The pier is drained to a depth of 7 m (cf Figure 5-1), which is barely above sea-level at 3000 AD. An inbuilt DarcyTools algorithm decreases conductivity for drained cells in comparison to the saturated profile.

Investigation Forsmark /Bosson et al. 2008, Hedenström et al. 2008/, the pier was modelled as a 3–4 m layer of artificial fill (i.e. coarse construction material; $K_h = 1.5 \times 10^{-4}$ m/s), on top of a 0.5 m layer of upper fractured bedrock ($K_h = 1.5 \times 10^{-6}$ m/s). Thus, the horizontal conductivity in the upper 4.5 m of the pier is actually lower in the current simulations than what was applied in the Site Investigation Forsmark model. The additional step of topographically removing the pier was therefore considered superfluous.

In the Site Investigation Forsmark model, the bedrock is modelled below these 4.5 m soil layers, with a HRD conductivity on the order 10^{-8} m/s. However, in the model setup the fictive HSD parameterisation continues down to 20 m depth, with a conductivity ranging from 10^{-5} m/s to 10^{-7} m/s (Figure 5-2). As a result, the groundwater level virtually drains down to sea level. This accentuates the need for an improved HSD parameterisation.

This exceptionally high horizontal conductivity is not only assigned to the pier, but also to the generic HSD layer. A high horizontal conductivity results in a simulated groundwater table that is less stringently tied to local variations in the topography of the ground surface. Instead the simulated groundwater table reflects a smoothed average of local variations in topography, which takes on its appearance as drained topographical peaks and flooded topographical depressions (see Figure 5-4c). In fact, the simulated groundwater table at 2000 AD is considerably deeper than measured groundwater levels in the Site Investigation Forsmark programme (Figure 5-20). However, in this comparison it should be kept in mind that low-topographic locations, where shallow groundwater tables can be expected, were overrepresented in the measurement programme, and that only two of the measure points were located above 7 m (RHB 70).

5.1.3 5000 AD

In 5000 AD the shoreline will have retreated to -14.96 m (RHB 70), which corresponds to a 4 km horizontal distance from the pier (Figure 5-4). The two discharge locations from the SFR area are a bay north of Charlie’s lake and a bay in southeast, just north of Kallrigafjärden (white areas; Figure 5-4). The simulated groundwater table reflects a smoothed average of the local variation in topography, which takes on its expression as drained topographical peaks and flooded topographical depressions (Figure 5-4c). Note that a simulated groundwater table below topography is shown in green/orange contours, while a water table above topography is shown in blue contour in Figure 5-4c. According to simulations, the areas south of the pier, west of the Biotest lake, and Charlie’s lake are submerged by surface water (i.e. groundwater table above topography; blue contour in Figure 5-4c). It should also be noted that the topography used in simulations is basin-filled, which means that the blue contour inside Charlie’s lake (Figure 5-4c) does not indicate the simulated lake depth, but the excess surface water above its actual basin threshold.

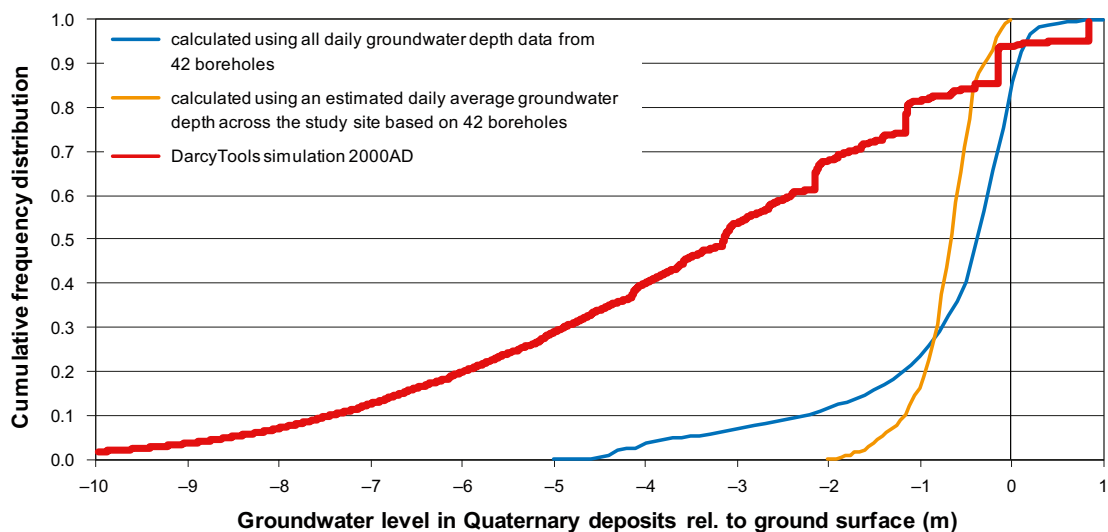


Figure 5-3. Comparison between measured and simulated depth to groundwater table. Measurements show the groundwater table is seldom deeper than 1 m below ground surface, whereas the simulated groundwater table for 2000 AD takes on a wide range of depths down to 10 m below ground surface. Modified from Figure 2-35 in /Johansson and Öhman 2008/.

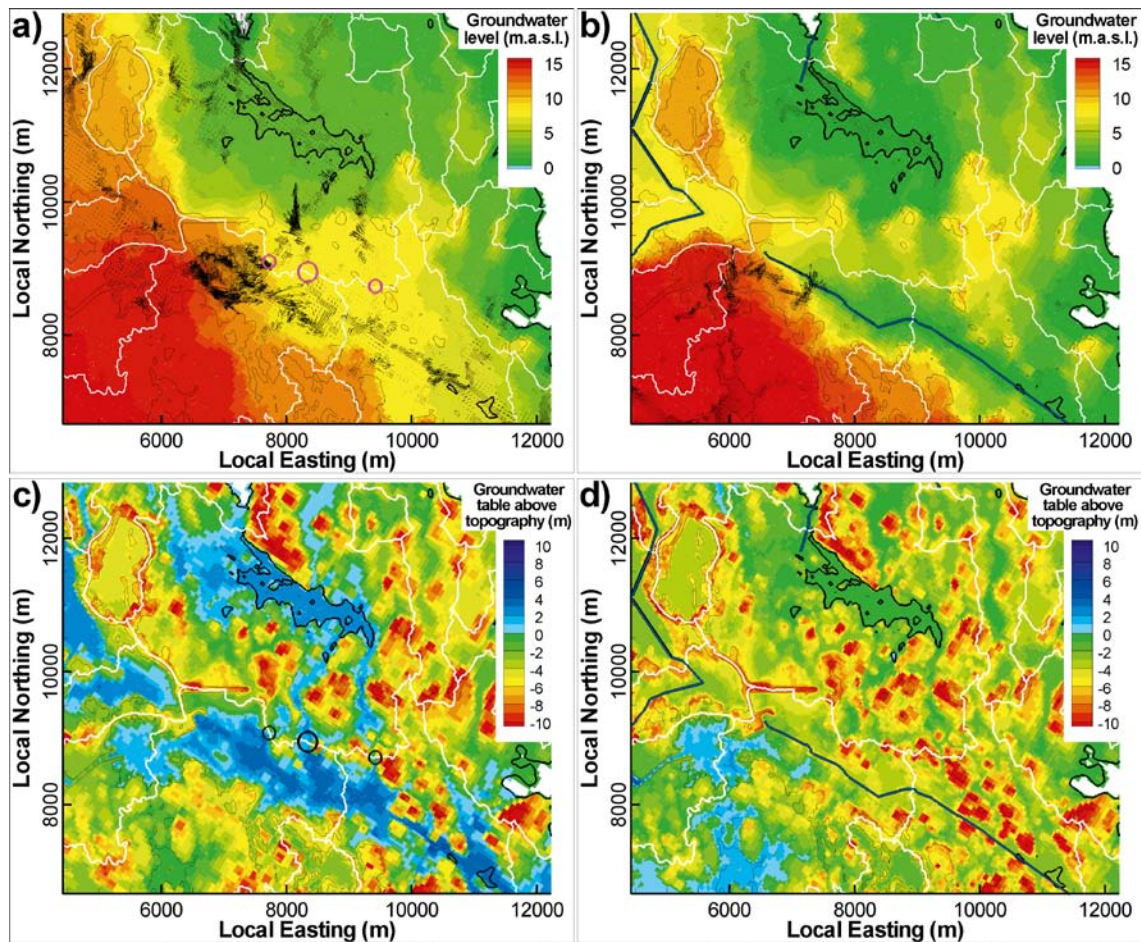


Figure 5-4. Simulated groundwater level in the vicinity of the pier at 5000 AD; a) and b) simulated ground water level relative to the sea level (shoreline at $z = -14.96$ m RHB 70), c) and d) are simulated groundwater table relative to the topography. Tentative “major future rivers” have been implemented in Figures b) and d) in order to drain excessive surface water. Note that the topography used in simulations is basin-filled, which means that the green colour of Charlie’s lake in d) does not indicate a drained lake, but a simulated lake level on par with its basin threshold.

The simulated excess surface water is due to an insufficient surface runoff in the model. The darcy flux vectors of surface runoff reveal the locations of bottlenecks (black arrows; Figure 5-4a). In fact, the flooding south of the pier (Asphällsfjärden) in combination with the low groundwater table inside the pier (and other topographical peaks), induces both surface flow and groundwater flow across the topographical water divide. There are flow lines from Asphällsfjärden that cross the topographical water divide over to the catchment of Charlie’s lake (pink circles; Figure 5-4a), which would imply that if Asphällsfjärden is flooded the ridge may not function as a local water divide at 5000 AD.

There are several reasons for the flooding of the current results:

1. Asphällsfjärden receives large inflows: a) surface runoff from large inland catchments, as well as, b) the groundwater flow from the underlying sheet joints which is re-directed upwards into Asphällsfjärden by the Singö deformation zone,
2. the high HSD conductivity parameterisation provides a smooth flat groundwater table, which is only partly connected to the local variation in ground topography (which implies that the topographical divide may not necessarily coincide with the actual water divide), and
3. the Singö topographical depression has a shallow topographical gradient downstream to Kallrigafjärden equal to $8 \text{ m}/6,000 \text{ m}$, which makes its discharge threshold highly exposed to bottleneck passages. In the simulation, the bottlenecks are artefacts of discretisation, but in reality bottlenecks may comprise of thresholds of non-erodible material (sediments, vegetation or bedrock; see Figure 3-8).

5.1.4 5000 AD with major future rivers

In order to examine the effect of a complete drainage of the Singö depression, the 5000 AD scenario was repeated with inclusion of “major future rivers” (Section 3.2.5). These major rivers are assigned a fictive high horizontal conductivity and modelled with a vertical depth of 4 m, which effectively could be interpreted a prescribed head condition draining the bottom of these riverbeds. Indeed, the Singö depression is successfully drained from excess surface water (Figure 5-4d), which effectively terminates the flux across the topographical divide (Figure 5-4b). A conclusion to be drawn from this is that the question to if the ridge acts as a water divide, or not, depends on the parameterisation of the HSD and the runoff.

5.2 Particle tracking

Particle tracking is performed for the steady state flow fields at 2000 AD, 3000 AD, 5000 AD, and an alternative 5000 AD scenario with major future rivers. Storage tunnel particles follow the intersection between zfmENE8031 and ZFMNNW1209 (zon6), while particles from the Silo follow the intersection between ZFMNE0870B (zon9) and zfmNW0805b (zon8)

An impracticality encountered in the particle tracking algorithm is its discretisation by a constant time step. Initially, the particles tend to move slowly until reaching, either a highly transmissive HCD, or the fictive conductivity at ground surface, which is used to mimic surface runoff (see Sections 4.2.2 and 4.2.3). As the particle approaches the ground surface it is channelled into to higher fluxes and its velocity accelerates by orders of magnitude. Given this circumstance, it is impossible to find a time step that is long enough for the initial slow phase of the particle motion, and yet short enough to resolve its fast movement at its later phase (i.e. considering the fact that not all particles are not simultaneously in the same phase; Figure 5-5). The next version of DarcyTools v 3.3 will allow particle motion discretisation by cell-jump, which would circumvent all such difficulties in resolving particle movement. In other words, particle location will not be tracked and recorded to an ASCII-file on a time step-basis, but instead each time the particle location has actually changed.

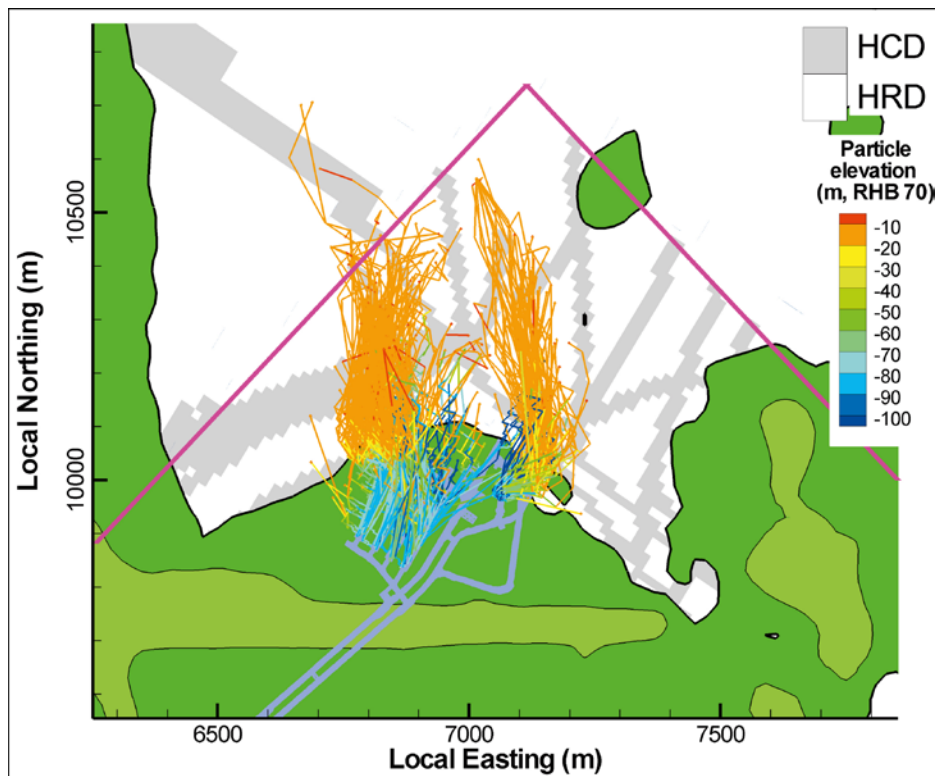


Figure 5-5. An example of simulated particle trajectories: at 3000 AD particles from the existing SFR move upwards to an elevation of -15 m, after which they are re-directed north.

It is common practise to use a particle collection box to define the endpoints of the particle trajectories. This may be convenient for analysis of deep storage repositories, where the resolution of particle motion close to ground surface is of lesser interest. However, in the previous application to SFR /Odén 2009/, it was found that the particle collection box required a vertical extent of approximately 30 m in order to catch all particles. This corresponds to about a third of the vertical depth of SFR, and thus constitutes a relatively indistinct boundary for particle trajectories (i.e. compared to the Site Investigation analysis, where the repository depth is 500 m). Therefore, an option was used where particle location printout occurs when the particle leaves the domain /Svensson et al. 2007/ (i.e. the option <event> = 3). The relative proportion of particle exit points on either side of the topographical divide between catchments 28 and 32 (i.e. Charlie's lake or the future Singö river) is used to evaluate the significance of the ridge as a potential local water divide (Table 5-1).

At 2000 AD and 3000 AD particles emerge to the ground surface inside the SFR Regional domain (Figure 5-5; Figure 5-6). These predictions are rather similar to previous modeling work /Holmén and Stigsson 2001, Odén 2009/. Layout 1 has the closest exit points to those of the existing SFR (primarily the Silo; Figure 5-6). Also the particles of Layout 2 exit relatively close to the existing SFR, although a larger proportion of the particles exit south of the topographical divide into catchment 28. Layout 3, which is located some 60 m below Layout 2, has significantly deeper trajectories with exit points in a widely spread plume. Layout 4 has clearly the highest proportion particles exit south of the topographical divide.

At 5000 AD, the implementation of major future rivers has the dominant control of the particle exit locations (Table 5-1). The reason for this is explained by the hydraulic gradients arising from the differences in simulated groundwater table (see Figure 5-4). It is interesting to note that, in the presence of major future rivers, the relative proportions of the particles exit on either side of the topographical divide are very similar between the 3000 AD and 5000 AD cases (Table 5-1).

The resulting performance measures are visualized in figures for each model setup, (see Appendices H and I). However, results should be interpreted with caution, as confidence is low. More importantly is the identification of modeling difficulties that need to be addressed in coming model versions, as summarized in Chapter 6.

Table 5-1. Fraction of particles exiting south of the topographical water divide.

| Scenario | Existing SFR | Layout 1 | Layout 2 | Layout 3 | Layout 4 |
|----------------------|--------------|----------|----------|----------|----------|
| 2000AD | 0.0% | 19.4% | 85.6% | 29.0% | 100.0% |
| 3000AD | 0.0% | 0.0% | 16.9% | 28.8% | 100.0% |
| 5000AD | 0.0% | 0.0% | 0.0% | 0.0% | 0.2% |
| 5000AD, Major rivers | 0.0% | 0.0% | 17.0% | 8.5% | 80.2% |

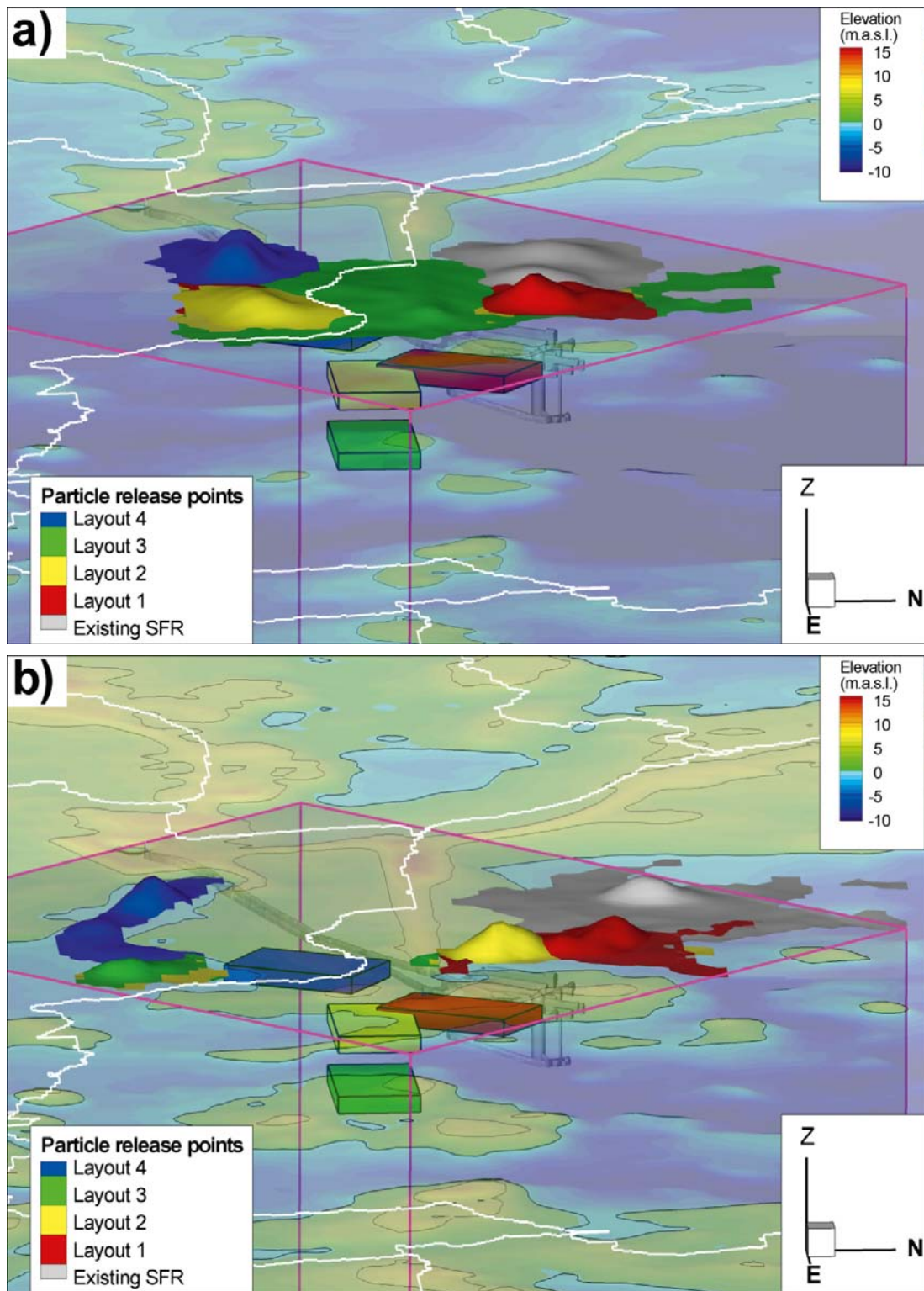


Figure 5-6. Particle exit locations from existing and candidate storage facilities in steady state flow solutions at different stages of land lift; a) 2000 AD and b) 3000 AD. Note that the flow fields have been solved separately with only one candidate layout implemented at the time, as the layouts influence the flow field.

6 Summary and conclusions

This study has demonstrated a numerical implementation of the hydrogeologic model SFR v 0.1 in the computational software DarcyTools v 3.1. In specific, the scope of this study was to evaluate the performance of four candidate layouts at different stages of land-lift, with respect to the overlying ridge, which constitutes a topographical (and hydrological) water divide. The model is uncalibrated with respect to tunnel inflow, point-water head measurements, interference tests, hydrochemistry see /Follin et al. 2007/ and therefore results should be considered preliminary and are highly uncertain. More importantly, a number of difficulties have been identified, which are summarised below. These need to be addressed in coming model versions.

In comparison to the planned deep repository for disposal of spent nuclear fuel, the SFR is a very shallow repository. This implies that in comparison to previous DarcyTools applications, the modelling of SFR is sensitive to the parameterisation of HSD and surface runoff; particularly in this study where one of the objectives was to evaluate the ridge's effect on the flow field (see Section 5.1). It is therefore strongly recommended that more attention is paid to the model description of the HSD, surface hydrology, and the groundwater table in the coming model versions.

Groundwater level measurements from the Site Investigation Forsmark show that the groundwater table is rarely more than 1 m below the ground surface, which is not reproduced in the current simulations (Figure 5-3). The groundwater table controls the hydraulic gradients, and in its turn, the groundwater flow. The DarcyTools computational software is a tool that has primarily been developed to target deep groundwater flow in fractured media, whereas the shallow hydrology is crudely represented by artificial conductivities. Therefore it must be questioned if the surface hydrology can be satisfactorily described in DarcyTools, or if it is more rational to use a different modelling tool for the shallow groundwater flow in SFR. If it is decided to continue using DarcyTools for the coming model versions, it may be preferable to re-consider the choice of top boundary condition. An alternative condition could be to assign a prescribed head of 1.0 m below the ground surface (see Figure 5-3), or perhaps, prescribed head along river beds. This could be a simple strategy to re-direct the modelling efforts to the modelling of flow in HCD/HRD. The drawback of changing to a prescribed-head boundary condition is that the conservation of flux is sacrificed (i.e. overland net precipitation versus total discharge to the sea). However, perhaps the conservation of flux is less important, as the SFR area appears to be dominated by saturated infiltration, with a groundwater table close to the ground surface. For the particular study of evaluating potential water divides, a prescribed head boundary is less appealing, as the results become pre-destined by the chosen boundary condition.

The land lift is modelled by successively elevating the topography relatively to the sea level. However, as the current seafloor is elevated above sea level, its topography will alter due to landscape dynamic processes. These include wave erosion at the retreating shoreline and surface runoff erosion in a second stage. The topography constitutes the driving potential for hydraulic gradients and the shallow groundwater flow. Therefore, the landscape development plays an important role for the performance assessment of the candidate layouts. In the coming model versions and simulations it is suggested that the future landscape dynamics are considered in more detail to improve modelling of soil-layer depth and surface runoff. For example, it appears more reasonable to parameterise the surface hydrology (river and lakes; Section 3.2) based on the regolith model after the removal of layers with highly erodible soil types, such as clay and silt.

Saltwater density is not included in the current model. In this model setup, the prescribed pressure on the seafloor must also reflect freshwater density in order to attain model consistency (see Appendix C).

Rotation of input objects proved to be a successful method to transform the orientation of computational mesh versus the flow field. However, in this case the water-dividing pier is aligned East-West, which would result in a North-South oriented flow. Therefore it is inconclusive whether the rotation improved the configuration of the mesh in this particular case.

In the modelling of sequential land lift, it was found that the topography must be basin-filled in order to prevent the inbuilt DarcyTools algorithm from erroneously interpreting deep lake bottoms as part of the discharge boundary (equated with the open sea; Section 3.2.4). The influence of such erroneous “inland seas” is probably particularly large for the exceptionally plain topography of the SFR area.

This ongoing SFR project is pioneering, in the sense that for the first time it has decided to use DarcyTools to deliver repository performance measures to Safety Analysis. This poses additional demands on the particle tracking algorithm, such as output options, robustness, and particle recovery rate in. It was found during the course of this project that the particle tracking algorithm must be improved to meet the demands. The suggested changes will be implemented in the DarcyTools version 3.3, which is intended to be released by August 2009.

There are seven HCDs defined inside the SFR Regional domain that terminate against the interface between the Regional and Super-regional domains (black ovals; Figure 4-3b). The reason for this is that these lineament data are based on surface lineaments /Curtis et al. 2009/ that were unavailable at the time when the HCDs of the Super-regional domain were defined /Stephens et al. 2007/. The truncation of HCDs is expected to force trajectories upwards towards the highly conductive HSD as particles move across the interface between the Regional and Super-regional model domains.

References

- Axelsson C-L, 1997.** Data for calibration and validation of numerical models at SFR Nuclear Waste Repository, Forsmark, Sweden. SKB R-98-48, Svensk Kärnbränslehantering AB.
- Axelsson C-L, Mærsk Hansen L, 1997.** Update of structural models at SFR nuclear waste repository, Forsmark, Sweden. SKB R-98-05, Svensk Kärnbränslehantering AB.
- Axelsson C-L, Ekstav A, Lindblad Pål A, 2002.** SFR – Utvärdering av hydrogeologi. SKB R-02-14, Svensk Kärnbränslehantering AB.
- Bosson E, Gustafsson L-G, Sassner M, 2008.** Numerical modelling of surface hydrology and near-surface hydrogeology at Forsmark. Site descriptive modelling, SDM-Site Forsmark. SKB R-08-09, Svensk Kärnbränslehantering AB.
- Brydsten L, 1999.** Shore line displacement in Öregrundsgrepen. SKB TR-99-16, Svensk Kärnbränslehantering AB.
- Brydsten L, 2006.** A model for landscape development in terms of shoreline displacement, sediment dynamics, lake formation, and choke-up processes, SKB TR-06-40, Svensk Kärnbränslehantering AB.
- Curtis P, Petersson J, Triumph C-A, 2009.** Site investigation SFR. Deformation zone modelling. Model version 0.1. SKB P-09-48, Svensk Kärnbränslehantering AB.
- Follin S, Hartley L, Jackson P, Roberts D, Marsic N, 2008.** Hydrogeological conceptual model development and numerical modelling using CONNECTFLOW, Forsmark modeling stage 2.3. SKB R-08-23, Svensk Kärnbränslehantering AB.
- Follin S, Johansson P-O, Levén J, Hartley L, Holton D, McCarthy R, Roberts D, 2007.** Updated strategy and test of new concepts for groundwater flow modelling in Forsmark in preparation of site descriptive modelling stage 2.2. SKB R-07-20, Svensk Kärnbränslehantering AB.
- Hedenström A, Risberg J, 2003.** Shore displacement in northern Uppland during the last 6,500 calendar years, SKB TR-03-17, Svensk Kärnbränslehantering AB.
- Hedenström A, Sohlenius G, Strömgren M, Brydsten L, Nyman H, 2008.** Depth and stratigraphy of regolith at Forsmark. Site descriptive modelling, SDM-Site Forsmark. SKB R-08-07, Svensk Kärnbränslehantering AB.
- Holmén J G, 2005.** Inverse modelling of inflow to tunnels and propagation of estimated uncertainties to predictive stages. SKB R-05-74, Svensk Kärnbränslehantering AB.
- Holmén J G, 2008.** Premodelling of the importance of the location of the upstream hydraulic boundary of a regional flow model of the Laxemar-Simpevarp area. Site descriptive modelling, SDM-Site Laxemar. SKB R-08-60, Svensk Kärnbränslehantering AB.
- Holmén J G, Stigsson M, 2001.** Modelling of future hydrogeological conditions at SFR. SKB R-01-02, Svensk Kärnbränslehantering AB.
- Johansson P-O, Öhman J, 2008.** Presentation of meteorological, hydrological and hydrogeological monitoring data from Forsmark. Site descriptive modeling, SDM-Site Forsmark. SKB R-08-10, Svensk Kärnbränslehantering AB.
- Kjellström E, Strandberg G, Brandefelt J, Näslund J-O, Smith B, Wohlfarth B, 2009.** Climate conditions in Sweden in a 100,000-year time perspective. SKB TR-09-04, Svensk Kärnbränslehantering AB.
- Odén M, 2009.** Site investigation SFR. Hydrogeological modelling at SFR using DarcyTools. Site description SFR version 0.0. SKB P-08-94, Svensk Kärnbränslehantering AB.
- Pål A, 2001.** An empirical model of glacio-isostatic movements and shore-level displacement in Fennoscandia, SKB R-01-41, Svensk Kärnbränslehantering AB.

Rhén I, Follin S, Hermanson J, 2003. Hydrogeological Site Descriptive Model – a strategy for its development during Site Investigations. SKB R-03-08, Svensk Kärnbränslehantering AB.

SKB, 2008. Geovetenskapligt undersökningsprogram för utbyggnad av SFR. SKB R-08-67, Svensk Kärnbränslehantering AB.

Stephens M B, Fox A, La Pointe P, Simeonov A, Isaksson H, Hermanson J, Öhman J, 2007. Geology Forsmark. Site descriptive modelling Forsmark stage 2.2. SKB R-07-45, Svensk Kärnbränslehantering AB.

Stigsson M, Follin S, Andersson J, 1998. On the simulation of variable density flow at SFR, Sweden. SKB R-99-08, Svensk Kärnbränslehantering AB.

Strömgren M, Brydsten L, 2008. Digital elevation models of Forsmark. Site descriptive modelling, SDM-Site Forsmark. SKB R-08-62, Svensk Kärnbränslehantering AB.

Svensson U, 2004. DarcyTools, version 2.1. Verification and validation. SKB R-04-21, Svensk Kärnbränslehantering AB.

Svensson U, Ferry M, 2004. DarcyTools, version 2.1. User's guide. SKB R-04-20, Svensk Kärnbränslehantering AB.

Svensson U, Kuylenstierna H-O, Ferry M, 2007. DarcyTools, Version 3.4. Concepts, methods, equations and demo simulations. SKB R-07-38, Svensk Kärnbränslehantering AB.

Öhman J, Follin S, 2010. Site investigation SFR. Parameterisation of the Hydrogeologic model SFR. Model version 0.1. SKB P-09-49, Svensk Kärnbränslehantering AB.

List of geometric objects used in the grid generation

Table A-1. Objects¹ used in the DarcyTools grid generation.

| Object name ² | Description |
|-----------------------------|-------------------|
| R_ansl_1BLA.dat | Connecting tunnel |
| R_ansl_1BMA.dat | Connecting tunnel |
| R_ansl_1BTF.dat | Connecting tunnel |
| R_ansl_2BTF.dat | Connecting tunnel |
| R_förvaring_1BLA.dat | Deposition tunnel |
| R_förvaring_1BMA.dat | Deposition tunnel |
| R_förvaring_1BTF.dat | Deposition tunnel |
| R_förvaring_2BTF.dat | Deposition tunnel |
| R_silo_del1.dat | Deposition silo |
| R_silo_del2.dat | Deposition silo |
| R_blå_del.dat | Access tunnel |
| R_blå_del2.dat | Access tunnel |
| R_gul_byggtunnel1.dat | Access tunnel |
| R_gul_byggtunnel2.dat | Access tunnel |
| R_gul_drifttunnel1.dat | Access tunnel |
| R_gul_drifttunnel2.dat | Access tunnel |
| R_gul_drifttunnel3.dat | Access tunnel |
| R_gul_drifttunnel4.dat | Access tunnel |
| R_gul_drifttunnel5.dat | Access tunnel |
| R_gul_drifttunnel6.dat | Access tunnel |
| R_gul_drifttunnel7.dat | Access tunnel |
| R_gulgrön_byggtunnel1.dat | Access tunnel |
| R_gulgrön_byggtunnel10.dat | Access tunnel |
| R_gulgrön_byggtunnel11.dat | Access tunnel |
| R_gulgrön_byggtunnel2.dat | Access tunnel |
| R_gulgrön_byggtunnel3.dat | Access tunnel |
| R_gulgrön_byggtunnel4.dat | Access tunnel |
| R_gulgrön_byggtunnel5.dat | Access tunnel |
| R_gulgrön_byggtunnel6.dat | Access tunnel |
| R_gulgrön_byggtunnel7.dat | Access tunnel |
| R_gulgrön_byggtunnel8.dat | Access tunnel |
| R_gulgrön_byggtunnel9.dat | Access tunnel |
| R_gulgrön_drifttunnel1.dat | Access tunnel |
| R_gulgrön_drifttunnel10.dat | Access tunnel |
| R_gulgrön_drifttunnel11.dat | Access tunnel |
| R_gulgrön_drifttunnel12.dat | Access tunnel |
| R_gulgrön_drifttunnel13.dat | Access tunnel |
| R_gulgrön_drifttunnel2.dat | Access tunnel |
| R_gulgrön_drifttunnel3.dat | Access tunnel |
| R_gulgrön_drifttunnel4.dat | Access tunnel |
| R_gulgrön_drifttunnel5.dat | Access tunnel |
| R_gulgrön_drifttunnel6.dat | Access tunnel |
| R_gulgrön_drifttunnel7.dat | Access tunnel |
| R_gulgrön_drifttunnel8.dat | Access tunnel |
| R_gulgrön_drifttunnel9.dat | Access tunnel |
| R_gulgrön_tvärtunnel1.dat | Access tunnel |
| R_gulgrön_tvärtunnel2.dat | Access tunnel |
| R_gulgrön_tvärtunnel3.dat | Access tunnel |
| R_gulgrön_tvärtunnel4.dat | Access tunnel |
| R_gulgrön_tvärtunnel5.dat | Access tunnel |

| | |
|-------------------------------|-----------------------------|
| R_gulgrön_tvärtunnel6.dat | Access tunnel |
| R_gulgrön_tvärtunnel7.dat | Access tunnel |
| R_gulgrön_tvärtunnel8.dat | Access tunnel |
| R_orange_del1.dat | Access tunnel |
| R_orange_del2.dat | Access tunnel |
| R_orange_del3.dat | Access tunnel |
| R_orange_del4.dat | Access tunnel |
| R_orange_del5.dat | Access tunnel |
| R_orange_del6.dat | Access tunnel |
| R_orange_del7.dat | Access tunnel |
| R_orange_del8.dat | Access tunnel |
| R_singözonen_byggtunnel1.dat | Access tunnel |
| R_singözonen_byggtunnel2.dat | Access tunnel |
| R_singözonen_drifttunnel1.dat | Access tunnel |
| R_singözonen_drifttunnel2.dat | Access tunnel |
| R_singözonen_drifttunnel3.dat | Access tunnel |
| R_singözonen_drifttunnel4.dat | Access tunnel |
| R_röd_BST_del1.dat | Access tunnel |
| R_röd_BST_del2.dat | Access tunnel |
| R_top_no_ridge.dat | Ground surface topography |
| R_top_with_ridge.dat | Ground surface topography |
| R_LAKES.dat | Topographical depressions |
| R_rivers.dat | River lines from GIS |
| R_riversm1.dat | River lines +/- 1 m |
| R_riversp1.dat | River lines +/- 1 m |
| R_riversm2.dat | River lines +/- 2 m |
| R_riversp2.dat | River lines +/- 2 m |
| R_Brydstens_rivers.dat | River lines /Brydsten 1999/ |
| R_SFR_modellområde_v01.dat | SFR regional domain |
| R_Doman.dat | Super-regional flow domain |
| R_kartong_läge1.dat | Particle release domain |
| R_kartong_läge2.dat | Particle release domain |
| R_kartong_läge3.dat | Particle release domain |
| R_kartong_läge4.dat | Particle release domain |

¹ SKBdoc 1223130 – Befintligt skannat SFR i STL-format, Version 0.1, 2010-06-08, (access might be given on request).

² The prefix "R_" indicates that objects have been rotated horizontally, Section 3.4.

Merging the PFM2.2 and SFR0.1 geologic models

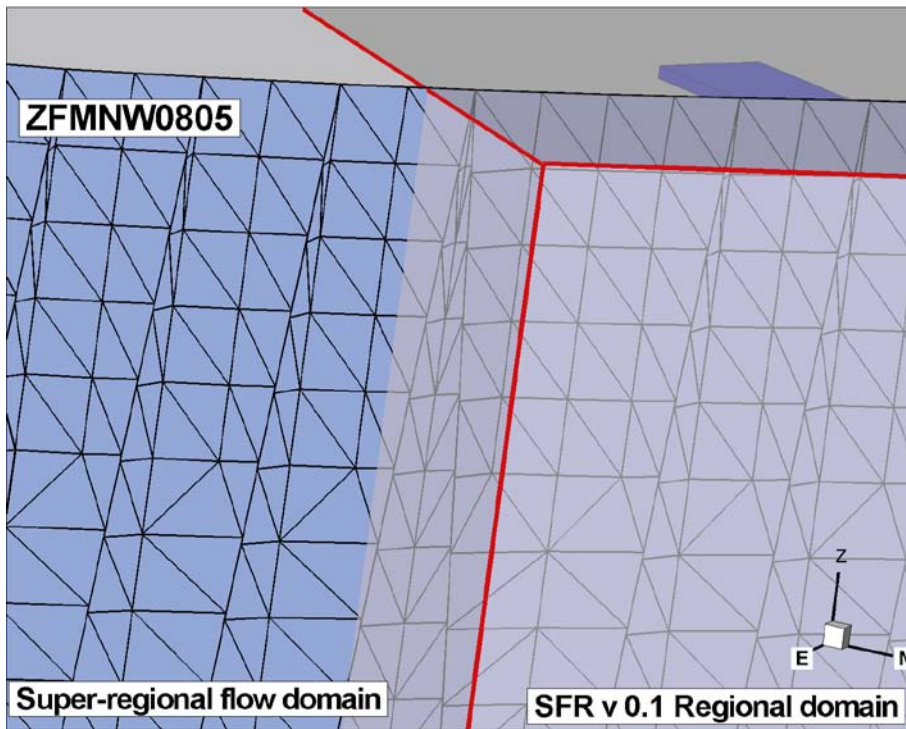


Figure B-1. ZFMNW0805 as defined in the PFM2.2 geologic model /Stephens et al. 2007/, meshed at the 100 m scale. The part inside the SFR v 0.1 Regional domain is to be replaced by the definition of the SFR v 0.1 geologic model /Curtis et al. 2009/.

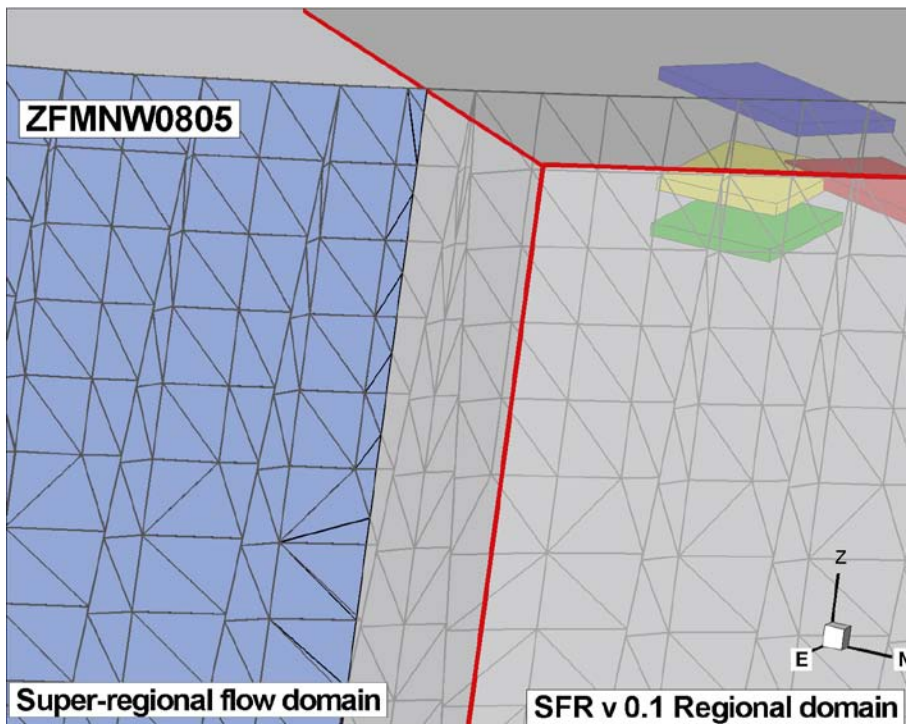


Figure B-2. The zone is re-meshed along its intersection with the SFR v 0.1 Regional domain, and all HCD area falling inside the Regional domain is excluded.

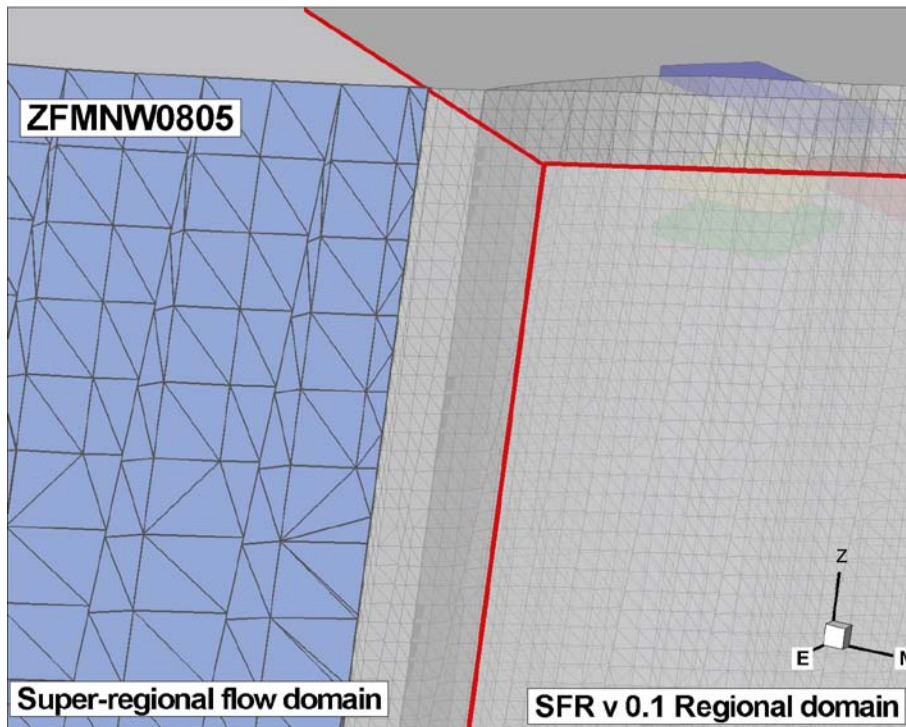


Figure B-3. The part of zone inside the SFR regional domain is substituted with the definition from the SFR v 0.1 geologic model /Curtis et al. 2009/, and is meshed at the 25 m scale.

Saltwater density in boundary conditions

This Appendix demonstrates why the Baltic sea must be modelled with a freshwater density, in order to attain model consistency at the seafloor boundary, eq. (4-2). In the current flow model, the impact of variable density on flow has been assumed negligible, and therefore the groundwater flow is modelled as solely freshwater (Section 2). The seafloor is the only discharge boundary of the model (Section 4.3). The seafloor boundary is assigned prescribed head in terms of a dynamic pressure, which is set equal to the excessive pressure of the overburden Baltic relative to hydrostatic freshwater pressure. This pressure depends on the density of the Baltic sea and depth below sea level (i.e. the excessive overburden weight of the saltwater column), eq. (4-2).

In the first model setup, the actual density of the brackish Baltic was used ($\rho_{\text{sea}} = 1,004 \text{ kg/m}^3$). This is the default approach in DarcyTools (Svensson, personal communication). However, when particle tracking was performed in the resulting steady state flow field solutions, it was found that this boundary condition imposes a converging flow field that forces all particles to exit exactly at the shoreline (Figure C-1). This is a paradoxical result, as the pier has been expected to act as a local waterdivide, which – conversely – would diverge flow away from the pier (Figure C-1). The reason for this lies in the inconsistency in taking saltwater density into account at a flow boundary, while solving the flow equation only for freshwater. The boundary condition imposes density driven gradients, which can only be levelled out by an equilibration in salt density (i.e. saltwater intrusion) – a process which is neglected in the flow model. In other words, the pressure difference between simulated groundwater (hydrostatic freshwater) and its overlying Baltic (hydrostatic salt water) impose gradients along the seafloor, depending on the seafloor elevation of underwater topography (Figure C-2a). This pressure difference is proportional to the height of the overlying saltwater column, and, by definition, takes on its minimum value at the shoreline (Figure C-3a). All gradients along the seafloor boundary are therefore directed towards the shoreline, which consequently forces all particle trajectories to exit at the shoreline, which by definition becomes the only discharge boundary of the model. This inconsistency can be described as an everlasting density-driven saltwater intrusion, which cannot reach steady state without incorporating variable fluid density in the flow solution.

Therefore, the second option was used instead; the density of the Baltic was set equal to the density of the simulated groundwater. This reduces eq. (4-2) to $P = \rho_{\text{fresh}} g z_{\text{sea}}$, where z_{sea} is the elevation of the sea (RHB 70), which is a constant value, independent of variability in seafloor topography. As a result, all density driven gradients along the seafloor are eliminated (see Figure C-2b), and the diverging flow of a water divide (Figure C-3b).

It may seem odd to use fresh water density in the calculation of excessive saltwater head at the seafloor boundary, but in essence this approach translates to the assumption of low density differences below the sea. This is a realistic assumption, since salt-water intrusion (which is a neglected process in the current model setup) tends to level out the density differences below sea. Which of the values, 1,000 or 1,004 kg/m^3 , is used for ρ_{sea} is of less importance. It is more important that to acknowledge the fact that both fluid densities, the groundwater and the overlying Baltic, will have approximately the same density at its discharge boundary. Furthermore, the shallow bay of Öregrundsgrepen can be expected to have lower density than in the proper Baltic (1,004 kg/m^3), and to continue decreasing over time with the retreating shoreline.

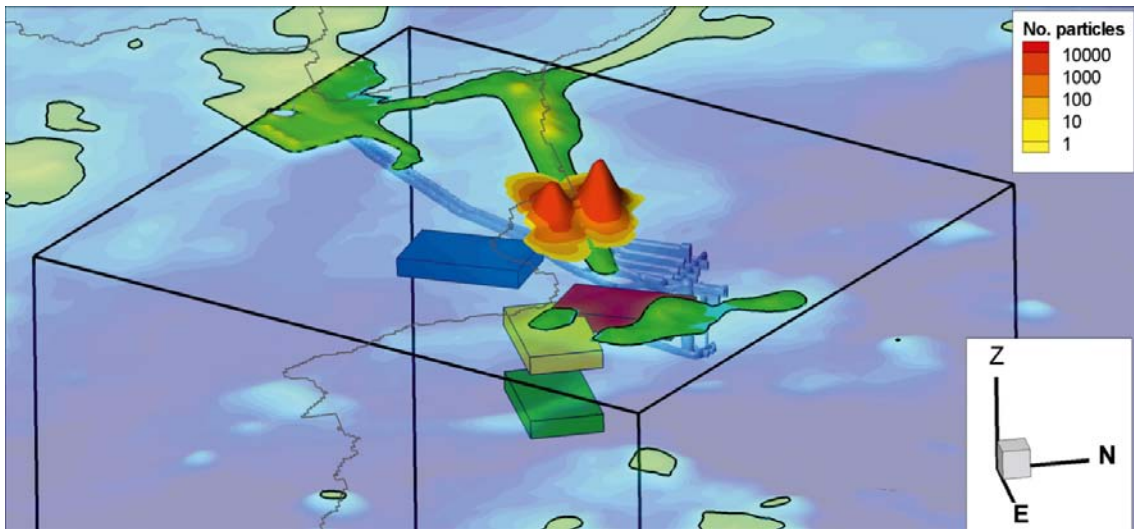


Figure C-1. Particle exit locations from the existing SFR at 2000 AD ($z_{sea} = -0.17$ m RHB 70), with brackish water density used in the calculation of seafloor boundary condition.

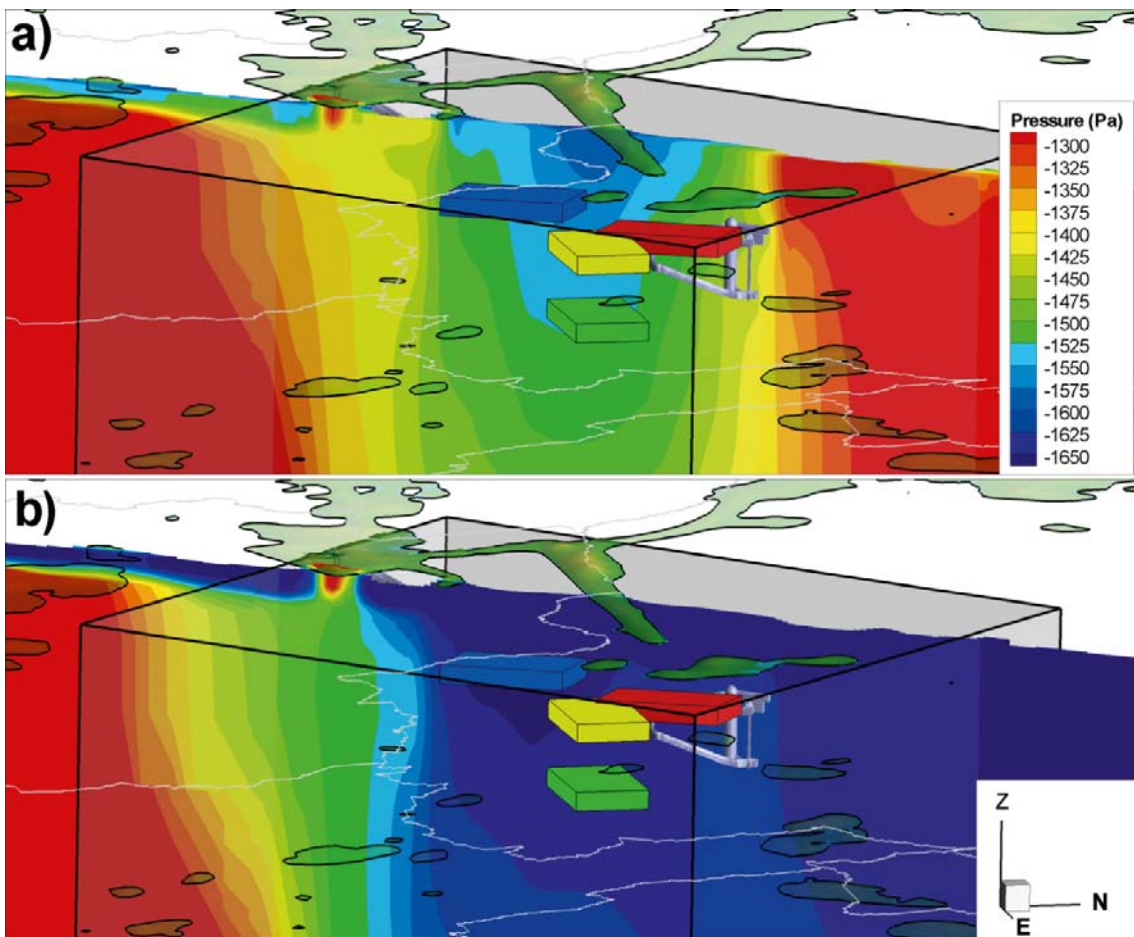


Figure C-2. Simulated pressure field at 2000 AD ($z_{sea} = -0.17$ m RHB 70), depending on boundary condition at the seafloor; a) brackish water density and b) freshwater density. Shown in a vertical cross section viewing towards the West, vertical exaggeration 2.5.

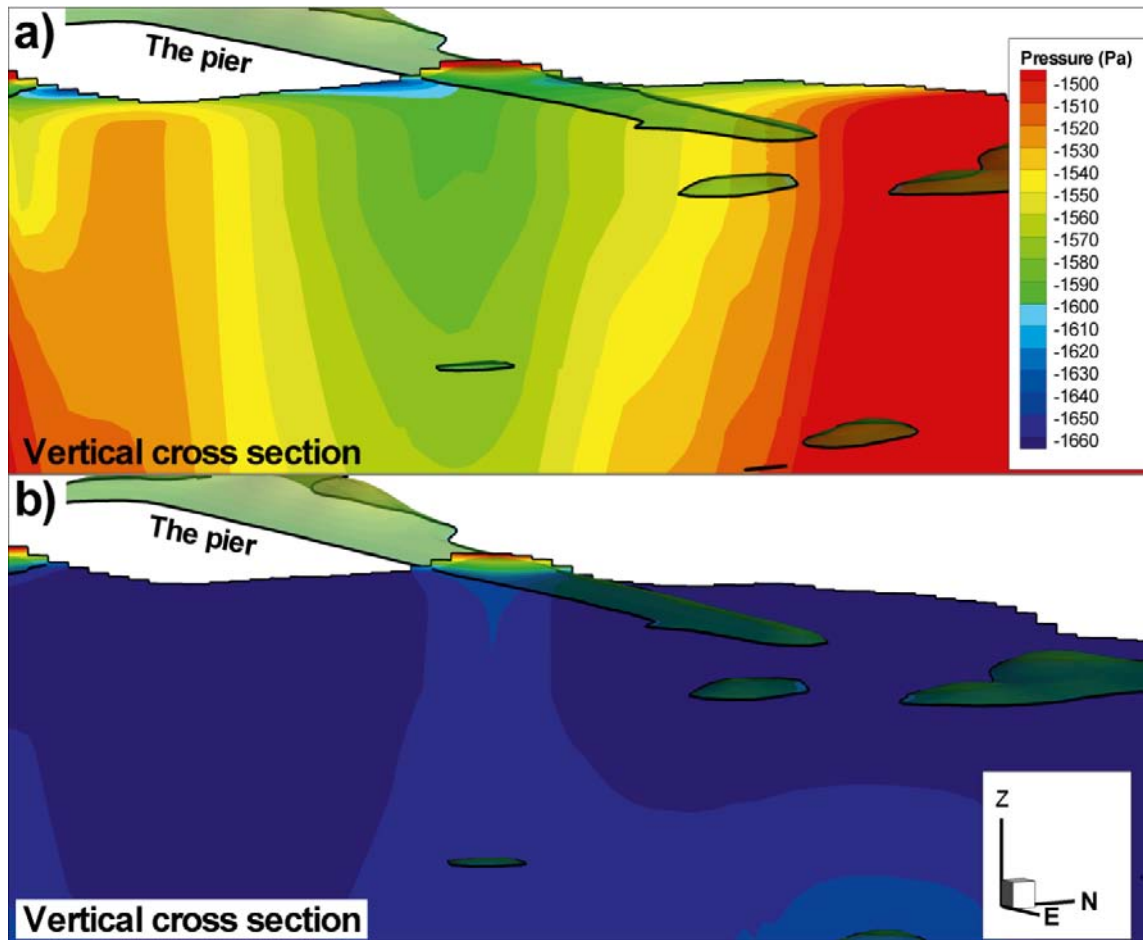


Figure C-3. Close-up of the simulated pressure field at 2000 AD ($z_{sea} = -0.17$ m RHB 70), depending on boundary condition at the seafloor; a) brackish water density and b) freshwater density. Shown in a vertical cross section viewing towards the West, vertical exaggeration 5.

Inconsistencies between the PFM2.2 and SFR0.1 geologic models

Table D-1. Geometric HCD inconsistencies between geologic models PFM2.2¹ and SFR 0.1².

| HCD | Comments | Action |
|------------|--|---|
| ZFM871 | Large discrepancy between models | Replaced by separate RVS feature |
| ZFMNNE0725 | Does not enter the SFR regional domain in PFM2.2, but included in the SFR model. | None |
| ZFMNNE0869 | Extends across domain boundaries in PFM2.2, but strictly inside SFR regional domain, in the SFR model. | PFM2.2 definition replaced by SFR0.1 |
| ZFMWNW0809 | The PFM2.2 definition crosses corner of SFR regional domain, but excluded in SFR 0.1. | PFM2.2 definition retained inside SFR regional domain 0.1 |
| ZFMNNE0808 | The PFM2.2 definition crosses corner of SFR regional domain, but excluded in SFR 0.1. | PFM2.2 definition retained inside SFR regional domain 0.1 |
| ZFMENE0060 | The PFM2.2 definition crosses corner of SFR regional domain 0.1, but excluded in SFR 0.1. | PFM2.2 definition retained inside SFR regional domain 0.1 |
| ZFMWNW1127 | The PFM2.2 definition crosses the SFR regional domain; replaced by ZFMWNW0001 and ZFMWNW0804 in SFR 0.1. | None |
| ZFMENE1057 | The PFM2.2 definition strictly inside SFR regional domain 0.1; removed in SFR 0.1. | PFM2.2 definition removed |
| ZFMWNW0001 | Unconnected across the domain boundaries. | None |
| ZFMWNW0813 | Unconnected across the domain boundaries. | None |
| ZFMWNW0835 | Unconnected across the domain boundaries. | None |
| ZFMWNW0836 | Unconnected across the domain boundaries. | None |
| ZFMWNW1056 | Unconnected across the domain boundaries. | None |
| ZFMNW0805 | Unconnected across the domain boundaries. | None |

¹ PFM2.2 refers to the geologic model SDM-Site Forsmark /Stephens et al. 2007/.

² SFR 0.1 refers to the SFR geologic model v 0.1 /Curtis et al. 2009/.

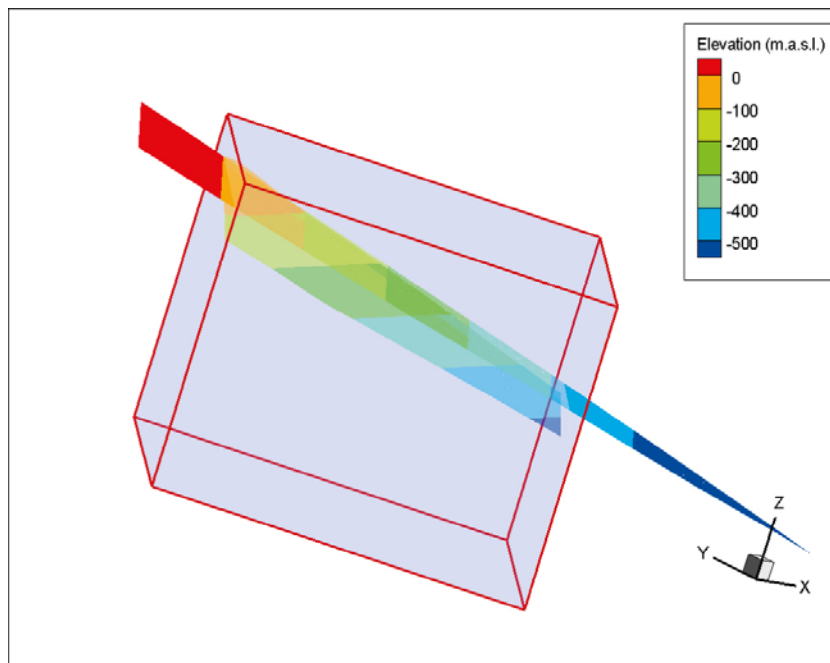


Figure D-1. Side view. Disagreement in definition of ZFM871 between the PFM2.2 (grey) and the SFR0.1 models at the boundary to the SFR regional domain.

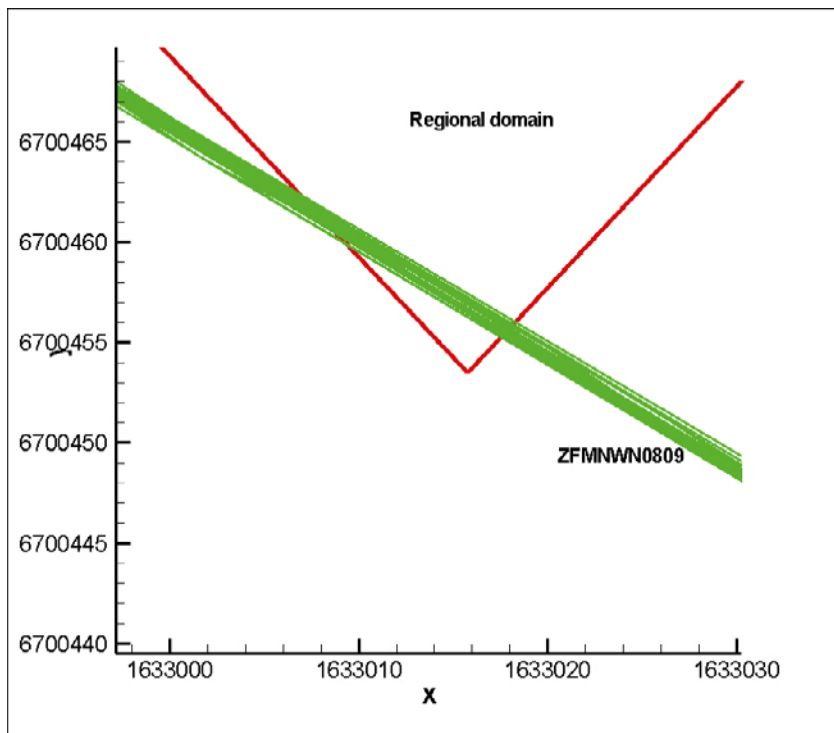


Figure D-2. Top view. The PFM2.2 definition of ZFMNNE0809 (green) touches corner of SFR regional domain.

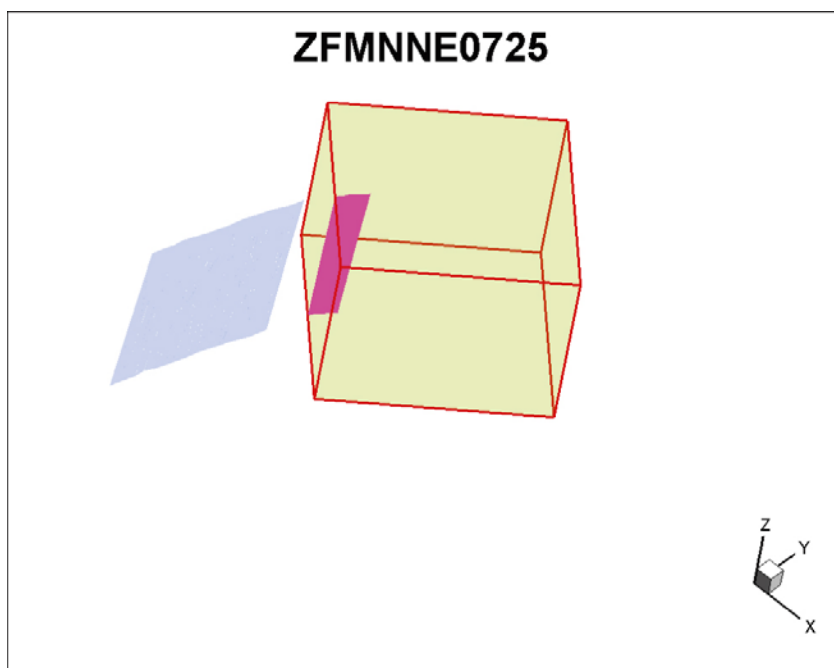


Figure D-3. Side view. Disagreement in definition of ZFMNNE0725 between the PFM2.2 (grey) and the SFR0.1 (pink) models at the boundary to the SFR regional domain (pale green).

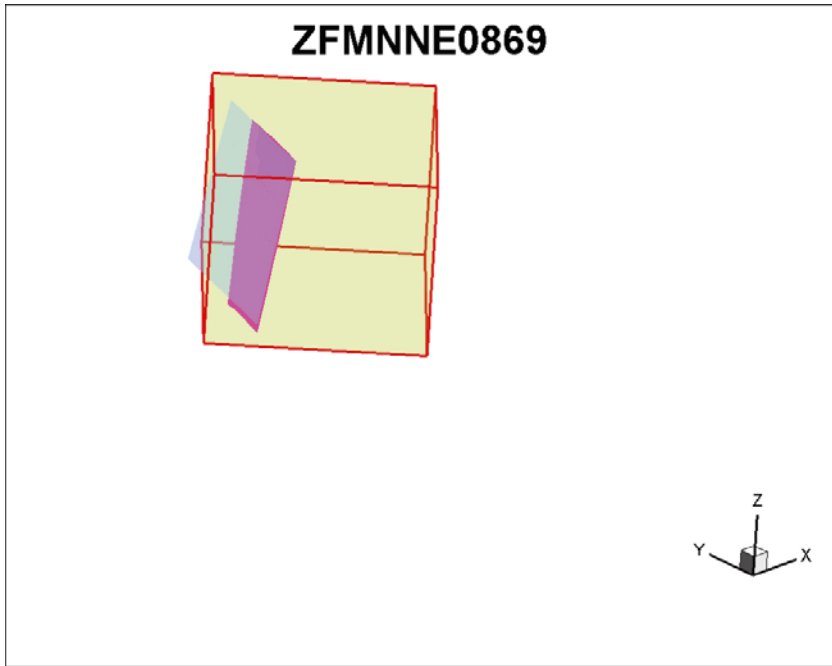


Figure D-4. Side view. ZFMNNE0869 (zon3) extends across domain boundaries in PFM2.2 (grey), but strictly inside SFR regional domain (pale green), in the SFR model (pink).

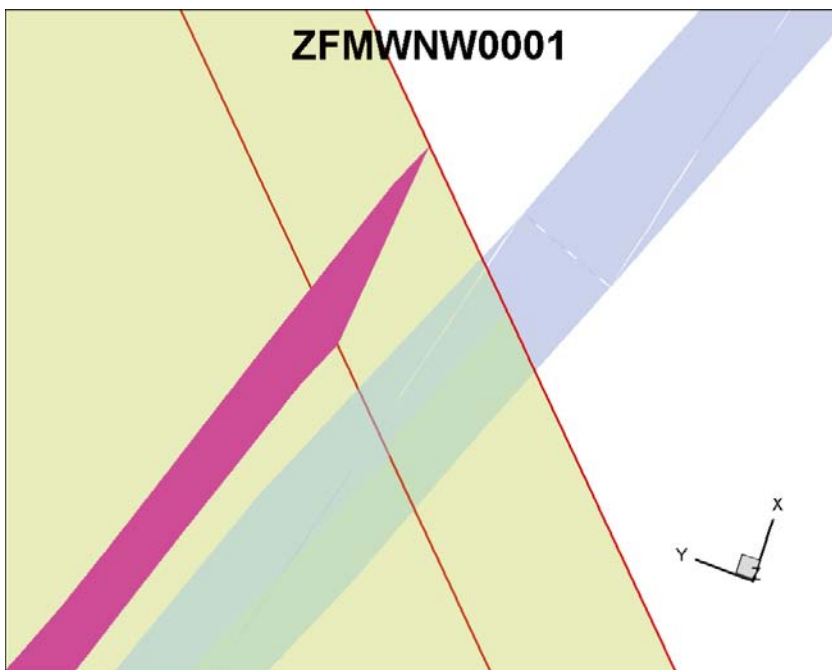


Figure D-5. Top view. Disagreement in definition of Singö between the PFM2.2 (grey) and the SFR0.1 (pink) models at the boundary to the SFR regional domain (pale green).

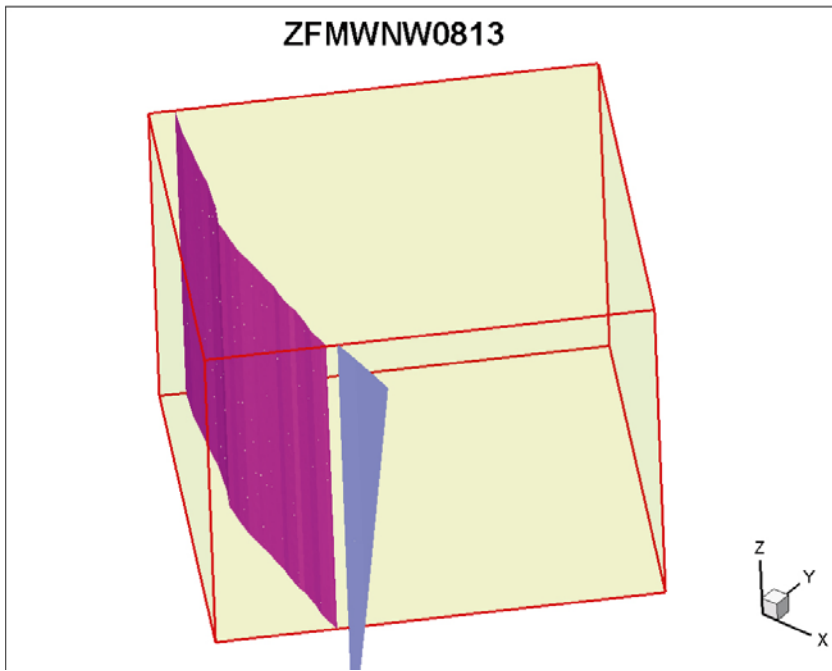


Figure D-6. Side view. Disagreement in definition of ZFMWNW0813 between the PFM2.2 (grey) and the SFR0.1 (pink) models at the boundary to the SFR regional domain (pale green).

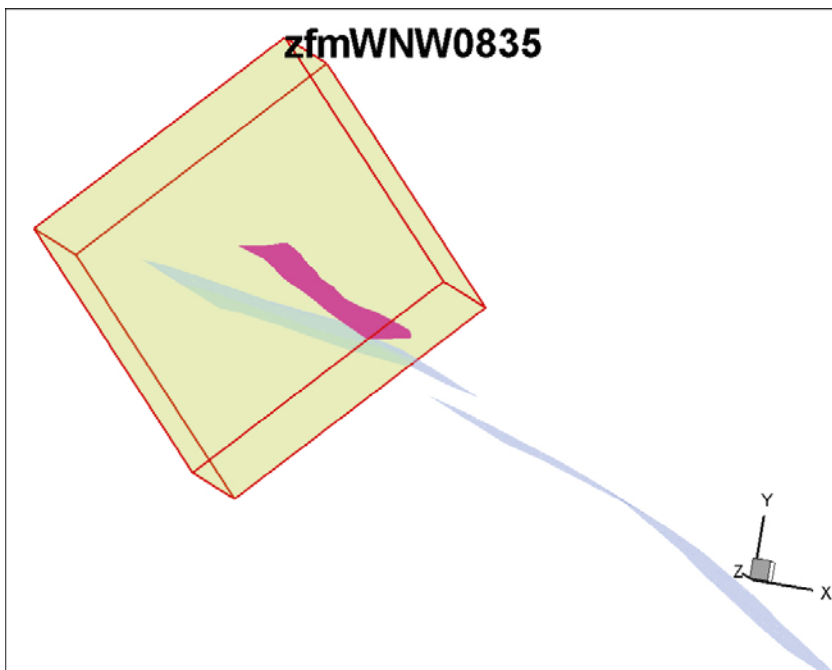


Figure D-7. Top view. Disagreement in definition of ZFMWNW0835 between the PFM2.2 (grey) and the SFR0.1 (pink) models at the boundary to the SFR regional domain (pale green).

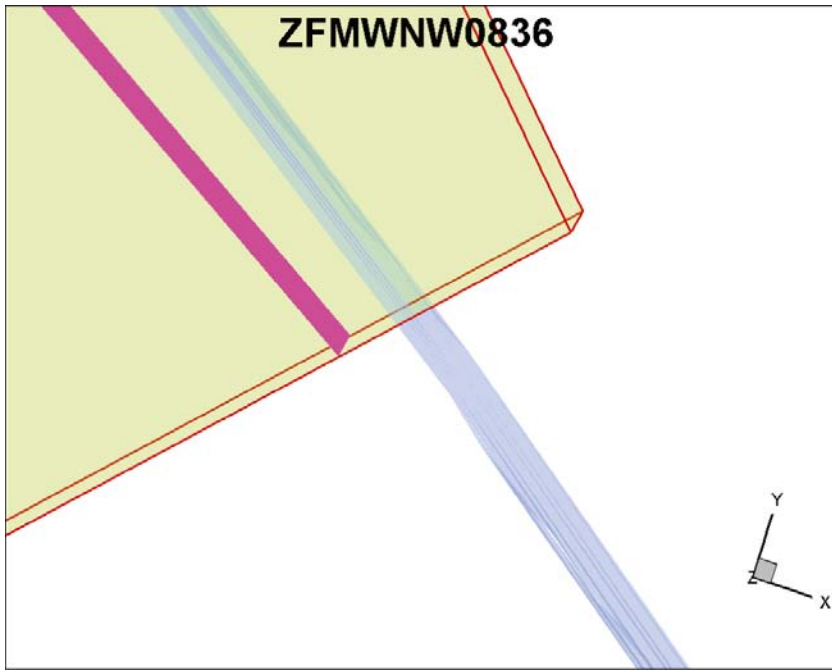


Figure D-8. Top view. Disagreement in definition of ZFMWNW0836 between the PFM2.2 (grey) and the SFR0.1 (pink) models at the boundary to the SFR regional domain (pale green).

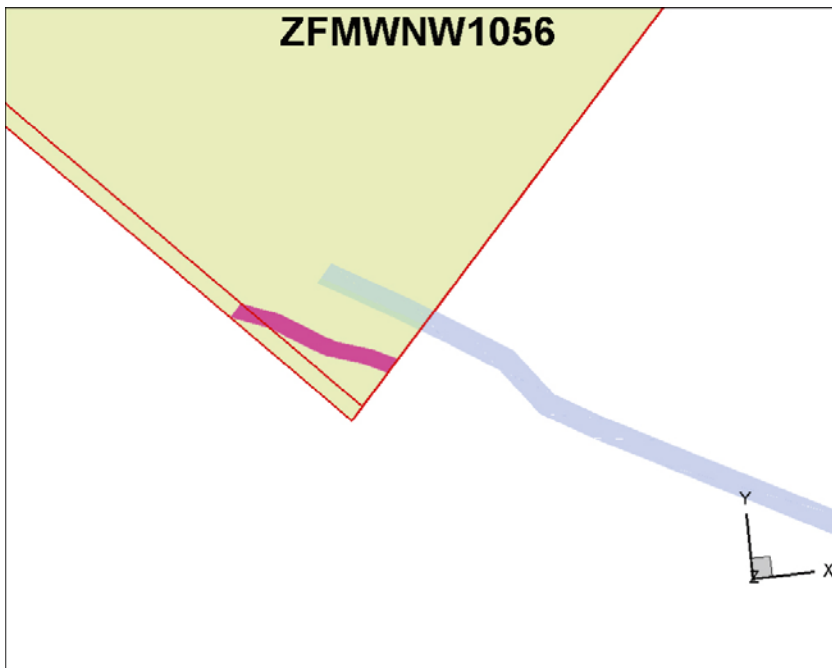


Figure D-9. Top view. Disagreement in definition of ZFMWNW1056 between the PFM2.2 (grey) and the SFR0.1 (pink) models at the boundary to the SFR regional domain (pale green).

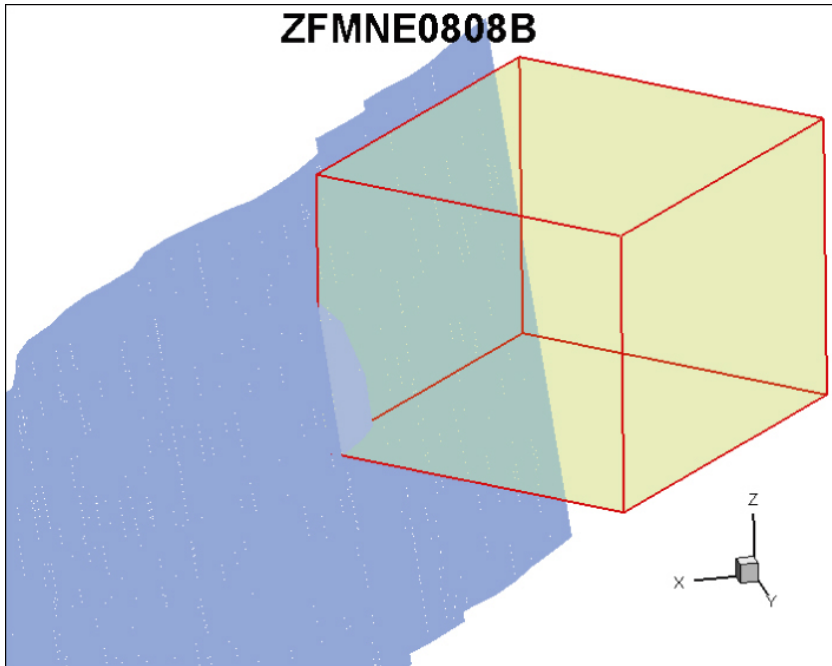


Figure D-10. Side view. The PFM2.2 definition of ZFMNNE0808 (grey) touches corner of SFR regional domain (pale green).

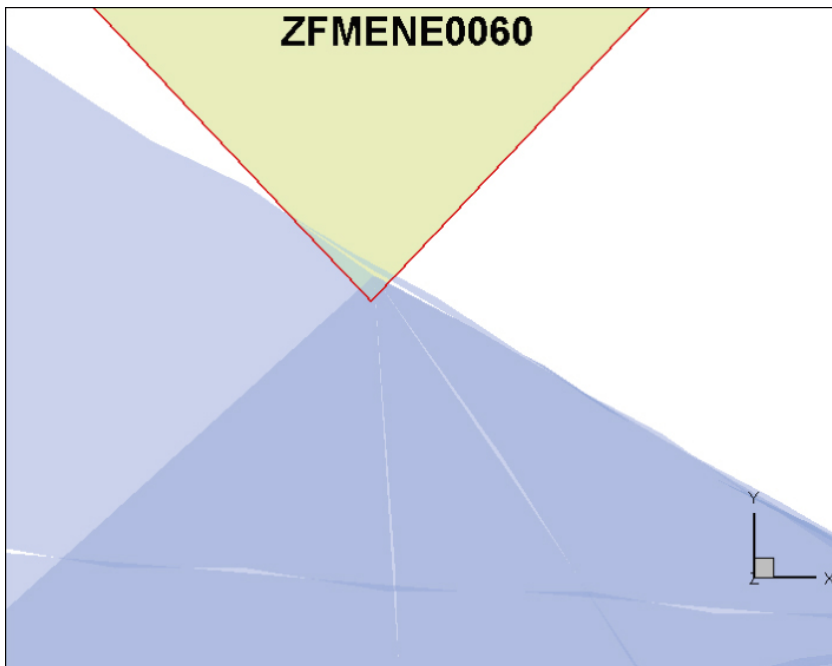


Figure D-11. Top view. The PFM2.2 definition of ZFMENE0060 (grey) touches corner of SFR regional domain (pale green).

DarcyTools input file: Grid generation

```

<cif>
<!--=====
<===== MAIN =====
<=====
<===== Case SFR Grid, Frac =====
<===== Date 2009-05-30 =====
<===== Author Johan Ohman =====
<=====
<tecplot>
<name>          ggnSFR          </name>
<title>         'SFRgrid'       </title>
<var>           cellmk          </var>
<obj>           SFR_regional_domain </obj>
<obj>           WD              </obj>
<obj>           rivers          </obj>
<obj>           Brydstens_rivers </obj>
<loc>           plane x'        </loc>
<loc>           plane y'        </loc>
<loc>           plane z80'      </loc>
<loc>           plane z0'       </loc>
<loc>           land            </loc>
<loc>           sea             </loc>
<loc>           'SURF_hydrology_1' </loc>
<loc>           'SURF_hydrology_2' </loc>
<loc>           'tunn10'        </loc>
<loc>           'tunn11'        </loc>
<loc>           'tunn12'        </loc>
<loc>           'tunn13'        </loc>
<loc>           'tunn14'        </loc>
<loc>           'tunn15'        </loc>
</tecplot>
<!--=====
<===== GRID GENERATION =====
<=====
<gridgen>
<ggn>           gg1            </ggn>
<ggn>           gg2            </ggn>
<ggn>           gg3            </ggn>
<ggn>           gg4            </ggn>
<ggn>           gg5            </ggn>
<ggn>           gg6            </ggn>
<ggn>           gg9            </ggn>
<ggn>           gg12           </ggn>
<ggn>           gg11           </ggn>
<ggn>           gg8            </ggn>
<ggn>           gg10           </ggn>
<ggn>           gg99           </ggn>
<span>          16384. 32768. 2048. </span>
<origin>        -1000. 0.-1100. </origin>
<tecplot>       ggnSFR         </tecplot>
</gridgen>
<ggn>
<name>          gg1            </name>

```

Objects exported to TecPlot

- SFR regional domain v 0.1
- SFR super-regional flow domain v 0.1
- Minor river system
- Major river system
- Intersection planes
- Rivers and lakes
- Access tunnels
- SFR storage facilities
- Mesh with 128 m cell size
- Mesh ground surface
- Remove cells above ground surface
- Mesh super- regional flow domain
- Mesh SFR storage facilities + layout
- Mesh rivers
- Mesh SFR regional domain v 0.1
- Again, remove cells above ground
- Mark SFR regional domain v 0.1
- Mark SFR storage facilities + layout
- Mark minor rivers
- Mark future major rivers + lakes

| | | | |
|------------|--------------------------|-------------|--|
| <isotropy> | F | </isotropy> | |
| <dxmax> | 128.1 | </dxmax> | |
| <dymax> | 128.1 | </dymax> | |
| <dzmax> | 128.1 | </dzmax> | |
| </ggn> | | | |
| <ggn> | | | |
| <name> | gg2 | </name> | |
| <isotropy> | F | </isotropy> | |
| <c221> | T | </c221> | |
| <l221> | T | </l221> | |
| <zone> | ztop | </zone> | |
| </ggn> | | | |
| <ggn> | | | |
| <name> | gg3 | </name> | |
| <isotropy> | F | </isotropy> | |
| <zone> | zoff | </zone> | |
| </ggn> | | | |
| <ggn> | | | |
| <name> | gg12 | </name> | |
| <isotropy> | F | </isotropy> | |
| <zone> | zoff | </zone> | |
| </ggn> | | | |
| <ggn> | | | |
| <name> | gg4 | </name> | |
| <isotropy> | F | </isotropy> | |
| <zone> | zWD | </zone> | |
| </ggn> | | | |
| <ggn> | | | |
| <name> | gg5 | </name> | |
| <isotropy> | F | </isotropy> | |
| <zone> | zTUNNEL | </zone> | |
| <zone> | zförvaring_1BTF | </zone> | Existing SFR storage facilities |
| <zone> | zförvaring_2BTF | </zone> | |
| <zone> | zförvaring_1BLA | </zone> | |
| <zone> | zförvaring_1BMA | </zone> | |
| <zone> | zsilo | </zone> | |
| <zone> | zkartong_läge1 | </zone> | Only one candidate layout meshed at the time |
| <zone> | zkartong_läge2 | </zone> | |
| <zone> | zkartong_läge3 | </zone> | |
| <zone> | zkartong_läge4 | </zone> | |
| <c221> | T | </c221> | |
| <l221> | T | </l221> | |
| </ggn> | | | |
| <ggn> | | | |
| <name> | gg11 | </name> | |
| <isotropy> | F | </isotropy> | |
| <zone> | zSFR_regional_domainMark | </zone> | |
| </ggn> | | | |
| <ggn> | | | |
| <name> | gg8 | </name> | |
| <isotropy> | F | </isotropy> | |
| <zone> | zTUNNELmark | </zone> | |
| <zone> | zförvaring_1BTFmark | </zone> | Existing SFR storage facilities |
| <zone> | zförvaring_2BTFmark | </zone> | |
| <zone> | zförvaring_1BLAmark | </zone> | |
| <zone> | zförvaring_1BMAmark | </zone> | |
| <zone> | zsilomark | </zone> | |

| | | | |
|------------|---------------------------------|-------------|---|
| <zone> | zkartong_läge1mark | </zone> | Only one at the time used |
| <zone> | zkartong_läge2mark | </zone> | |
| <zone> | zkartong_läge3mark | </zone> | |
| <zone> | zkartong_läge4mark | </zone> | |
| </ggn> | | | |
| <ggn> | | | |
| <name> | gg6 | </name> | |
| <isotropy> | F | </isotropy> | |
| <zone> | zrivers | </zone> | |
| <c221> | T | </c221> | |
| <l221> | T | </l221> | |
| </ggn> | | | |
| <ggn> | | | |
| <name> | gg9 | </name> | |
| <zone> | zSFR_regional_domain | </zone> | |
| </ggn> | | | |
| <ggn> | | | |
| <name> | gg10 | </name> | |
| <zone> | zriversMark | </zone> | |
| </ggn> | | | |
| <ggn> | | | |
| <name> | gg99 | </name> | |
| <zone> | z_Future_surface_hydrology_Mark | </zone> | |
| </ggn> | | | |
| <zone> | | | |
| <name> | ztop | </name> | |
| <dzmax> | 1.1 | </dzmax> | Max cell size |
| <dxmax> | 64.1 | </dxmax> | At ground surface |
| <dymax> | 64.1 | </dymax> | |
| <blur> | 1 | </blur> | |
| <mask> | border top | </mask> | |
| </zone> | | | |
| <zone> | | | |
| <name> | zSFR_regional_domain | </name> | Max cell size |
| <dzmax> | 16.1 | </dzmax> | Inside regional domain |
| <dxmax> | 16.1 | </dxmax> | |
| <dymax> | 16.1 | </dymax> | |
| <mask> | inside SFR_regional_domain | </mask> | |
| <mask> | border SFR_regional_domain | </mask> | |
| </zone> | | | |
| <zone> | | | |
| <name> | zSFR_regional_domainMark | </name> | Mark SFR regional domain v 0.1 |
| <marker> | 16 | </marker> | |
| <mask> | inside SFR_regional_domain | </mask> | |
| <mask> | border SFR_regional_domain | </mask> | |
| </zone> | | | |
| <zone> | | | |
| <name> | zoff | </name> | Remove cells above topography |
| <marker> | -2 | </marker> | |
| <mask> | high top | </mask> | |
| </zone> | | | |
| <zone> | | | |
| <name> | zWD | </name> | Remove cells outside super-regional flow domain |
| <marker> | -3 | </marker> | |
| <mask> | outside WD | </mask> | |
| </zone> | | | |
| <zone> | | | |
| <name> | zrivers | </name> | |

| | | | |
|----------|---------------------------------|-----------|--|
| <dzmax> | 1.1 | </dzmax> | Max cell size |
| <dxmax> | 33 | </dxmax> | In all rivers & lakes |
| <dymax> | 33 | </dymax> | |
| <mask> | borderBrydstens_rivers | </mask> | |
| <mask> | borderrivers | </mask> | |
| <mask> | borderriversp1 | </mask> | |
| <mask> | borderriversm1 | </mask> | |
| <mask> | borderLAKES | </mask> | |
| <mask> | highLAKES | </mask> | |
| </zone> | | | |
| <zone> | | | |
| <name> | zriversMark | </name> | Identify river system, defined by GIS |
| <marker> | 4 | </marker> | |
| <mask> | borderrivers | </mask> | |
| <mask> | borderriversp1 | </mask> | |
| <mask> | borderriversm1 | </mask> | |
| </zone> | | | |
| <zone> | | | |
| <name> | z_Future_surface_hydrology_Mark | </name> | Identify Major rivers and lake objects |
| <marker> | 9 | </marker> | |
| <mask> | borderBrydstens_rivers | </mask> | |
| <mask> | highLAKES | </mask> | |
| </zone> | | | |
| <zone> | | | |
| <name> | zTUNNEL | </name> | |
| <dxmax> | 2.1 | </dxmax> | Max cell size |
| <dymax> | 2.1 | </dymax> | In tunnels |
| <dzmax> | 2.1 | </dzmax> | |
| <mask> | border blå_del | </mask> | |
| <mask> | border orange_del1 | </mask> | |
| <mask> | border orange_del2 | </mask> | |
| <mask> | border orange_del3 | </mask> | |
| <mask> | border orange_del4 | </mask> | |
| <mask> | border orange_del5 | </mask> | |
| <mask> | border orange_del6 | </mask> | |
| <mask> | border orange_del7 | </mask> | |
| <mask> | border orange_del8 | </mask> | |
| <mask> | border röd_BST_del1 | </mask> | |
| <mask> | border röd_BST_del2 | </mask> | |
| <mask> | inside blå_del | </mask> | |
| <mask> | inside orange_del1 | </mask> | |
| <mask> | inside orange_del2 | </mask> | |
| <mask> | inside orange_del3 | </mask> | |
| <mask> | inside orange_del4 | </mask> | |
| <mask> | inside orange_del5 | </mask> | |
| <mask> | inside orange_del6 | </mask> | |
| <mask> | inside orange_del7 | </mask> | |
| <mask> | inside orange_del8 | </mask> | |
| <mask> | inside röd_BST_del1 | </mask> | |
| <mask> | inside röd_BST_del2 | </mask> | |
| <mask> | border gul_byggtunnel1 | </mask> | |
| <mask> | border gul_byggtunnel2 | </mask> | |
| <mask> | border gul_drifttunnel1 | </mask> | |
| <mask> | border gul_drifttunnel2 | </mask> | |
| <mask> | border gul_drifttunnel3 | </mask> | |
| <mask> | border gul_drifttunnel4 | </mask> | |
| <mask> | border gul_drifttunnel5 | </mask> | |
| <mask> | border gul_drifttunnel6 | </mask> | |


```

<mask>         inside gulgrön_byggtunnel9          </mask>
<mask>         inside gulgrön_drifftunnel1       </mask>
<mask>         inside gulgrön_drifftunnel10      </mask>
<mask>         inside gulgrön_drifftunnel11      </mask>
<mask>         inside gulgrön_drifftunnel12      </mask>
<mask>         inside gulgrön_drifftunnel13      </mask>
<mask>         inside gulgrön_drifftunnel2       </mask>
<mask>         inside gulgrön_drifftunnel3       </mask>
<mask>         inside gulgrön_drifftunnel4       </mask>
<mask>         inside gulgrön_drifftunnel5       </mask>
<mask>         inside gulgrön_drifftunnel6       </mask>
<mask>         inside gulgrön_drifftunnel7       </mask>
<mask>         inside gulgrön_drifftunnel8       </mask>
<mask>         inside gulgrön_drifftunnel9       </mask>
<mask>         inside gulgrön_tvärtunnel1        </mask>
<mask>         inside gulgrön_tvärtunnel2        </mask>
<mask>         inside gulgrön_tvärtunnel3        </mask>
<mask>         inside gulgrön_tvärtunnel4        </mask>
<mask>         inside gulgrön_tvärtunnel5        </mask>
<mask>         inside gulgrön_tvärtunnel6        </mask>
<mask>         inside gulgrön_tvärtunnel7        </mask>
<mask>         inside gulgrön_tvärtunnel8        </mask>
<mask>         inside singözonen_byggtunnel1     </mask>
<mask>         inside singözonen_byggtunnel2     </mask>
<mask>         inside singözonen_drifftunnel1     </mask>
<mask>         inside singözonen_drifftunnel2     </mask>
<mask>         inside singözonen_drifftunnel3     </mask>
<mask>         inside singözonen_drifftunnel4     </mask>
<mask>         inside blå_del2                   </mask>
<mask>         border blå_del2                   </mask>
<mask>         inside ansI_1BLA                   </mask>
<mask>         inside ansI_1BMA                   </mask>
<mask>         inside ansI_1BTF                   </mask>
<mask>         inside ansI_2BTF                   </mask>
<mask>         border ansI_1BLA                   </mask>
<mask>         border ansI_1BMA                   </mask>
<mask>         border ansI_1BTF                   </mask>
<mask>         border ansI_2BTF                   </mask>
<blur>         2                                 </blur>
</zone>
<zone>
<name>         zTUNNELmark                       </name>
<marker>      10                               </marker>
<mask>         border blå_del                     </mask>
<mask>         border orange_del1                 </mask>
<mask>         border orange_del2                 </mask>
<mask>         border orange_del3                 </mask>
<mask>         border orange_del4                 </mask>
<mask>         border orange_del5                 </mask>
<mask>         border orange_del6                 </mask>
<mask>         border orange_del7                 </mask>
<mask>         border orange_del8                 </mask>
<mask>         border röd_BST_del1                </mask>
<mask>         border röd_BST_del2                </mask>
<mask>         inside blå_del                     </mask>
<mask>         inside orange_del1                 </mask>
<mask>         inside orange_del2                 </mask>
<mask>         inside orange_del3                 </mask>

```


<mask> inside orange_del4 </mask>
<mask> inside orange_del5 </mask>
<mask> inside orange_del6 </mask>
<mask> inside orange_del7 </mask>
<mask> inside orange_del8 </mask>
<mask> inside röd_BST_del1 </mask>
<mask> inside röd_BST_del2 </mask>
<mask> border gul_byggtunnel1 </mask>
<mask> border gul_byggtunnel2 </mask>
<mask> border gul_drifttunnel1 </mask>
<mask> border gul_drifttunnel2 </mask>
<mask> border gul_drifttunnel3 </mask>
<mask> border gul_drifttunnel4 </mask>
<mask> border gul_drifttunnel5 </mask>
<mask> border gul_drifttunnel6 </mask>
<mask> border gul_drifttunnel7 </mask>
<mask> border gulgrön_byggtunnel1 </mask>
<mask> border gulgrön_byggtunnel10 </mask>
<mask> border gulgrön_byggtunnel11 </mask>
<mask> border gulgrön_byggtunnel2 </mask>
<mask> border gulgrön_byggtunnel3 </mask>
<mask> border gulgrön_byggtunnel4 </mask>
<mask> border gulgrön_byggtunnel5 </mask>
<mask> border gulgrön_byggtunnel6 </mask>
<mask> border gulgrön_byggtunnel7 </mask>
<mask> border gulgrön_byggtunnel8 </mask>
<mask> border gulgrön_byggtunnel9 </mask>
<mask> border gulgrön_drifttunnel1 </mask>
<mask> border gulgrön_drifttunnel10 </mask>
<mask> border gulgrön_drifttunnel11 </mask>
<mask> border gulgrön_drifttunnel12 </mask>
<mask> border gulgrön_drifttunnel13 </mask>
<mask> border gulgrön_drifttunnel2 </mask>
<mask> border gulgrön_drifttunnel3 </mask>
<mask> border gulgrön_drifttunnel4 </mask>
<mask> border gulgrön_drifttunnel5 </mask>
<mask> border gulgrön_drifttunnel6 </mask>
<mask> border gulgrön_drifttunnel7 </mask>
<mask> border gulgrön_drifttunnel8 </mask>
<mask> border gulgrön_drifttunnel9 </mask>
<mask> border gulgrön_tvärtunnel1 </mask>
<mask> border gulgrön_tvärtunnel2 </mask>
<mask> border gulgrön_tvärtunnel3 </mask>
<mask> border gulgrön_tvärtunnel4 </mask>
<mask> border gulgrön_tvärtunnel5 </mask>
<mask> border gulgrön_tvärtunnel6 </mask>
<mask> border gulgrön_tvärtunnel7 </mask>
<mask> border gulgrön_tvärtunnel8 </mask>
<mask> border singözonerna_byggtunnel1 </mask>
<mask> border singözonerna_byggtunnel2 </mask>
<mask> border singözonerna_drifttunnel1 </mask>
<mask> border singözonerna_drifttunnel2 </mask>
<mask> border singözonerna_drifttunnel3 </mask>
<mask> border singözonerna_drifttunnel4 </mask>
<mask> inside gul_byggtunnel1 </mask>
<mask> inside gul_byggtunnel2 </mask>
<mask> inside gul_drifttunnel1 </mask>
<mask> inside gul_drifttunnel2 </mask>

```

<mask>         inside gul_drifftunnel3         </mask>
<mask>         inside gul_drifftunnel4         </mask>
<mask>         inside gul_drifftunnel5         </mask>
<mask>         inside gul_drifftunnel6         </mask>
<mask>         inside gul_drifftunnel7         </mask>
<mask>         inside gulgrön_byggtunnel1       </mask>
<mask>         inside gulgrön_byggtunnel10     </mask>
<mask>         inside gulgrön_byggtunnel11     </mask>
<mask>         inside gulgrön_byggtunnel2     </mask>
<mask>         inside gulgrön_byggtunnel3     </mask>
<mask>         inside gulgrön_byggtunnel4     </mask>
<mask>         inside gulgrön_byggtunnel5     </mask>
<mask>         inside gulgrön_byggtunnel6     </mask>
<mask>         inside gulgrön_byggtunnel7     </mask>
<mask>         inside gulgrön_byggtunnel8     </mask>
<mask>         inside gulgrön_byggtunnel9     </mask>
<mask>         inside gulgrön_drifftunnel1     </mask>
<mask>         inside gulgrön_drifftunnel10    </mask>
<mask>         inside gulgrön_drifftunnel11    </mask>
<mask>         inside gulgrön_drifftunnel12    </mask>
<mask>         inside gulgrön_drifftunnel13    </mask>
<mask>         inside gulgrön_drifftunnel2     </mask>
<mask>         inside gulgrön_drifftunnel3     </mask>
<mask>         inside gulgrön_drifftunnel4     </mask>
<mask>         inside gulgrön_drifftunnel5     </mask>
<mask>         inside gulgrön_drifftunnel6     </mask>
<mask>         inside gulgrön_drifftunnel7     </mask>
<mask>         inside gulgrön_drifftunnel8     </mask>
<mask>         inside gulgrön_drifftunnel9     </mask>
<mask>         inside gulgrön_tvärtunnel1      </mask>
<mask>         inside gulgrön_tvärtunnel2      </mask>
<mask>         inside gulgrön_tvärtunnel3      </mask>
<mask>         inside gulgrön_tvärtunnel4      </mask>
<mask>         inside gulgrön_tvärtunnel5      </mask>
<mask>         inside gulgrön_tvärtunnel6      </mask>
<mask>         inside gulgrön_tvärtunnel7      </mask>
<mask>         inside gulgrön_tvärtunnel8      </mask>
<mask>         inside singözonen_byggtunnel1   </mask>
<mask>         inside singözonen_byggtunnel2   </mask>
<mask>         inside singözonen_drifftunnel1  </mask>
<mask>         inside singözonen_drifftunnel2  </mask>
<mask>         inside singözonen_drifftunnel3  </mask>
<mask>         inside singözonen_drifftunnel4  </mask>
<mask>         border blå_del2                 </mask>
<mask>         inside blå_del2                 </mask>
<mask>         inside ans1_1BMA                 </mask>
<mask>         inside ans1_1BTF                 </mask>
<mask>         inside ans1_2BTF                 </mask>
<mask>         border ans1_1BLA                 </mask>
<mask>         border ans1_1BMA                 </mask>
<mask>         border ans1_1BTF                 </mask>
<mask>         border ans1_2BTF                 </mask>
</zone>
<zone>
<name>         zförvaring_1BTF                 </name>
<dxmax>       2.1                             </dxmax>
<dymax>       2.1                             </dymax>
<dzmax>       2.1                             </dzmax>

```

```

<mask>         border förvaring_1BTF         </mask>
<mask>         inside förvaring_1BTF         </mask>
</zone>
<zone>
<name>         zförvaring_1BTFmark           </name>
<marker>      11                           </marker>
<mask>         inside förvaring_1BTF         </mask>
<mask>         border förvaring_1BTF         </mask>
</zone>
<zone>
<name>         zförvaring_2BTF              </name>
<dxmax>       2.1                          </dxmax>
<dymax>       2.1                          </dymax>
<dzmax>       2.1                          </dzmax>
<mask>         border förvaring_2BTF         </mask>
<mask>         inside förvaring_2BTF         </mask>
</zone>
<zone>
<name>         zförvaring_2BTFmark          </name>
<marker>      12                           </marker>
<mask>         inside förvaring_2BTF         </mask>
<mask>         border förvaring_2BTF         </mask>
</zone>
<zone>
<name>         zförvaring_1BLA              </name>
<dxmax>       2.1                          </dxmax>
<dymax>       2.1                          </dymax>
<dzmax>       2.1                          </dzmax>
<mask>         border förvaring_1BLA         </mask>
<mask>         inside förvaring_1BLA         </mask>
</zone>
<zone>
<name>         zförvaring_1BLAmark          </name>
<marker>      13                           </marker>
<mask>         inside förvaring_1BLA         </mask>
<mask>         border förvaring_1BLA         </mask>
</zone>
<zone>
<name>         zförvaring_1BMA              </name>
<dxmax>       2.1                          </dxmax>
<dymax>       2.1                          </dymax>
<dzmax>       2.1                          </dzmax>
<mask>         border förvaring_1BMA         </mask>
<mask>         inside förvaring_1BMA         </mask>
</zone>
<zone>
<name>         zförvaring_1BMAmark          </name>
<marker>      14                           </marker>
<mask>         inside förvaring_1BMA         </mask>
<mask>         border förvaring_1BMA         </mask>
</zone>
<zone>
<name>         zsilos                        </name>
<dxmax>       2.1                          </dxmax>
<dymax>       2.1                          </dymax>
<dzmax>       2.1                          </dzmax>
<mask>         inside silo_del1              </mask>
<mask>         border silo_del1              </mask>

```

```

<mask>         inside silo_del2           </mask>
<mask>         border silo_del2          </mask>
</zone>
<zone>
<name>         zsilomark                 </name>
<marker>      15                       </marker>
<mask>         inside silo_del1          </mask>
<mask>         border silo_del1          </mask>
<mask>         inside silo_del2          </mask>
<mask>         border silo_del2          </mask>
</zone>
<zone>
<name>         zkartong_läge1            </name>
<dxmax>       2.1                      </dxmax>
<dymax>       2.1                      </dymax>
<dzmax>       2.1                      </dzmax>
<mask>         border kartong_läge1      </mask>
<mask>         inside kartong_läge1      </mask>
</zone>
<zone>
<name>         zkartong_läge1mark        </name>
<marker>      20                       </marker>
<mask>         inside kartong_läge1      </mask>
<mask>         border kartong_läge1      </mask>
</zone>
<zone>
<name>         zkartong_läge2            </name>
<dxmax>       2.1                      </dxmax>
<dymax>       2.1                      </dymax>
<dzmax>       2.1                      </dzmax>
<mask>         border kartong_läge2      </mask>
<mask>         inside kartong_läge2      </mask>
</zone>
<zone>
<name>         zkartong_läge2mark        </name>
<marker>      21                       </marker>
<mask>         inside kartong_läge2      </mask>
<mask>         border kartong_läge2      </mask>
</zone>
<zone>
<name>         zkartong_läge3            </name>
<dxmax>       2.1                      </dxmax>
<dymax>       2.1                      </dymax>
<dzmax>       2.1                      </dzmax>
<mask>         border kartong_läge3      </mask>
<mask>         inside kartong_läge3      </mask>
</zone>
<zone>
<name>         zkartong_läge3mark        </name>
<marker>      22                       </marker>
<mask>         inside kartong_läge3      </mask>
<mask>         border kartong_läge3      </mask>
</zone>
<zone>
<name>         zkartong_läge4            </name>
<dxmax>       2.1                      </dxmax>
<dymax>       2.1                      </dymax>
<dzmax>       2.1                      </dzmax>

```



```

<mask>         border kartong_läge4           </mask>
<mask>         inside kartong_läge4          </mask>
</zone>
<zone>
<name>         zkartong_läge4mark           </name>
<marker>      23                           </marker>
<mask>         inside kartong_läge4          </mask>
<mask>         border kartong_läge4          </mask>
</zone>
<!--=====
<===== FRACTURE NETWORK =====
<=====-->
<fracgen>
<seed>         0.12345                       </seed>
<knwfile>      R_PFM_zoner_med_hål_i_mitten </knwfile>      HCDs from PFM2.2
<knwfile>      R_PLU_sheet_joints           </knwfile>      Sheet joints /Follin et al. 2007/
<knwfile>      R_SFRs_REGIONAL_DZs          </knwfile>      HCDs from SFR geologic model v 0.1
</fracgen>
<fraccmds>
<genknw>       keptfracs                     </genknw>
<cellprop>     keptfracs .dat                </cellprop>
</fraccmds>
<!--=====
<===== OBJECTS & LOCATIONS =====
<=====-->
<!-- objects -->
<obj>
<name>         SFR_regional_domain           </name>
<file>         R_SFR_modellområde_v01.dat    </file>
</obj>
<obj>
<name>         top                           </name>
<file>         R_top_with_ridge.dat          </file>
</obj>
<obj>
<name>         WD                             </name>      Super-regional flow domain
<file>         R_Doman.dat                   </file>
</obj>
<obj>
<name>         rivers                         </name>
<file>         R_rivers.dat                  </file>
</obj>
<obj>
<name>         riversm1                       </name>      1 m deep rivers
<file>         R_riversm1.dat                </file>
</obj>
<obj>
<name>         riversp1                       </name>
<file>         R_riversp1.dat                </file>
</obj>
<obj>
<name>         Brydstens_rivers               </name>      Major future rivers
<file>         R_Brydstens_rivers.dat        </file>
</obj>
<obj>
<name>         LAKES                         </name>
<file>         R_LAKES.dat                   </file>
</obj>

```

```

<obj>
<name>          TUNNEL          </name>
<file>          R_TUNNEL.dat     </file>
</obj>
<obj>
<name>          kartong_läge1    </name>      Candidate layout volume 1
<file>          R_kartong_läge1.dat </file>
</obj>
<obj>
<name>          kartong_läge2    </name>      Candidate layout volume 2
<file>          R_kartong_läge2.dat </file>
</obj>
<obj>
<name>          kartong_läge3    </name>      Candidate layout volume 3
<file>          R_kartong_läge3.dat </file>
</obj>
<obj>
<name>          kartong_läge4    </name>      Candidate layout volume 4
<file>          R_kartong_läge4.dat </file>
</obj>
<obj>
<name>          förvaring_1BTF   </name>
<file>          R_förvaring_1BTF.dat </file>
</obj>
<obj>
<name>          förvaring_2BTF   </name>
<file>          R_förvaring_2BTF.dat </file>
</obj>
<obj>
<name>          förvaring_1BLA   </name>
<file>          R_förvaring_1BLA.dat </file>
</obj>
<obj>
<name>          förvaring_1BMA   </name>
<file>          R_förvaring_1BMA.dat </file>
</obj>
<obj>
<name>          blå_del          </name>
<file>          R_blå_del.dat     </file>
</obj>
<obj>
<name>          orange_del1      </name>
<file>          R_orange_del1.dat </file>
</obj>
<obj>
<name>          orange_del2      </name>
<file>          R_orange_del2.dat </file>
</obj>
<obj>
<name>          orange_del3      </name>
<file>          R_orange_del3.dat </file>
</obj>
<obj>
<name>          orange_del4      </name>
<file>          R_orange_del4.dat </file>
</obj>
<obj>
<name>          orange_del5      </name>

```

```

<file>          R_orange_del5.dat          </file>
</obj>
<obj>
  <name>         orange_del6         </name>
  <file>         R_orange_del6.dat    </file>
</obj>
<obj>
  <name>         orange_del7         </name>
  <file>         R_orange_del7.dat    </file>
</obj>
<obj>
  <name>         orange_del8         </name>
  <file>         R_orange_del8.dat    </file>
</obj>
<obj>
  <name>         röd_BST_del1        </name>
  <file>         R_röd_BST_del1.dat   </file>
</obj>
<obj>
  <name>         röd_BST_del2        </name>
  <file>         R_röd_BST_del2.dat   </file>
</obj>
<obj>
  <name>         gul_byggtunnel1     </name>
  <file>         R_gul_byggtunnel1.dat </file>
</obj>
<obj>
  <name>         gul_byggtunnel2     </name>
  <file>         R_gul_byggtunnel2.dat </file>
</obj>
<obj>
  <name>         gul_drifttunnel1    </name>
  <file>         R_gul_drifttunnel1.dat </file>
</obj>
<obj>
  <name>         gul_drifttunnel2    </name>
  <file>         R_gul_drifttunnel2.dat </file>
</obj>
<obj>
  <name>         gul_drifttunnel3    </name>
  <file>         R_gul_drifttunnel3.dat </file>
</obj>
<obj>
  <name>         gul_drifttunnel4    </name>
  <file>         R_gul_drifttunnel4.dat </file>
</obj>
<obj>
  <name>         gul_drifttunnel5    </name>
  <file>         R_gul_drifttunnel5.dat </file>
</obj>
<obj>
  <name>         gul_drifttunnel6    </name>
  <file>         R_gul_drifttunnel6.dat </file>
</obj>
<obj>
  <name>         gul_drifttunnel7    </name>
  <file>         R_gul_drifttunnel7.dat </file>
</obj>

```

```

<obj>
  <name>          gulgrön_byggtunnel1          </name>
  <file>          R_gulgrön_byggtunnel1.dat    </file>
</obj>
<obj>
  <name>          gulgrön_byggtunnel10        </name>
  <file>          R_gulgrön_byggtunnel10.dat   </file>
</obj>
<obj>
  <name>          gulgrön_byggtunnel11        </name>
  <file>          R_gulgrön_byggtunnel11.dat   </file>
</obj>
<obj>
  <name>          gulgrön_byggtunnel2         </name>
  <file>          R_gulgrön_byggtunnel2.dat    </file>
</obj>
<obj>
  <name>          gulgrön_byggtunnel3         </name>
  <file>          R_gulgrön_byggtunnel3.dat    </file>
</obj>
<obj>
  <name>          gulgrön_byggtunnel4         </name>
  <file>          R_gulgrön_byggtunnel4.dat    </file>
</obj>
<obj>
  <name>          gulgrön_byggtunnel5         </name>
  <file>          R_gulgrön_byggtunnel5.dat    </file>
</obj>
<obj>
  <name>          gulgrön_byggtunnel6         </name>
  <file>          R_gulgrön_byggtunnel6.dat    </file>
</obj>
<obj>
  <name>          gulgrön_byggtunnel7         </name>
  <file>          R_gulgrön_byggtunnel7.dat    </file>
</obj>
<obj>
  <name>          gulgrön_byggtunnel8         </name>
  <file>          R_gulgrön_byggtunnel8.dat    </file>
</obj>
<obj>
  <name>          gulgrön_byggtunnel9         </name>
  <file>          R_gulgrön_byggtunnel9.dat    </file>
</obj>
<obj>
  <name>          gulgrön_drifttunnel1        </name>
  <file>          R_gulgrön_drifttunnel1.dat    </file>
</obj>
<obj>
  <name>          gulgrön_drifttunnel10       </name>
  <file>          R_gulgrön_drifttunnel10.dat   </file>
</obj>
<obj>
  <name>          gulgrön_drifttunnel11       </name>
  <file>          R_gulgrön_drifttunnel11.dat   </file>
</obj>
<obj>
  <name>          gulgrön_drifttunnel12       </name>

```

```

<file>          R_gulgrön_drifftunnel12.dat      </file>
</obj>
<obj>
<name>          gulgrön_drifftunnel13      </name>
<file>          R_gulgrön_drifftunnel13.dat  </file>
</obj>
<obj>
<name>          gulgrön_drifftunnel2      </name>
<file>          R_gulgrön_drifftunnel2.dat  </file>
</obj>
<obj>
<name>          gulgrön_drifftunnel3      </name>
<file>          R_gulgrön_drifftunnel3.dat  </file>
</obj>
<obj>
<name>          gulgrön_drifftunnel4      </name>
<file>          R_gulgrön_drifftunnel4.dat  </file>
</obj>
<obj>
<name>          gulgrön_drifftunnel5      </name>
<file>          R_gulgrön_drifftunnel5.dat  </file>
</obj>
<obj>
<name>          gulgrön_drifftunnel6      </name>
<file>          R_gulgrön_drifftunnel6.dat  </file>
</obj>
<obj>
<name>          gulgrön_drifftunnel7      </name>
<file>          R_gulgrön_drifftunnel7.dat  </file>
</obj>
<obj>
<name>          gulgrön_drifftunnel8      </name>
<file>          R_gulgrön_drifftunnel8.dat  </file>
</obj>
<obj>
<name>          gulgrön_drifftunnel9      </name>
<file>          R_gulgrön_drifftunnel9.dat  </file>
</obj>
<obj>
<name>          gulgrön_tvärtunnel1      </name>
<file>          R_gulgrön_tvärtunnel1.dat  </file>
</obj>
<obj>
<name>          gulgrön_tvärtunnel2      </name>
<file>          R_gulgrön_tvärtunnel2.dat  </file>
</obj>
<obj>
<name>          gulgrön_tvärtunnel3      </name>
<file>          R_gulgrön_tvärtunnel3.dat  </file>
</obj>
<obj>
<name>          gulgrön_tvärtunnel4      </name>
<file>          R_gulgrön_tvärtunnel4.dat  </file>
</obj>
<obj>
<name>          gulgrön_tvärtunnel5      </name>
<file>          R_gulgrön_tvärtunnel5.dat  </file>
</obj>

```



```

<obj>
  <name>      gulgrön_tvärtunnel6      </name>
  <file>      R_gulgrön_tvärtunnel6.dat </file>
</obj>
<obj>
  <name>      gulgrön_tvärtunnel7      </name>
  <file>      R_gulgrön_tvärtunnel7.dat </file>
</obj>
<obj>
  <name>      gulgrön_tvärtunnel8      </name>
  <file>      R_gulgrön_tvärtunnel8.dat </file>
</obj>
<obj>
  <name>      singözonen_byggtunnel1    </name>
  <file>      R_singözonen_byggtunnel1.dat </file>
</obj>
<obj>
  <name>      singözonen_byggtunnel2    </name>
  <file>      R_singözonen_byggtunnel2.dat </file>
</obj>
<obj>
  <name>      singözonen_drifttunnel1    </name>
  <file>      R_singözonen_drifttunnel1.dat </file>
</obj>
<obj>
  <name>      singözonen_drifttunnel2    </name>
  <file>      R_singözonen_drifttunnel2.dat </file>
</obj>
<obj>
  <name>      singözonen_drifttunnel3    </name>
  <file>      R_singözonen_drifttunnel3.dat </file>
</obj>
<obj>
  <name>      singözonen_drifttunnel4    </name>
  <file>      R_singözonen_drifttunnel4.dat </file>
</obj>
<obj>
  <name>      silo_del1                  </name>
  <file>      R_silo_del1.dat            </file>
</obj>
<obj>
  <name>      silo_del2                  </name>
  <file>      R_silo_del2.dat            </file>
</obj>
<obj>
  <name>      blå_del2                   </name>
  <file>      R_blå_del2.dat             </file>
</obj>
<obj>
  <name>      ansl_1BLA                  </name>
  <file>      R_ansl_1BLA.dat            </file>
</obj>
<obj>
  <name>      ansl_1BMA                  </name>
  <file>      R_ansl_1BMA.dat            </file>
</obj>
<obj>
  <name>      ansl_1BTF                  </name>

```

```

<file>          R_ansl_1BTF.dat          </file>
</obj>
<obj>
<name>          ansl_2BTF                </name>
<file>          R_ansl_2BTF.dat          </file>
</obj>
<!-- locations -->
<loc>
<name>          'plane x'                </name>
<xplane>        6875                    </xplane>
</loc>
<loc>
<name>          'plane y'                </name>
<yplane>        9940                    </yplane>
</loc>
<loc>
<name>          'plane z0'               </name>
<zplane>        0                       </zplane>
</loc>
<loc>
<name>          'plane z80'              </name>
<zplane>        -80                     </zplane>
</loc>
<loc>
<name>          LOC_kartong_läge1        </name>
<marker>        cell 20                 </marker>
</loc>
<loc>
<name>          LOC_kartong_läge2        </name>
<marker>        cell 21                 </marker>
</loc>
<loc>
<name>          LOC_kartong_läge3        </name>
<marker>        cell 22                 </marker>
</loc>
<loc>
<name>          LOC_kartong_läge4        </name>
<marker>        cell 23                 </marker>
</loc>
<loc>
<name>          tunn10                   </name>
<marker>        cell 10                 </marker>
</loc>
<loc>
<name>          tunn11                   </name>
<marker>        cell 11                 </marker>
</loc>
<loc>
<name>          tunn12                   </name>
<marker>        cell 12                 </marker>
</loc>
<loc>
<name>          tunn15                   </name>
<marker>        cell 15                 </marker>
</loc>
<loc>
<name>          tunn13                   </name>
<marker>        cell 13                 </marker>

```

```
</loc>
<loc>
  <name>      tunn14      </name>
  <marker>    cell 14    </marker>
</loc>
<loc>
  <name>      SURF_hydrology_1  </name>
  <marker>    cell 4          </marker>
</loc>
<loc>
  <name>      SURF_hydrology_2  </name>
  <marker>    cell 9          </marker>
</loc>
</cif>
```

DarcyTools input file: Flow simulation and particle tracking

```

<cif>
<!--===== >
<===== MAIN =====>
<===== >
<===== Case SFR Grid, Frac =====>
<===== Date 2009-05-30 =====>
<===== Author Johan Ohman =====>
<===== >
<!-- Physical models -->
<!-- ***** -->
<law_mu>
<a0>          0.002          </a0>
<!-- Variables -->
<!-- ***** -->
<var>
<name>        permx          </name>
<infile>      PERMX          </infile>
</var>
<var>
<name>        permy          </name>
<infile>      PERMY          </infile>
</var>
<var>
<name>        permz          </name>
<infile>      PERMZ          </infile>
</var>
<var>
<name>        poros          </name>
<infile>      PORO           </infile>
</var>
<var>
<name>        stora          </name>
<ini>         domain 5.E-6   </ini>
</var>
<var>
<name>        uvel           </name>
<ini>         domain 0.      </ini>
<pos>         xface         </pos>
</var>
<var>
<name>        vvel           </name>
<ini>         domain 0.      </ini>
<pos>         yface         </pos>
</var>
<var>
<name>        wvel           </name>
<ini>         domain 0.      </ini>
<pos>         zface         </pos>
</var>
<spt>
<s0>          0              </s0>
<s1>          0              </s1>
<dspd>        0              </dspd>

```

```

<dwt>          6          </dwt>
</spt>
<flux>
<name>         fluxrep    </name>
<loc>         reploc     </loc>
</flux>
<flux>
<name>         fluxEck    </name>
<loc>         rivlocEck  </loc>
<faces>       north     </faces>
</flux>
<flux>
<name>         fluxBol    </name>
<loc>         rivlocBol  </loc>
<faces>       north     </faces>
</flux>
<flux>
<name>         fluxsilo   </name>
<loc>         silo       </loc>
</flux>
<flux>
<name>         fluxtunn10 </name>
<loc>         tunn10    </loc>
</flux>
<flux>
<name>         fluxtunn11 </name>
<loc>         tunn11    </loc>
</flux>
<flux>
<name>         fluxtunn12 </name>
<loc>         tunn12    </loc>
</flux>
<flux>
<name>         fluxtunn13 </name>
<loc>         tunn13    </loc>
</flux>
<flux>
<name>         fluxtunn14 </name>
<loc>         tunn14    </loc>
</flux>
<flux>
<name>         fluxtunn15 </name>
<loc>         tunn15    </loc>
</flux>
<!-- Boundary Conditions, Sources & Sinks -->
<!-- ***** -->
<defbc>
<ssea>         0          </ssea>
<pme>         4.7E-09    </pme>    net precipitation = 150 mm/year
</defbc>
<!-- Special models -->
<!-- ***** -->
<gwt>
<relax>       0.005      </relax>    This value is decreased, with converg-
ing flow solution
<facmin>     0.001      </facmin>
</gwt>
<partrack>

```



```

<method>                2                                </method>
<traj>                  500, 26, 500                      </traj>
<locfile>               Release_kartong_1.txt            </locfile>    Only one at the time
<locfile>               Release_kartong_2.txt            </locfile>    Only one at the time
<locfile>               Release_kartong_3.txt            </locfile>    Only one at the time
<locfile>               Release_kartong_4.txt            </locfile>    Only one at the time
<locfile>               BEFINTLIG_starting_locations.txt </locfile>    Only one at the time
</partrack>
<tracks>
<file>                  PARTICLES_OUTPUT                 </file>
<binary>                F                               </binary>
<ievent>                3                               </ievent>
</tracks>
<!-- Equations -->
<!-- ***** -->
<eqn>
<name>                  mass                             </name>        Deactivated, if particle tracking
</eqn>
<eqs>
<name>                  mass                             </name>
<relin>                 0.4                             </relin>
<liter>                 16                              </liter>
<nbrelax>               9                               </nbrelax>
<resfac>                0.0001                         </resfac>
<ipreco>                3                              </ipreco>
<igmres>                4                              </igmres>
</eqs>
<!-- Solver -->
<!-- ***** -->
<time>
<order>                 1                               </order>
<dt>                   3150000                         </dt>          3.15E7 = 1 year
</time>
<!-- loops -->
<loop>
<name>                  step                             </name>
<nbit>                  10000                           </nbit>
<eqs>                   mass                             </eqs>
<hist>                  hist1                           </hist>
<hist>                  hist2                           </hist>
<hist>                  hist3                           </hist>
<hist>                  hist4                           </hist>
<hist>                  hist5                           </hist>
<hist>                  hist6                           </hist>
<hist>                  hist7                           </hist>
<hist>                  hist8                           </hist>
<hist>                  hist9                           </hist>
</loop>
<loop>
<name>                  main                             </name>
<tecplot>               SFRtrans                       </tecplot>
<tecplot>               trajSFRtrans                   </tecplot>
</loop>
<!--=====
===== INPUT-OUTPUT =====
=====
<!-- Run % store -->
<!-- ***** -->

```

```

<run>
<title>          THE SFR REPOSITORY'          </title>
</run>
<slv>
<restart>        t          </restart>
<reset>         F          </reset>
</slv>
<rst>
<var>           gwt_fill    </var>
<var>           gwt_gh      </var>
</rst>
<!-- Screen -->
<!-- ***** -->
<hist>          <name>
<var>           pressure    </var>
<var>           fluxrep      </var>
<var>           fluxrep-     </var>
<var>           fluxrep+     </var>
<var>           fluxsilo     </var>
<var>           fluxsilo-    </var>
<var>           fluxsilo+    </var>
<var>           fluxEck      </var>
<var>           fluxBol      </var>
</hist>
<hist>          <name>
<var>           fluxtunn10-  </var>
<var>           fluxtunn10+  </var>
<var>           fluxtunn11-  </var>
<var>           fluxtunn11+  </var>
<var>           fluxtunn12-  </var>
<var>           fluxtunn12+  </var>
<var>           fluxtunn13-  </var>
<var>           fluxtunn13+  </var>
<var>           fluxtunn14-  </var>
<var>           fluxtunn14+  </var>
<var>           fluxtunn15-  </var>
<var>           fluxtunn15+  </var>
<spot>         North       </spot>
</hist>
<hist>          <name>
<var>           pressure    </var>
<var>           gwt_fill     </var>
<var>           darcy-w      </var>
<spot>         South       </spot>
</hist>
<hist>          <name>
<var>           pressure    </var>
<var>           darcy-u      </var>
<var>           darcy-v      </var>
<var>           darcy-w      </var>
<spot>         Rep80_1     </spot>
</hist>
<hist>          <name>
<var>           pressure    </var>
<var>           darcy-u      </var>
<var>           darcy-v      </var>
<var>           darcy-w      </var>
<spot>         Rep80_2     </spot>

```

```

</hist>
<hist>                                <name>
<var>          pressure                 </var>
<var>          gwt_fill                 </var>
<var>          darcy-w                 </var>
<spot>        North                    </spot>
</hist>
<hist>                                <name>
<var>          pressure                 </var>
<var>          darcy-u                 </var>
<var>          darcy-v                 </var>
<var>          darcy-w                 </var>
<var>          gwt_fill                 </var>
<profile>     vertical_rep             </profile>
</hist>
<hist>                                <name>
<var>          pressure                 </var>
<var>          darcy-u                 </var>
<var>          darcy-v                 </var>
<var>          darcy-w                 </var>
<var>          gwt_fill                 </var>
<profile>     vertical_Fisk            </profile>
</hist>
<hist>                                <name>
<var>          pressure                 </var>
<expand>      8                       </expand>
<cut>         plane x'                 </cut>
</hist>
<!-- Tecplot -->
<!-- ***** -->
<tecplot>
<name>          SFRtrans                </name>
<title>        FORSMRep'               </title>
<var>          pressure                 </var>
<var>          cellmk                   </var>
<var>          poros                    </var>
<var>          permx                    </var>
<var>          permy                    </var>
<var>          permz                    </var>
<var>          darcy-u                  </var>
<var>          darcy-v                  </var>
<var>          darcy-w                  </var>
<var>          gwt_fill                 </var>
<var>          gwt_gh                   </var>
<var>          ghdel                     </var>
<loc>          plane x'                 </loc>
<loc>          plane y'                 </loc>
<loc>          plane z0'                </loc>
<loc>          plane z60'               </loc>
<loc>          land                     </loc>
</tecplot>
<tecplot>
<name>          trajSFRtrans            </name>
<traj>         0                      </traj>
</tecplot>
<!--=====>
===== OBJECTS & LOCATIONS =====
<!--=====

```

```

<!-- locations -->
<loc>
  <name>          reoloc          </name>
  <patch>        6350. 8000. 9350. 10150. -145. -20. </patch>
</loc>
<loc>
  <name>          silo            </name>
  <patch>        7040. 7090. 9955. 10000. -140. -60. </patch>
</loc>
<loc>
  <name>          rivlocEck       </name>
  <patch>        5750. 6050. 5900. 5900. -10.10. </patch>
</loc>
<loc>
  <name>          rivlocBol       </name>
  <patch>        5910. 6110. 8170. 8170. -10.10. </patch>
</loc>
<loc>
  <name>          tunn10          </name>
  <marker>       cell 10        </marker>
</loc>
<loc>
  <name>          tunn11          </name>
  <marker>       cell 11        </marker>
</loc>
<loc>
  <name>          tunn12          </name>
  <marker>       cell 12        </marker>
</loc>
<loc>
  <name>          tunn15          </name>
  <marker>       cell 15        </marker>
</loc>
<loc>
  <name>          tunn13          </name>
  <marker>       cell 13        </marker>
</loc>
<loc>
  <name>          tunn14          </name>
  <marker>       cell 14        </marker>
</loc>
<!-- planes -->
<loc>
  <name>          plane x'        </name>
  <xplane>       6500            </xplane>
</loc>
<loc>
  <name>          plane y'        </name>
  <yplane>       9940            </yplane>
</loc>
<loc>
  <name>          plane z0'       </name>
  <zplane>       0                </zplane>
</loc>
<loc>
  <name>          plane z60'      </name>
  <zplane>       -60              </zplane>
</loc>

```

```
<loc>
  <name>          depthz3          </name>
  <dplane>        3                </dplane>
</loc>
<!-- spots -->
<loc>
  <name>          Rep80_1'         </name>
  <spot>          6942. 9932. -80. </spot>
</loc>
<loc>
  <name>          Rep80_2'         </name>
  <spot>          6860. 9900. -80. </spot>
</loc>
<loc>
  <name>          South'           </name>
  <spot>          7000. 5000. 00.  </spot>
</loc>
<loc>
  <name>          North'           </name>
  <spot>          3000. 8000. 00.  </spot>
</loc>
<!-- profiles -->
<loc>
  <name>          vertical_rep'     </name>
  <zline>         6942. 9932.       </zline>
</loc>
<loc>
  <name>          vertical_Fisk'    </name>
  <zline>         8000. 5000.       </zline>
</loc>
</cif>
```

Main changes between the preliminary v 0.1 model delivery and the 'final' post review model delivery.

By Phillip Curtis, Golder Associates AB

No lineaments or the deformation zone ground surface traces have been modified. Estimates of the span of various properties have been removed from the property tables since it was judged that sufficient information is lacking.

| Deformation zone ID | Parameter | Preliminary v0.1 | Final v0.1 | Comment |
|---------------------|-------------------|------------------|---|--|
| ZFM871 | Orientation | 070/19 | 071/19 | |
| | Thickness | 20 m | 24 m | |
| | Length | 1,400 m | 1,200 m | There is still no associated lineament, only a change in the estimated projected length |
| | Bh intercepts | | Additional intercepts have been included from KFR24, KFR25 and KFR57 | Additional intercepts based on /Axelsson and Mærsk Hansen 1997/ |
| | Tunnel intercepts | | Very minor adjustments to RVS control point intercepts, no change in interpretation | |
| ZFMNE0870B | Orientation | 227/74 | 227/73 | Adjustment in position interpreted in KFR09 and added intercept position from KFR36 |
| | Tunnel intercepts | | Very minor adjustments to RVS control point intercepts, no change in interpretation | |
| ZFMNNE0869 | Orientation | 200/80 | 201/86 | |
| | Thickness | 50 m | 60 m | More weight given to SHI thickness estimates. |
| | Tunnel intercepts | | Very minor adjustments to RVS control point intercept, no change in interpretation | |
| ZFMNNW0999 | Confidence | High | Medium | There is a geometrical intercept with KFR08 SHI DZ2. However, this interval is now inferred as being dominated by ZFMNW0805A and no exclusive evidence for the existence of ZFMNNW0999 has been identified |
| | Thickness | 20 m | 5 m | Return to a default thickness due to reinterpretation of the KFR08 intercept (see above) |
| ZFMNW0805A | Orientation | 134/90 | 314/83 | Steep dip to the NE (leads to a 180° change in strike notation) based on adjusted intercept position with SHI DZ2 in KFR08. |
| | Thickness | 20 m | 60 m | Adjusted to correspond to the entire extent of SHI DZ2 in KFR08 |
| | Bh intercepts | | | Adjusted position in KFR08. Very minor adjustment to position in KFR7A |

| Deformation zone ID | Parameter | Preliminary v0.1 | Final v0.1 | Comment |
|---------------------|---------------|------------------|------------|--|
| ZFMNW0805B | Bh intercepts | | | No significant change in zone geometry. However, target intercepts in KFR7A and KFR08 are no longer quoted since the respective intervals are inferred as being dominated by other zones and no exclusive evidence for the existence of ZFMNW0805B has been identified |
| ZFMNW0002 | Name | ZFMWNW0804 | ZFMNW0002 | The preliminary model name of zone ZFMWNW0804 has been replaced by ZFMNW0002 |
| | Thickness | 40 m | 58 m | Change based on a re-assessment of tunnel mapping results |

Simulated exit locations from candidate layouts at different stages of land-lift.

This appendix visualizes the simulated exit locations from the four suggested candidate layouts. The exit locations of particle trajectories are shown for the land-lift at 2000 AD, 3000 AD and 5000 AD.

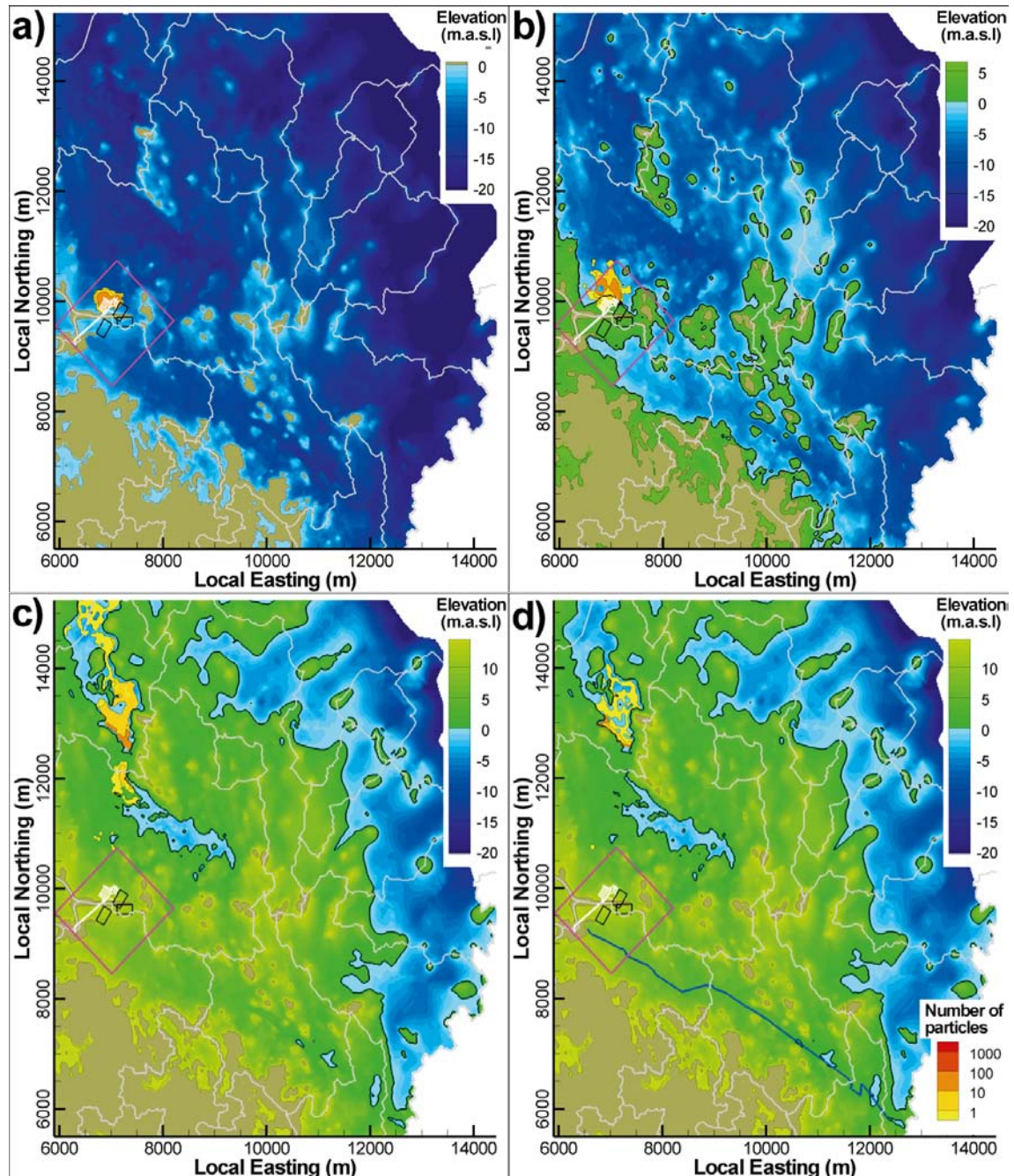


Figure H-1. Particle exit locations from the existing SFR; a) 2000 AD, b) 3000 AD, c) 5000 AD, and d) 5000 AD with major future rivers implemented. No particles exit south of the topographical divide.

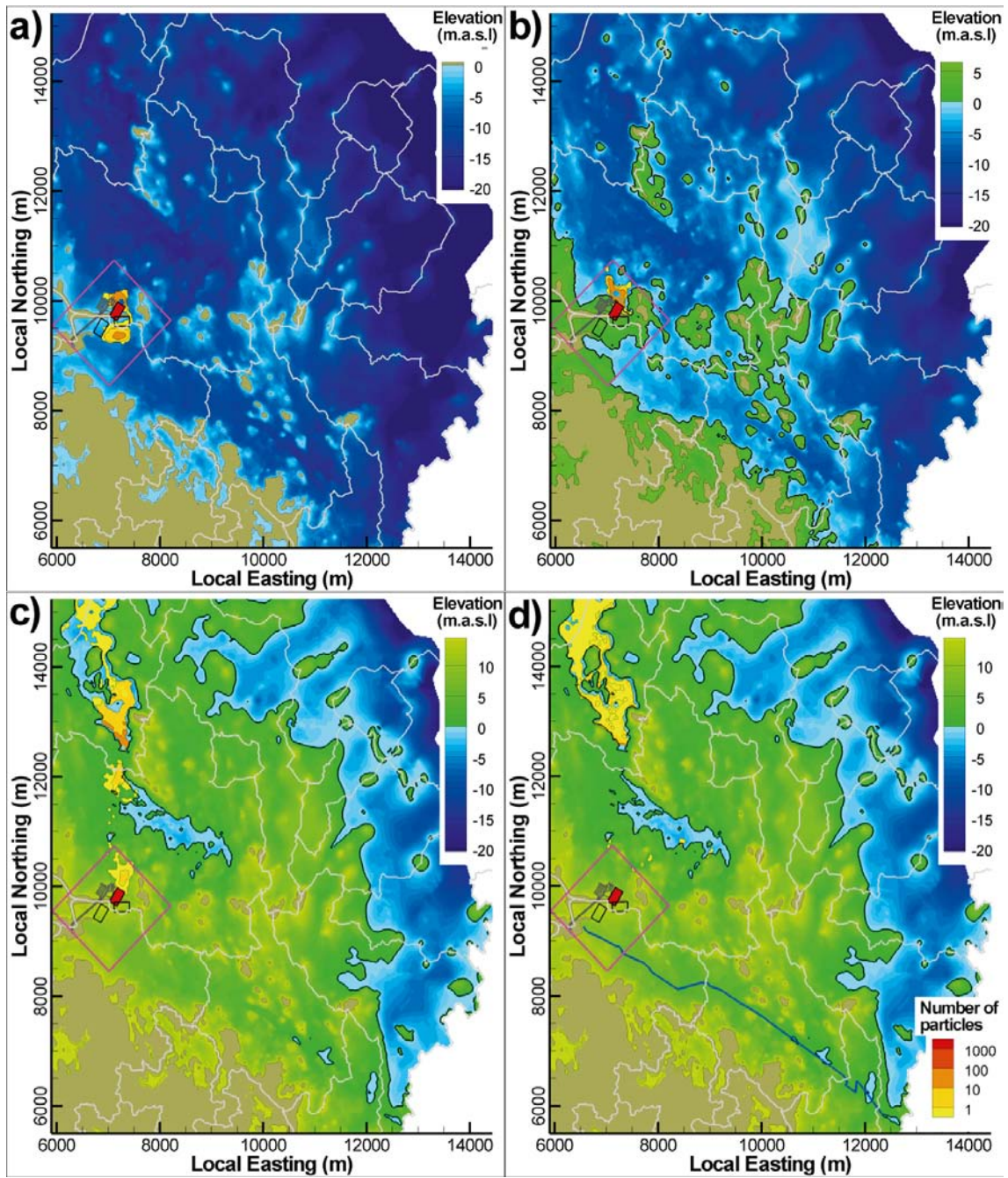


Figure H-2. Particle exit locations from the candidate layout 1; a) 2000 AD, b) 3000 AD, c) 5000 AD, and d) 5000 AD with major future rivers implemented. 19% exit south of the topographical divide at 2000 AD.

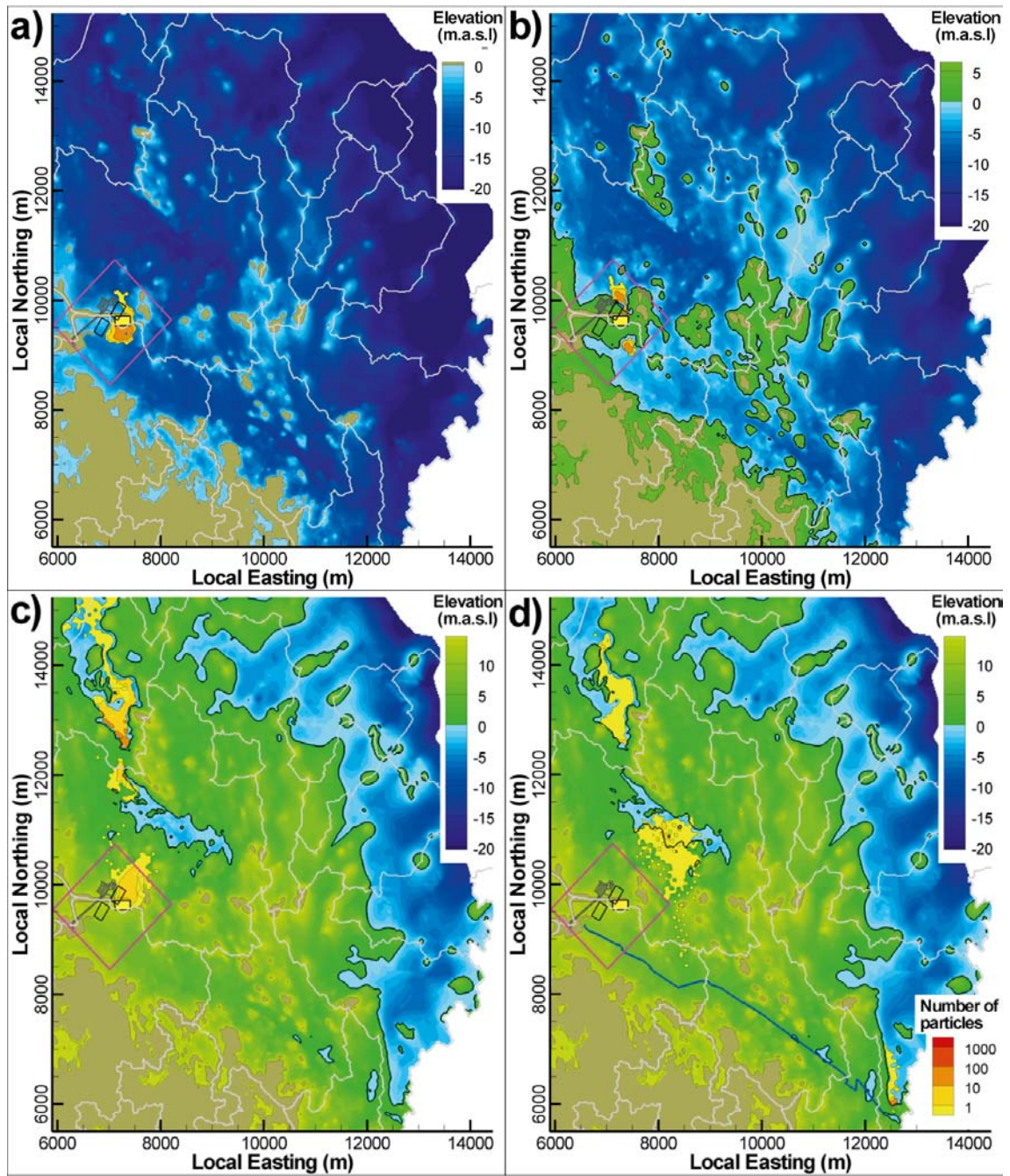


Figure H-3. Particle exit locations from the candidate layout 2; a) 2000 AD, b) 3000 AD, c) 5000 AD, and d) 5000 AD with major future rivers implemented. 85% exit south of the topographical divide at 2000 AD, while 17% exit south of the topographical divide at 3000 AD and 5000 AD. If the Singö river is not implemented, no particles exit south of the topographical divide at 5000 AD.

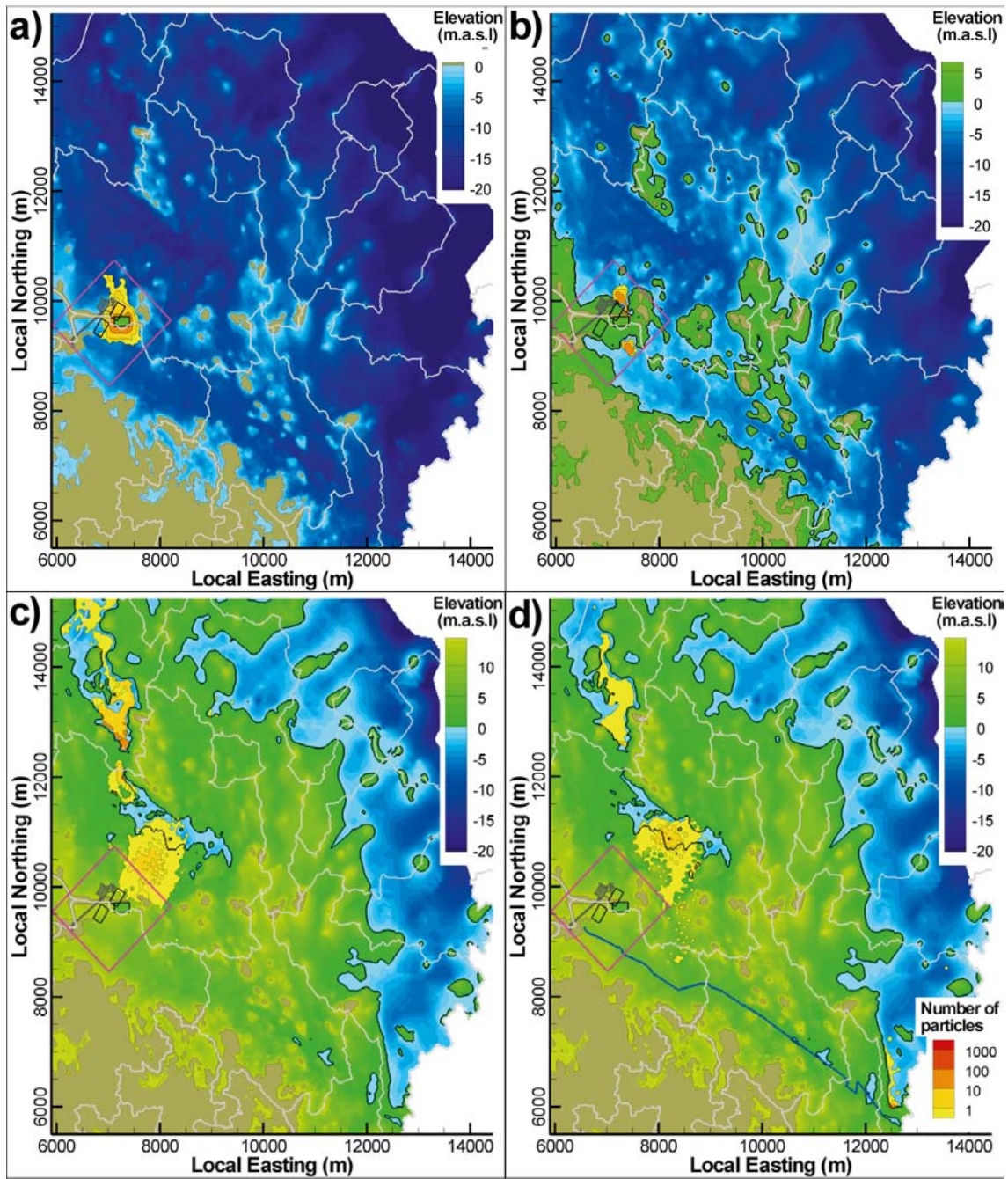


Figure H-4. Particle exit locations from the candidate layout 3; a) 2000 AD, b) 3000 AD, c) 5000 AD, and d) 5000 AD with major future rivers implemented. 29% exit south of the topographical divide at 2000 AD, respectively, 3000 AD. If the Singö river is implemented, 9% will exit south of the topographical divide at 5000 AD, otherwise all exit to the north.

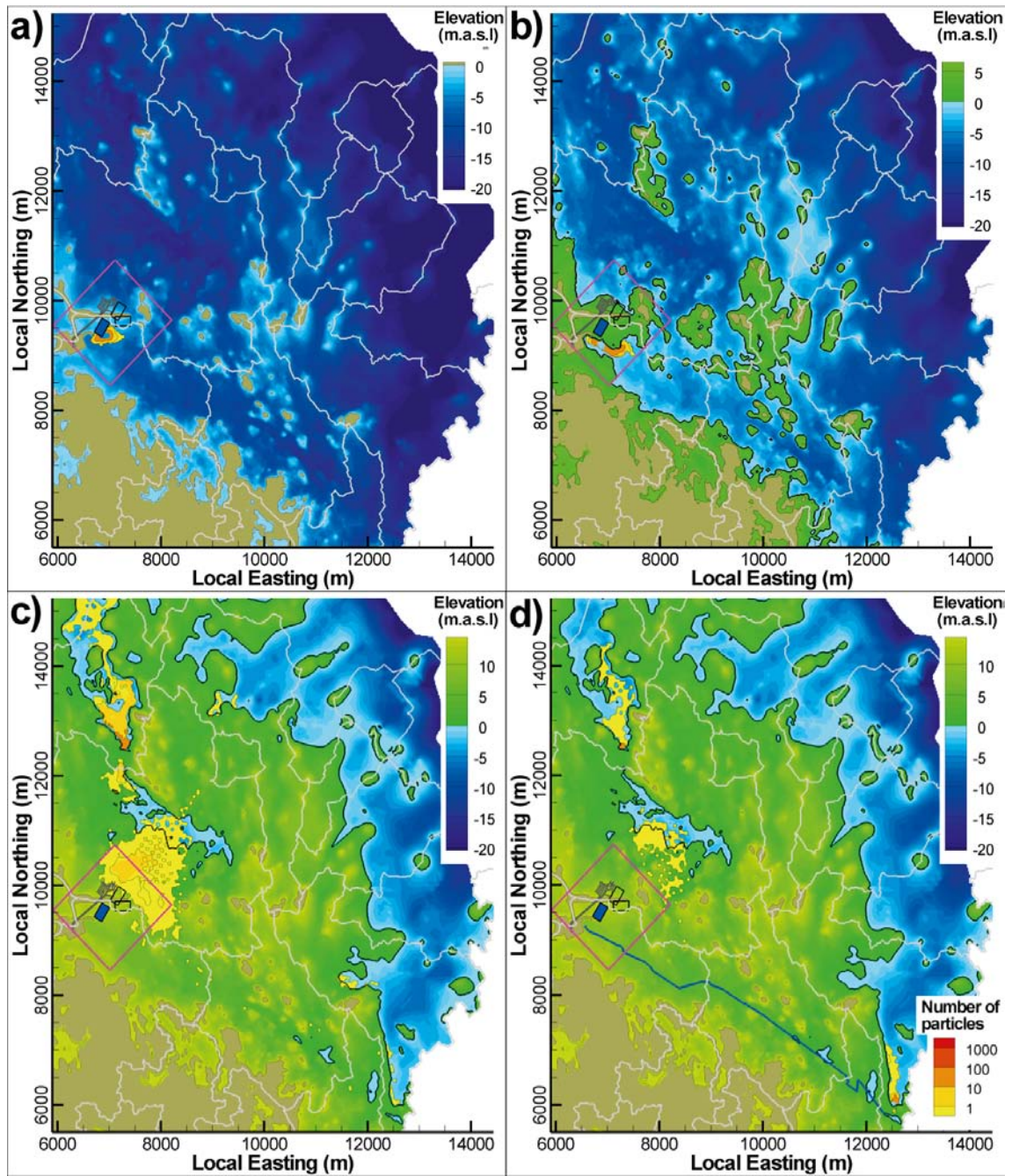


Figure H-5. Particle exit locations from the candidate layout 4; a) 2000 AD, b) 3000 AD, c) 5000 AD, and d) 5000 AD with major future rivers implemented. 100% exit south of the topographical divide at 2000 AD, respectively, 3000 AD. If the Singö river is implemented, 80% will exit south of the topographical divide at 5000 AD, otherwise all exit to the north.

Simulated flow-field of Candidate layouts.

This Appendix visualizes the simulated near flow field for each of the Candidate layouts at different stages of land-lift: 2000 AD, 3000 AD, and 5000 AD. Only the outward-directed flux is shown, representing the particle exit locations from the Candidate layouts.

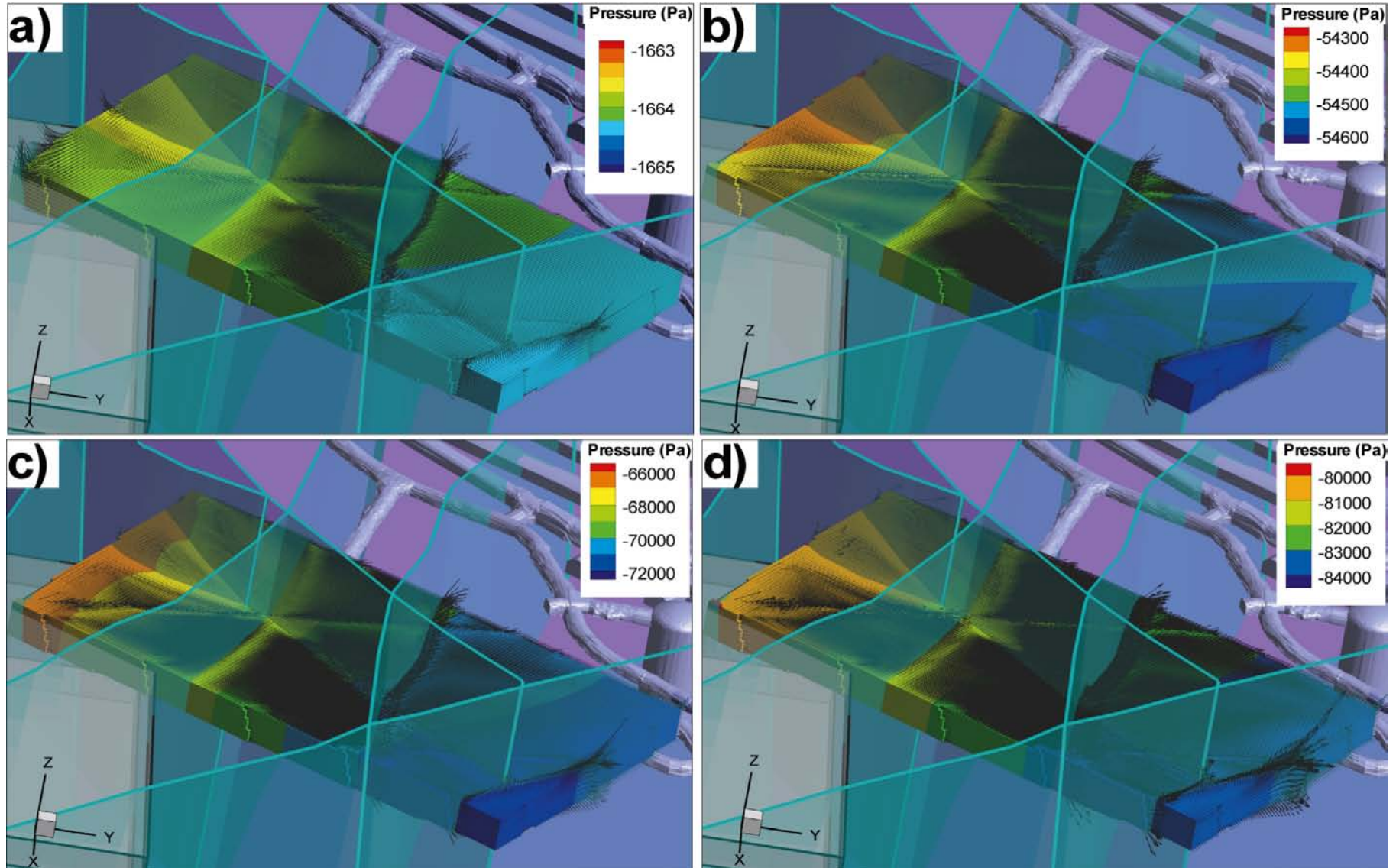


Figure I-1. Outward-directed Darcy velocity for layout 1; a) 2000 AD, b) 3000 AD, c) 5000 AD, and d) 5000 AD with major future rivers.

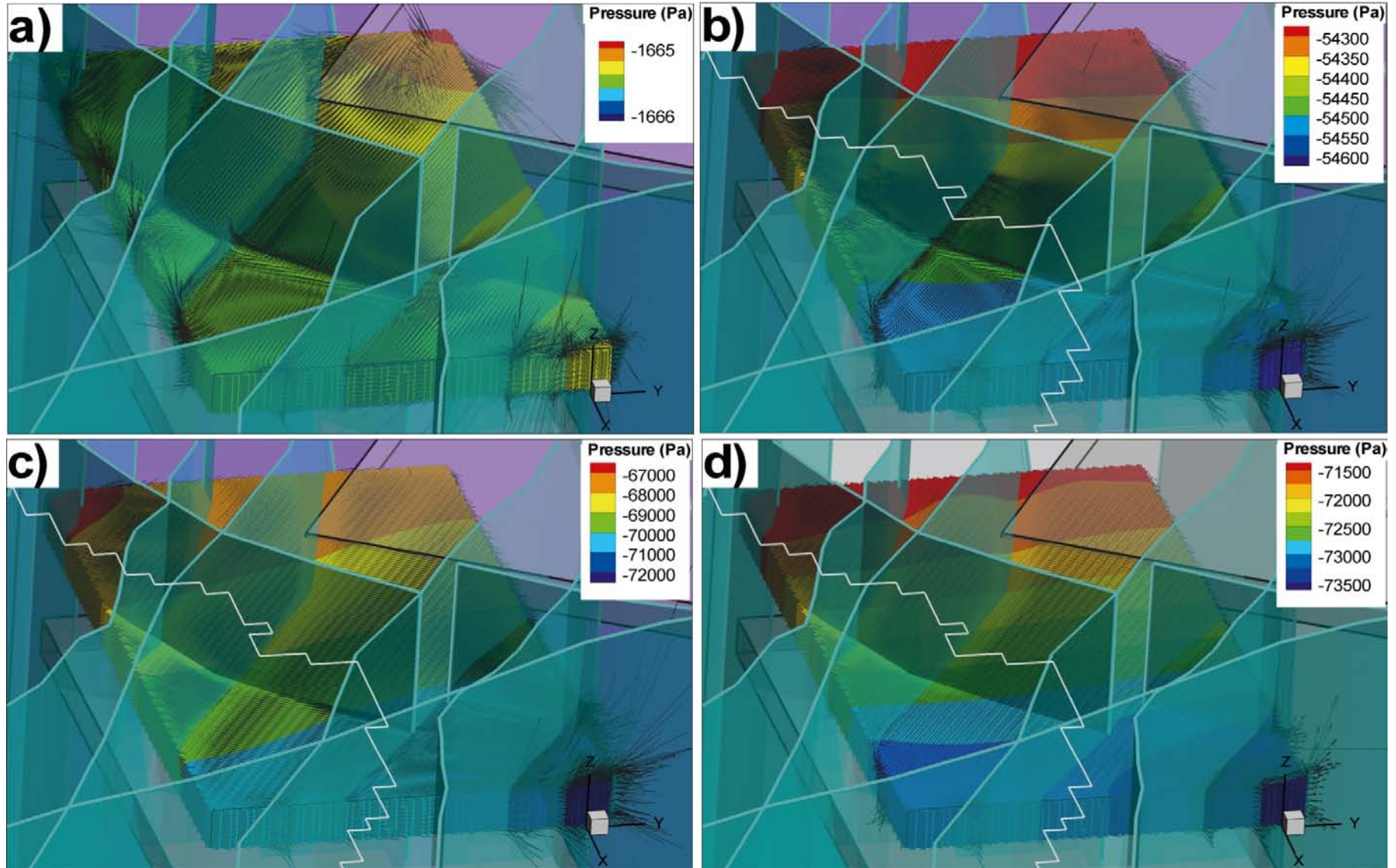


Figure I-2. Outward-directed Darcy velocity for layout 2; a) 2000 AD, b) 3000 AD, c) 5000 AD, and d) 5000 AD with major future rivers.

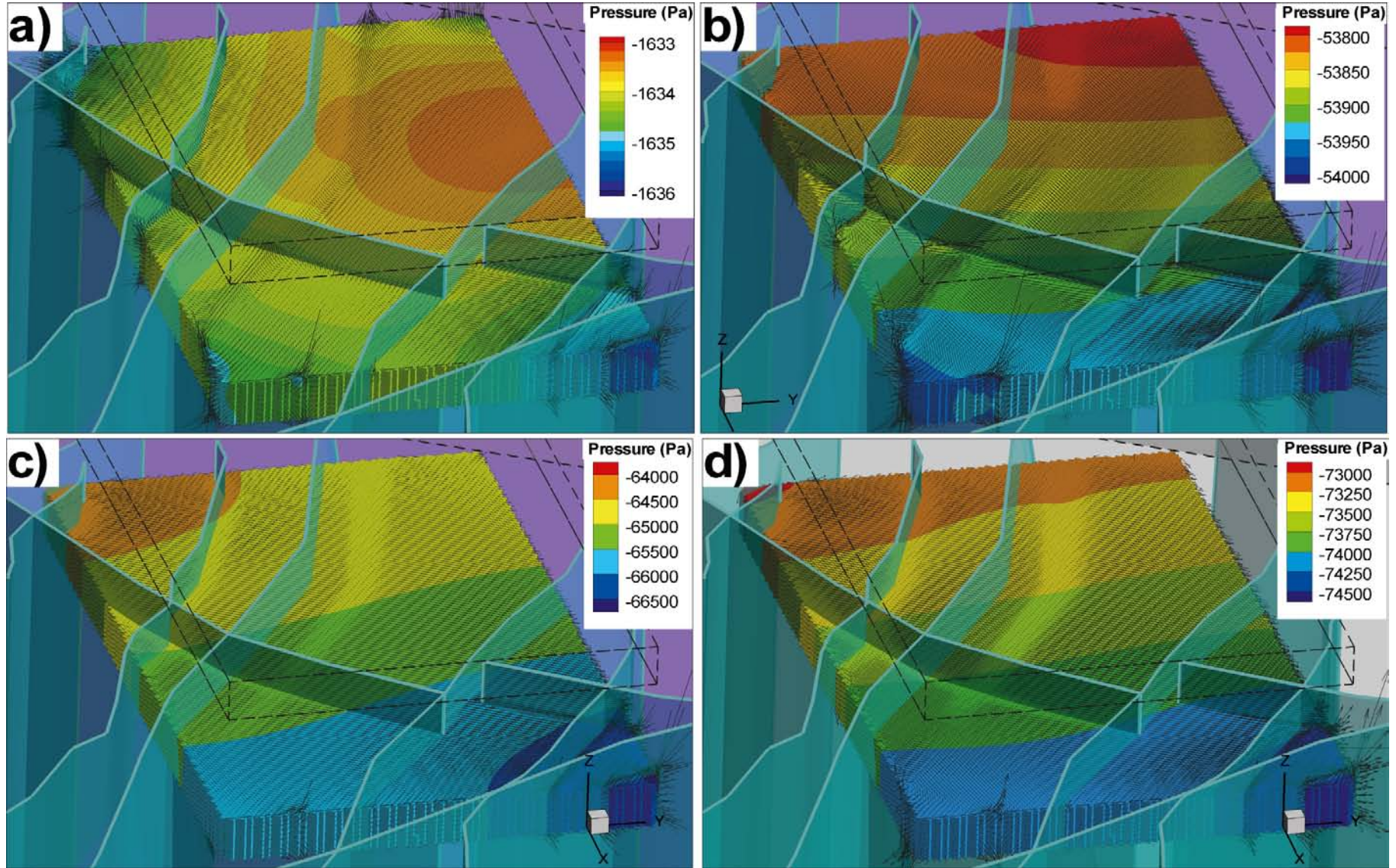


Figure I-3. Outward-directed Darcy velocity for layout 3; a) 2000 AD, b) 3000 AD, c) 5000 AD, and d) 5000 AD with major future rivers.

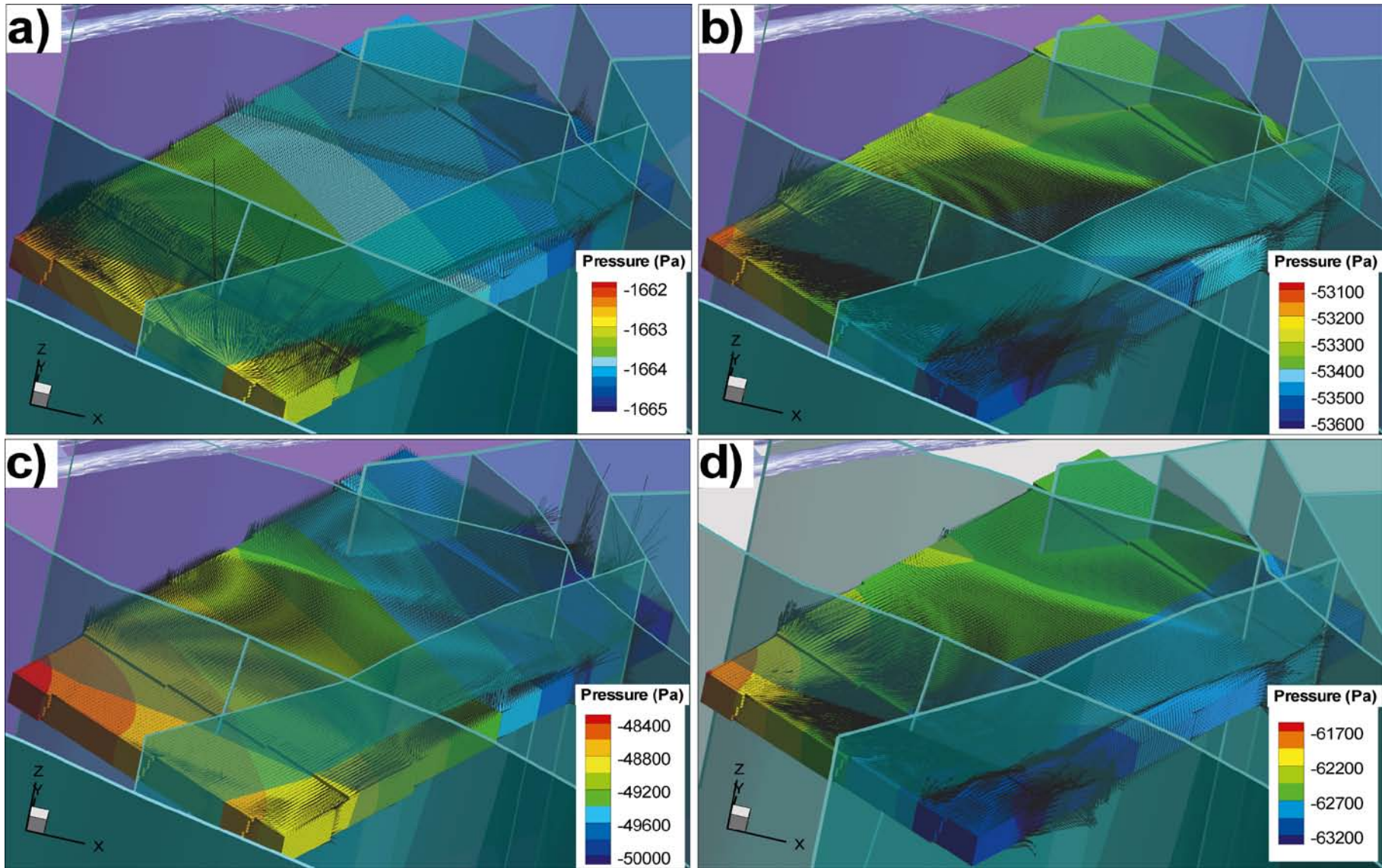


Figure I-4. Outward-directed Darcy velocity for layout 4; a) 2000 AD, b) 3000 AD, c) 5000 AD, and d) 5000 AD with major future rivers.